DPST-AFCT-77-1-2

SAVANNAH RIVER LABORATORY QUARTERLY REPORT

ALTERNATE FUEL CYCLE TECHNOLOGIES

APRIL – JUNE 1977

SAVANNAH RIVER LABORATORY
AIKEN, SOUTH CAROLINA 29801

PREPARED FOR THE U.S. ENERGY RESEARCH AND DEVELOPMENT ADMINISTRATION UNDER CONTRACT AT(07-2)-1

DPST-AFCT-77-1-2

Indexing Term: Water Cooled
Reactor/Fuel Cycle

SAVANNAH RIVER LABORATORY QUARTERLY REPORT

ALTERNATE FUEL CYCLE TECHNOLOGIES

APRIL – JUNE 1977

Publication Date: September 1977

E. I. DU PONT DE NEMOURS AND COMPANY
SAVANNAH RIVER LABORATORY
AIKEN, SOUTH CAROLINA 29801

PREPARED FOR THE U. S. ENERGY RESEARCH AND DEVELOPMENT ADMINISTRATION UNDER CONTRACT AT(07-2)-1

FOREWORD

This quarterly report describes Savannah River Laboratory (SRL) research and development studies to assist ERDA in providing information needed by industry to close the back end of the commercial light-water reactor (LWR) fuel cycle. These efforts are directed primarily at reprocessing and recycle of uranium and plutonium from spent LWR fuel.

The process steps in the front end of the nuclear fuel cycle are uranium ore mining and milling, uranium enrichment, and uranium fuel fabrication. Process steps in the back end of the fuel cycle are spent fuel reprocessing, actinide recycle (mixed uranium-plutonium oxide), recycle fuel fabrication, and waste management. The front end of the cycle is well developed and is providing suitable fuel for commercial power reactors. However, the back end is only partially developed. Spent reactor fuel is presently being stored underwater in basins until facilities become available for reprocessing, fuel recycle, and waste management.

Processing areas under study are head-end treatment of the spent fuel, treatment of offgas from various parts of the reprocessing system, and recovery and purification of uranium and plutonium by the Purex solvent extraction process. Additional information is being provided by economic and environmental studies, and by general support activities such as corrosion and shielding studies and development of improved online process control methods.

The LWR fuel recycle research and development program includes the following categories:

Economic Studies
Environmental Studies
Fuel Receipt
Head-End Processes
Off-Gas Treatment
Purex Process
Finishing Processes
Waste Management
Environmental Effects
Safeguards
General Support (Corrosion and Materials Development, Analytical Methods, and Criticality and Shielding Studies)

SRL is also coordinating LWR fuel recycle studies at other ERDA sites. These research and Development activities are summarized quarterly by SRL in a separate report (DPST-AFCT-year-2-quarter).

CONTENTS

ENVIRONMENTAL STUDIES

ENVIRONMENTAL IMPACT OF REPROCESSING LWR FUEL AND FABRICATING MIXED-OXIDE FUEL

The environmental impacts of model plants for reprocessing LWR fuel and fabricating mixed-oxide (MOX) fuel were assessed as part of a larger assessment of an LWR fuel reprocessing and recycle industry. The environmental effects of particular interest were associated with radioactive releases. This study shows that these releases and the resulting population doses would be small; the dose to the local population would be about 0.03% of that received from natural radiation sources.

Description of Process Plant

The model fuel reprocessing plant (FRP) is based on the Purex solvent-extraction process for separation of uranium and plutonium products from the waste stream. The plant is sized to process 1500 MTU per year and includes facilities to convert uranium to UF_6 and plutonium to PuO_2. The primary process steps are:

- Fuel element chopping
- Nitric acid leaching
- Purex solvent extraction
- UF_6 production from uranyl nitrate by thermal decomposition and anhydrous fluorination
- PuO_2 production from plutonium nitrate by the oxalate calcination process.

UO_2-PuO_2 fuel is assumed to be fabricated in an MOX plant colocated or integral with the FRP. The model MOX plant has a capacity of 350 MT/yr of fuel containing less than 5% PuO_2. The process includes:

- Oxide powder preparation
- Mechanical blending of UO_2 and PuO_2 powders
- Pelletizing, sintering, and grinding of the mixed oxide
- Scrap recovery
- Waste treatment to recover plutonium and to prepare the waste for disposal.

Plant Design

Each plant is assumed to be designed to withstand design-basis earthquakes and other natural phenomena (such as tornadoes, hurricanes, and floods) as appropriate for its location. Plant auxiliaries include standby diesels for emergency power, fire protection systems, water treatment systems, boilers to produce plant steam, electrical switchgear, and sanitary waste treatment systems.

Personnel exposure to radiation is controlled by shielding for normal operations and by use of special work permits for maintenance operations. Contamination of air in areas occupied by personnel is minimized by controlled-flow ventilation with air flow from areas of low contamination to areas of progressively higher contamination.

Multiple levels of confinement limit release of plutonium from the MOX manufacturing building. The manufacturing building is maintained at a negative pressure relative to the outside. Plutonium-handling operations are carried out inside equipment within process enclosures (glove boxes or shielded cells) maintained at negative pressures relative to adjacent areas of the manufacturing building. Pressure differentials are maintained so that air flows from noncontaminated areas into areas of potentially higher contamination levels, to limit any possible spread of radioactivity. Ventilation air discharged from the manufacturing building to the atmosphere is filtered through high-efficiency particulate air (HEPA) filters.

Waste Management

Solids

Solid wastes, such as hulls and fuel hardware containing transuranic elements in excess of 10 nCi/g, are expected to be stored onsite in vaults or equivalent facilities, and then shipped to a Federal repository. Other low-specific-activity solid wastes are packaged and shipped to commercial burial grounds or stored onsite.

Liquids

High level liquid wastes (HLLW) from the FRP are expected to be retained as concentrated acid wastes held in cooled, multibarrier stainless-steel tanks on the FRP site for a year or more to allow

short-lived fission products to decay before further processing. Federal regulations[1] require that within five years after generation, HLLW must be solidified, and within ten years after their generation the solids must be transferred to a Federal repository.

Gases

Atmospheric releases of radionuclides from an FRP will be reduced by effluent control systems currently available or under development. These controls include voloxidation to remove tritium, fluorocarbon absorption of ^{85}Kr and ^{14}C (after the carbon is catalytically oxidized to CO_2), volatilization of iodine from the dissolver solution followed by sorption of iodine in a scrubber system, and improved filtration for collection of particulates.

All exhausts from the processes are discharged through a 100-meter stack after filtration and purification.

Releases from an FRP/MOX Plant

Radioactive

Table 1 summarizes annual releases of radionuclides from the model FRP/MOX plant to the atmosphere. These estimates are based on cooling spent fuel one year before processing.

No radionuclides are expected to be released to the environment with liquid effluents.

Chemical

All emissions of SO_2, NO_x, CO, fluorides, and hydrocarbons from the model FRP/MOX plant and support facilities were calculated to result in ambient air concentrations within the National Primary Standards. Chemical concentrations in liquid effluents were calculated to be within standards for public water supplies.

Radiation Doses from Normal Operations

Radiation doses resulting from radioactive releases during routine operation of the model FRP/MOX plant were estimated for the hypothetical individual who receives the maximum dose and also for the general population (local, U.S., and worldwide.).

---

1. U. S. Code of Federal Regulations, Title 10, Part 50, Appendix F.

TABLE 1

Annual Release of Radionuclides to the Atmosphere from the Model FRP/MOX Plant[a]

Nuclide	*Ci/yr*	*Nuclide*	*Ci/yr*
^{3}H	11,000	^{134}Cs	0.49
^{14}C	7	^{137}Cs	0.50
^{85}Kr	140,000	^{141}Ce	0.001
^{89}Sr	0.02	^{144}Ce	1.3
^{90}Sr	0.2	^{147}Pm	0.26
^{90}Y	0.2	^{154}Eu	0.022
^{91}Y	0.03	^{155}Eu	0.020
^{95}Zr	0.07	^{238}Pu	0.0077
^{95}Nb	0.02	^{239}Pu	0.00037
^{103}Ru	0.003	^{240}Pu	0.00078
^{106}Ru	0.52	^{241}Pu	0.22
^{110m}Ag	0.006	^{242}Pu	0.000006
^{125}Sb	0.025	^{241}Am	0.00023
^{127m}Te	0.005	^{243}Am	0.000063
^{129}I	0.3	^{242}Cm	0.011
^{131}I	3×10^{-7}	^{244}Cm	0.015

a. An integrated or colocated fuel reprocessing plant (1500 MTU/yr) and mixed-oxide fuel fabrication plant. Spent fuel is LWR-Pu fuel cooled one year to allow decay of short-lived fission products.

The dose commitment that accrues during the remaining lifetime of the individual is defined as the total radiation dose to a particular organ resulting from an intake of a radionuclide. This definition includes the contribution of any radioactive daughters that are formed in the body as the parent radionuclide decays. For this study, the exposed individual was assumed to be an adult, who is 20 years old at the time of intake and lives to an age of 70 years. Radiation doses and dose commitments were calculated for dose pathways based on external exposure to radiation from radionuclides in the air, inhalation, transpiration by vegetation (for tritium oxide only), contamination of ground surfaces, and contamination of agricultural commodities produced near the facility.

Maximum for an Individual

The hypothetical individual receiving the maximum dose was assumed to reside continuously at the site boundary at the point of highest atmospheric concentrations. The 50-year dose commitment to this individual from one year's operation was calculated to be about 0.4 mrem to the whole body and 5.9 mrem to the thyroid. For comparison, exposure to natural radiation sources in the U.S. ranges from 100 to 250 mrem/yr averaging 130 mrem/yr.

General Population

Predicted population doses from one year's operation of the model FRP/MOX plant are shown in Table 2 for the nuclides and dose pathways contributing significantly to the total dose commitment. Effects of long-lived nuclides for 100 years following the year of release are included to assess the effects of persistent nuclides. The release was assumed to occur in year 2000, and the year 2001 was taken as the start of the 100-year period.

TABLE 2

Population Radiation Dose from Operation of the Model FRP/MOX Plant in Year 2000[a]

		Population Dose, man-rem[b]			
Critical Organ	*Nuclide or Pathway*	*Local (50-mi. radius)*	*U.S. (less local)*	*World (less U.S.)*	*Total*
Whole body	^{14}C	1.2	27	410	440
	^{85}Kr	0.29	3.4	45	49
	^{3}H	12	35	5.7	53
	Exposure to contaminated ground	13	51	-	64
	Inhalation[c]	2.6	7.9	-	10
	Foodstuffs[c]	0.53	2.1	-	2.6
	Total	*30*	*130*	*460*	*620*
Thyroid[d]	^{129}I	260	950	-	1200
Bone[d]	Inhalation[c]	86	260	-	350
	Foodstuffs[c]	6.3	25	-	32
	Total	*92*	*290*	-	*380*
Lung[d]	^{85}Kr	0.60	7.0	93	100
Red Marrow[d]	^{14}C	2.1	47	710	760

a. Continued effects of year 2000 releases are included through the year 2100.

b. To two significant figures.

c. Includes contribution from nuclides other than ^{3}H, ^{14}C, ^{85}Kr, and ^{129}I.

d. Doses in addition to organ dose from whole body irradiation.

Local Population

The calculated whole-body dose commitment to a population of one million people living within 50 miles of the model FRP/MOX plant is 30 man-rem (Table 2). This dose commitment is 0.03% of that received by the same population from natural radiation sources.

United States

Several radionuclides released in gaseous effluents from the model FRP/MOX plant would spread from the localities of the plants to part of the continental United States land area, and some would eventually be transported worldwide. ^{85}Kr, ^{14}C, and ^{3}H would expose the United States population before subsequent dispersion throughout the world, but ^{129}I and radioactive particulates (primarily actinides) were assumed to be deposited only on U.S. soil. Because FRP/MOX plants are assumed to be located in the east or midwest, only the population in the eastern U.S. is considered to be exposed to releases of radioactivity before worldwide distribution.

Table 2 includes the total dose to the U.S. population from releases from one model FRP/MOX plant during the year 2000. The anticipated 130 man-rem whole body dose is only 4×10^{-4}% of the 3×10^{7} man-rem dose from natural radiation sources received by the U.S. population in the year 2000, assuming 100 mrem/yr natural radiation per person.

World

Environmental effects from ^{3}H, ^{14}C, and ^{85}Kr released in fuel reprocessing include worldwide population doses resulting from global cycling. The estimated 460 man-rem whole body dose commitment (Table 2) is 7×10^{-5}% of the 6×10^{8} man-rem dose from natural radiation sources received by the world population in the year 2000, assuming 100 mrem/yr natural radiation per person.

Radiation Doses from Postulated Accidents

Radiation doses were estimated for criticality incidents, fires, and explosions in FRP/MOX plants based on information in WASH-1327[2] and ORNL-4992.[3] The expected maximum individual doses are all less than one rem, well within current or anticipated future standards for such infrequent events. All explosions, fires, and pressure surges arising from postulated accidents were assumed to be less than required to breach the facility structure; filters located away from the accident were assumed to remain intact.

---

2. *Draft Generic Environmental Statement on Mixed-Oxide Fuels (GESMO).* USAEC Report WASH-1327, U.S. Atomic Energy Commission, Washington, DC (1974).

3. *A Methodology for Calculating Radiation Doses from Radioactive Releases to the Environment.* ERDA Report ORNL-4992, Oak Ridge National Laboratory, Oak Ridge, TN (1976).

Population Health Effects

Public health effects of radioactive releases from the model FRP/MOX plant were calculated from the population doses given in Table 2 by applying the linear dose-effect relationships (Table 3) derived by the EPA[4,5] from the BEIR report.[6] No threshold dose was assumed. Most other interpretations[7] of the BEIR report lead to dose-effect estimates that are lower than those predicted from the EPA factors, and the probability that the actual number of health effects will be lower than those calculated must be recognized when using the estimates in a cost-benefit assessment. The NCRP has cautioned against assuming as actual risks those estimates of carcinogenic risks that are derived for low radiation levels by linear extrapolation from data obtained at high doses and dose rates. The NCRP has also cautioned against basing unduly restrictive policies on such estimates.[8]

The factors used by the EPA to estimate health effects from man-rem population doses and their estimate of the frequency of mortality from cancers are given in Table 3. The genetic effects are the very serious effects, such as congenital anomalies and constitutional and degenerative diseases.

The calculated statistical incidence of serious cancers and genetic effects attributed to radioactive releases from operation of the model FRP/MOX plant in the year 2000 are given in Table 4. These estimates are so much lower than the number of cancers diagnosed in the United States that it is impossible to identify

---

4. *Environmental Analysis of the Uranium Fuel Cycle, Part I - Fuel Supply.* Report EPA-520/9-73-003B, U.S. Environmental Protection Agency, Washington, DC (1973).

5. *Environmental Analysis of the Uranium Fuel Cycle, Part III - Nuclear Fuel Reprocessing.* Report EPA-520/9-73-003D, U.S. Environmental Protection Agency, Washington, DC (1973).

6. *The Effects on Populations of Exposure to Low Levels of Ionizing Radiation, BEIR Report.* National Academy of Sciences and National Research Council (November 1972).

7. *Reactor Safety Study.* Report WASH-1400 (NUREG-75/014), Appendix VI, An Assessment of Accident Risks in U.S. Commercial Nuclear Power Plants, U.S. Nuclear Regulatory Commission, Washington, DC (1975).

8. *Review of the Current State of Radiation Protection Philosophy.* NCRP Report 43, National Council on Radiation Protection Measurements, Washington, DC (1975).

TABLE 3

EPA Dose-Effect Factors

Organ	Number of Health Effects per Million Man-rem		
	Cancers	Fatal Cancers	Genetic Damage
Whole Body	400	200	-
Lung	50	50	-
Bone	32	16	-
Red Marrow	54[a]	54[a]	-
Thyroid	60	15	-
Gonads	-	-	300[b]

a. Leukemia.

b. Serious genetic effects; one-half the exposed population is assumed to be subject to genetic effects.

TABLE 4

Population Health Effects from Operation of the Model FRP/MOX Plant in the Year 2000[a]

Malignancies in	Calculated Incidence, cases/year[b]			
	Local (50-mi. radius)	U.S. (less local)	World (less U.S.)	Total
Whole Body	0.012	0.052	0.18	0.24
Lung[c]	0.000030	0.00035	0.00046	0.0050
Bone[c]	0.0029	0.0090	-	0.012
Red Marrow[c] (Leukemia)	0.00011	0.0025	0.038	0.041
Thyroid[c]	0.016	0.057	-	0.073
Total	0.031	0.12	0.22	0.37
Genetic Damage[d]	0.0038	0.014	0.060	0.078

a. Based on population doses and dose-effect factors given in Tables 2 and 3, respectively.

b. To two significant figures.

c. Organ health effects in addition to those included in whole body dose estimates.

d. For genetic dose, multiply whole body dose from tritium, carbon-14, and krypton-85 by 1.0, 0.39, and 0.74, respectively.

statistically any cases of cancer as being caused specifically by FRP/MOX operations. For example, even for the local population within 50 miles of the FRP/MOX plant, the expected 0.03 additional cases of cancer due to operation of the plant for one year is only 0.001% of the 3000 cancers expected to be diagnosed each year in this population.[9]

Occupational Health Effects

Radiological

In the model plant, personnel exposure is limited by shielding and procedural controls to "as low as reasonably achievable." This study assumed a maximum exposure of 1 rem/yr, the limit for new ERDA plutonium facilities.[10] Average exposure was assumed to be 40% of the 1 rem limit. The total work force was assumed to be 1200 for a colocated reprocessing and MOX fabrication plant; the annual occupational exposure would therefore be 480 man-rem.

Calculations with EPA linear dose-effect factors (Table 12) predict that this exposure would result in 0.2 cancers (50% fatal) and 0.1 serious genetic effects (assuming 75%* of the work force to be susceptible to genetic damage for each year's operation of the model FRP/MOX plant. For comparison, about 0.7 members of the plant's work force would die each year of cancer from other causes, assuming 60 cancer deaths per year per 100,000 persons between the ages of 18 and 64 in the United States.[8]

Accidental

Occupational accidents in the model FRP/MOX plant are expected to cause about 0.08 deaths each year, based on an observed frequency of 0.03 deaths per 10^6 man-hours worked in the chemical industry.[11]

---

* Higher than the 50% assumed in Table 12 because the average age of employees would be less than that of the general population.

9. *'76 Cancer Facts and Figures.* American Cancer Society.

10. USERDA Manual, Appendix 6301 (1974).

11. *Accidental Facts.* National Safety Council, Chicago, IL (1974).

Environmental Standards for the Uranium Fuel Cycle

The EPA has issued standards[12] that limit public radiation doses caused by planned discharges from uranium fuel cycle facilities to 25 mrem/yr for the whole body, 75 mrem/yr for the thyroid, and 25 mrem/yr for other organs. The dose for the hypothetical individual receiving the maximum dose from the model FRP/MOX plant is well within this standard.

The EPA standard also limits the release of ^{85}Kr to 5×10^4 Ci, ^{129}I to 5 mCi, and transuranium (TRU) alpha emitters (half-life >1 yr) to 0.5 mCi for each gigawatt-year of electrical energy produced by the fuel cycle. A 1500-MTU/yr reprocessing plant can service spent fuel from the generation of about 50 GWe each year. The release allowed by the standard for each 50 gigawatt-years of electricity generated are compared in Table 5 with releases from the model FRP/MOX plant. As shown in the table, the assumed controls for the model plant are adequate for ^{85}Kr, but additional improvement is required for ^{129}I and TRU alpha emitters.

TABLE 5

Annual Releases of Radioactivity from the Model FRP/MOX Plant Compared to EPA Standards

	Annual Release, curies/year	
Nuclide	*EPA Standard (40 CFR 190)*[a]	*Model Plant, 1500 MTU/yr*
^{85}Kr	2.5×10^6	0.14×10^6
^{129}I	0.25	0.3
TRU Alpha Emitters	0.025	0.024

a. For generation of 50 gigawatt-years of electrical energy.

12. U.S. Code of Federal Regulations, Title 49, Part 190.

FUEL RECEIPT

SHIPPING CASK HANDLING FACILITY

The minimum size of the cask-handling facility required for the conceptual reprocessing plant has been determined. The component subfacilities listed in Table 6 would be able to process casks containing slightly more than 10 metric tons of heavy metal (MTHM) per day. Determination of facility size was based on types of existing spent fuel casks, existing or planned power-reactor cask loading capabilites, and measured cask handling times.

Design Capacity

With this facility, a reprocessing plant could receive and process daily 8 legal-weight truck casks containing 1 pressurized water reactor (PWR) assembly or 2 boiling water reactor (BWR) assemblies and 2.2 rail casks containing 7 PWR or 18 BWR assemblies (equivalent to the receipt of 30% of the fuel weight in legal-weight truck casks and 70% in rail casks).

The design capacity for receiving and placing spent fuel in storage is achieved by specifying enough subfacilities for each unloading function (Figure 1). The required number of each type of subfacility was determined by the time required for each handling operation and the capacity of the casks. The number of subfacilities should be increased if the detailed design shows that any of them might be subject to frequent or prolonged outages. This increase has already been made for the fuel unloading pools. Although only two pools are required for the design throughput, a third pool was added because of the possibility that gross contamination might occasionally require isolation of a pool.

Cask Turnaround Time

Cask turnaround experience at the West Valley Reprocessing Plant (Nuclear Fuel Services),[1,2] the Midwest Fuel Recovery Plant

1. J. R. Clark. "Modifying the West Valley Reprocessing Plant." *Nuclear Engineering International*, February 1976, p. 27.
2. K. H. Dufrane. "Design, Manufacturing, and Operational Experience with the NFS-4 Spent Fuel Shipping Cask." *Proceedings of the International Symposium on Packaging and Transportation of Radioactive Materials, Miami Beach, Florida, September 1974*, pp. 138-149.

TABLE 6

Number of Cask-Handling Subfacilities for 10 Metric Tons/Day of Spent Fuel

Operation	*Number of Subfacilities*
Preparation and Cask Offloading and Loading[a]	4
Cask Cooling and Washing	2
Fuel Unloading (Pool)	3
Cask Decontamination	3

a. Each subfacility in the Preparation Area is paired with a subfacility in the Cask Offload (Load) Area.

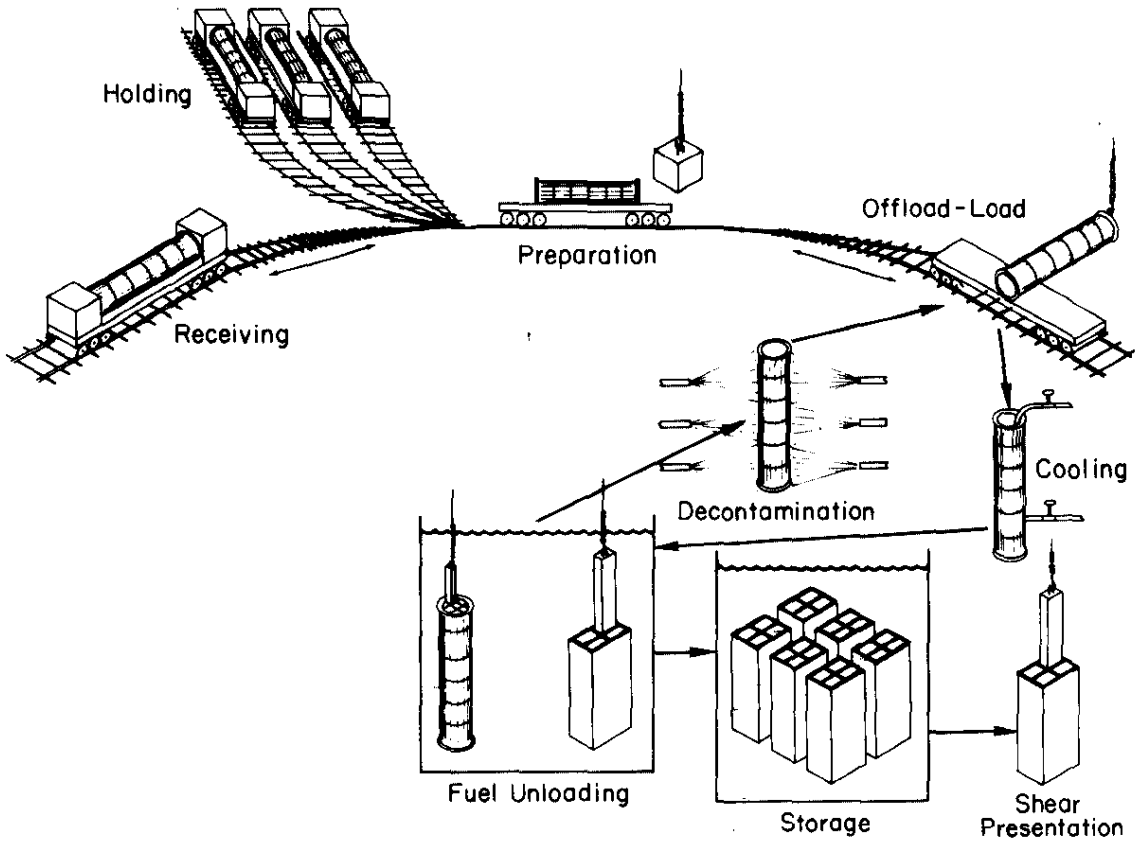

FIGURE 1. Proposed Facility for Receipt and Storage of Spent LWR Fuel

(General Electric), and Savannah River's Receiving Basin for Off-site Fuel (RBOF) varies widely (Table 7).

Nuclear Fuel Services made a special effort to reduce turn-around time at West Valley. Initially, turnaround time was much higher than the routine 4 to 8 hours achieved later.

General Electric studied the time required to process the NAC-1 type (or NFS-4) cask from the San Onofre Reactor and the Wisconsin Electric Power Company (WEPCO) Reactor. Table 8 shows their best estimate of the time required for each major operation at Midwest for a WEPCO cask shipment. The 18-hour total time is judged to be conservative, based on reports of processing the same cask in an average of 4 to 8 hours at West Valley. The Midwest times are judged to be long because the measurements were made early in their program and because they had little incentive to speed up processing. For example, General Electric did not use the protective shroud devised by Nuclear Fuel Services to minimize cask contamination in the Fuel Unloading Pool, or develop special equipment to facilitate decontamination.

The recommended conservative cask turnaround times shown in Table 8 were used to determine the number of subfacilities (cask unloading bays, decontamination pits, etc.) required to perform each function at the design throughput rate of 10 MTHM/day.

Expected Mix of Rail and Truck Casks

Three types of LWR fuel casks are presently being used (Table 9). The small legal-weight truck casks hold 1 PWR assembly or 2 BWR assemblies. Slightly larger casks hold 2 PWR assemblies or 4 BWR assemblies, but require overweight trucks. The very large casks contain 7 to 10 PWR assemblies or 18 to 24 BWR assemblies, but must be transported by rail or barge.

The number of casks to be handled at a receiving basin depends on the mix of the three types of casks. If rail casks alone were received, only 3 casks per day would deliver 10 MTHM/day. If only legal-weight truck casks were received, up to 24 casks per day would be handled.

Factors that could (but are not expected to) dictate the relative numbers of cask types include cask availability and transportation economics. However, spent fuel has a high value (about $280/kg), and transportation costs are relatively low (about $6/kg) so that transportation economics are not critical.[3]

3. *Benefit Analysis of Reprocessing and Recycling Light Water Reactor Fuel.* USERDA Report ERDA-76/121 (1976).

TABLE 7

Cask Turnaround Time Experience

Site	*Average Turnaround Time for a Legal-Weight Truck Cask, hr*
West Valley Reprocessing Plant[a]	4 to 8
Midwest Fuel Recovery Plant[b]	18 to 26
RBOF (Savannah River)	8 to 24[c]

a. Nuclear Fuel Services, West Valley, NY

b. General Electric, Morris, IL

c. The longer turnaround times generally occurred when special fuels (e.g., Hallam fuel) were handled.

TABLE 8

Recommended Cask Processing Times

Operation[a]	*Handling Time, hours, for Legal-Weight Truck Casks*[b] *Expected*	*Upper Limit*	*Rail Casks*[c] *Expected*	*Upper Limit*
Preparation, Offloading				
Cask from Vehicle	4.0	8.0	4.9	9.1
Cooling of Cask	4.0	8.0	4.9	9.1
Unloading Fuel from Cask	2.8	7.2	7.0	11.4
Decontamination of Cask	3.3	11.0	14.0	22.4
Preparation, Reloading				
Cask onto Vehicle	4.0	10.5	6.1	13.3
Total Turnaround Time	*18*	*45*	*37*	*65*

a. See Figure 1.

b. NAC-1, NFS-4, and NLI 1/2 casks (Table 9).

c. GE IF-300 cask (Table 9) for shipment by special overweight truck to nearby railhead.

TABLE 9

Status of Domestic Spent-Fuel Casks

Type Cask	*Cask Designation*	*Capacity, fuel assemblies*	*Loaded Cask Weight, short tons*	*Design License Status*	*Operational Status*
LWT[a]	NFS-4[b]	1 PWR or 2 BWR	25	Issued	2 casks in use
LWT	NAC-1[b]	1 PWR or 2 BWR	25	Issued	4 casks in use
LWT	NLI 1/2	1 PWR or 2 BWR	23.8	Issued	3 casks in use
OWT[c]	IF-200	2 PWR or 4 BWR	28	Issued	2 casks in use
OWT	TN-9	7 BWR	38	Issued	1 to 2 casks under construction
OWT	TN-8	3 PWR	38	Issued	1 to 2 casks under construction
Rail/water	IF-300[d]	7 PWR or 18 BWR	70	Issued	4 casks in use
Rail/water	NLI 10/24	10 PWR or 24 BWR	98.9	Issued	1 cask under construction and 12 casks planned

a. Legal-weight truck.

b. Identical casks with different designations by users.

c. Overweight truck.

d. The GE IF-300 cask is designed for shipment by special overweight truck to nearby railhead.

Additionally, cask procurement times (after initial licensing) are relatively short, so that supply can meet demand.

The types of casks used will probably be determined by what the reactors are capable of handling. All reactors can ship by truck cask, but not all reactors have access to railroads or barges. Table 10 shows three projections of the number that will be able to ship spent fuel by rail-type casks. According to the 1987 projection, reactors with rail access will account for 75.2% of the total fuel weight and will be distributed geographically as shown in Table 11. The trend is for newer, larger reactors to have rail access.

Required Number of Subfacilities

The minimum number of handling subfacilities of each type required to attain the desired daily throughput of 8 legal-weight truck casks and 2.2 rail casks was determined by computer simulation of the various operations. The simulation program uses a Monte Carlo technique in which a large number of casks are received at a facility with a fixed number of subfacilities. As a cask enters each subfacility, the time to process the cask in that subfacility is selected at random from a log-normal distribution of the process times shown in Table 8.

The cask throughput (at a fixed ratio of 8 lightweight truck casks to 2.2 rail casks) was determined for different numbers of subfacilities of each type. Typical results are shown in Table 12. The minimum number of subfacilities to achieve at least 10 MTHM/day throughput is shown in Case 2. The effect of the rail/truck mix is shown in Table 13.

TABLE 10

Anticipated Proportion of Reactors with Rail Access for Shipment of Spent Fuel

Year	*Reactors with Rail Access, %*
1980	56[a]
1987	73[b]
1975 to 2020	90[c]

a. *Draft Environmental Statement, Handling and Storage of Spent Light Water Power Reactor Fuel.* United States Nuclear Regulatory Commission, October 1976.

b. *U. S. Light Water Reactor Spent Fuel Cask Transportation — Status of Current Capabilities and Limitations.* Nuclear Assurance Corporation, Atlanta, Georgia (1977). Prepared at the request of the ERDA for use in conceptual design studies.

c. "Estimated % of Fuel Shipped by Rail Cask." *Transportation Accident Risks in the Nuclear Power Industry 1975-2020.* Report No. EPA-520/3-75-023. Environmental Protection Agency, Washington, DC, Office of Radiation Programs (1975).

TABLE 11

Anticipated Geographical Distribution of Reactors with Rail Access in 1987

Section of U.S.A.	*Reactors with Rail Access, %*
Midwest	92.0
West	85.0
South	76.1
Northeast	47.3

TABLE 12

Simulation Study of Size of Cask Handling Facility

Spent Fuel Receipt: 70% in Rail Casks
30% in Legal-Weight Truck Casks

	Case 1	*Case 2*[a]	*Case 3*
Number of Subfacilities for:			
Cask Preparation	12	4	4
Cash Offloading/Loading	12	4	4
Cask Cooling, Washing	6	2	2
Fuel Unloading (Pool)	6	2[b]	2[b]
Cask Decontamination	7	3	2
Capacity: Casks/day	28.4	10.6	8.5
MTHM/day	29.7	11.0	8.9

a. Minimum number of subfacilities for nominal throughput of 10 MTHM/day.

b. A third pool is recommended to allow for possible outages caused by release of radioactivity in an unloading pool.

TABLE 13

Effect of Rail/Truck Cask Mix on the Cask-Handling Capacity of a Minimum Facility[a]

	Spent Fuel Receipt, % in rail casks/ % in legal-weight truck casks			
	70/30	*65/35*	*60/40*	*50/50*
Number of Subfacilities for:				
Cask Preparation	4	5	6	6
Cask Offloading/Loading	4	5	6	6
Cask Cooling, Washing	2	2	3	3
Fuel Unloading (Pool)	2	2	2	2
Cask Decontamination	3	3	3	3
Capacity: Casks/day	10.6	11.5	13.8	14.6
MTHM/day	11.0	10.8	11.9	10.6

a. Case 2, Table 11, nominal throughput of 10 MTHM/day.

Elimination of any one subfacility would significantly decrease the throughput, as shown by Case 3 of Table 12. Conversely, Table 14 shows that addition of any one subfacility except a Preparation Area and a Cask Offloading/Loading Area would not increase throughput; an additional Preparation Area and Cask Offloading/Loading Area would increase throughput about 7%.

Conservative Assumptions

The number of subfacilities required to process casks containing 10 MTHM/day of spent LWR fuel could be determined conservatively by arbitrarily assuming more fuel would arrive by legal-weight trucks. However, there are already several conservative assumptions built into the study which are equivalent to large assumed changes in the rail/truck split. For the recommended subfacilities, these include:

- *Overweight Casks.* The analysis assumed no use of overweight trucks, which have twice the capacity of legal-weight trucks. If 1/3 of the trucks were overweight (the current mix, Table 9), the recommended facility could handle about 45% of the fuel on trucks rather than 30% as designed.

- *Cask Unloading Times.* If the 18-hour truck-cask unloading time were reduced to 12 hours (50% longer than NFS's longest reported time), the recommended facility could handle about 50% of all fuel by truck shipments.

- *Trend to Rails.* Either a delay in reprocessing or an acceleration in reactor construction will result in a larger fraction of reactors with rail access.

- *Definition of Rail Access.* The 1987 projection (Table 10) does not include five reactors that do not have railheads onsite but from which it is planned to ship a full-size rail cask on a special truck a short distance to a railhead. Also not included are three reactors with railheads onsite which would require only minor modifications for shipment of rail casks. If these eight reactors were included in the 1987 projection, the percent (by fuel weight) of reactors with rail access would have been almost 80%.

- *Attainment.* For design purposes, the attainment of the receiving facility has been assumed the same (300 days) as that of the reprocessing plant. However, because of the multiple process subfacilities, the attainment should be much higher.

TABLE 14

Effect of Additional Subfacilities on Capacity of Minimum Cask-Handling Facility

Spent Fuel Receipt: 70% in Rail Casks
30% in Legal-Weight Truck Casks

	Number of Subfacilities				
	Case 2[a]	*Case 4*	*Case 5*	*Case 6*	*Case 7*
Number of Subfacilities for:					
Cask Preparation	4	5[b]	4	4	4
Cask Offloading/Loading	4	5[b]	4	4	4
Cask Cooling, Washing	2	2	3[b]	2	2
Fuel Unloading (Pool)	2	2	2	3[b]	2
Cask Decontamination	3	3	3	3	4[b]
Capacity, casks/day	10.6	11.4	10.6	10.6	10.6

a. Minimum facility for nominal throughput of 10 MTHM/day, Table 12.

b. Number of subfacilities increased by one over the minimum required. Number of other subfacilities unchanged.

COMPUTER MODEL FOR LWR FUEL STORAGE

A computer model was developed to forecast inventories in fuel storage basins and the consequences of limited storage capacity. The forecasts are based on projections of fuel discharges and reprocessing schedules. Testing of the model has been completed: results predicted by the model agreed well with ERDA data for the cases reported in ERDA-76-25, "LWR Spent Fuel Disposition Capabilities."

The model considers the general problems of movement of material through the LWR fuel cycle.[4] This movement is impeded because the projected capacity for reprocessing spent fuel has not kept pace with the projected output of spent fuel. Until reprocessing capacity is adequate, interim storage of spent fuel is required.

4. *Savannah River Laboratory Quarterly Report, Light Water Reactor Fuel Recycle, July-September 1976.* USERDA Report, DPST-LWR-76-1-3, p. 23.

HEAD-END PROCESSES

ENCLOSED FUEL ROD SHEAR

An enclosed shear has been fabricated, tested, and installed in the high-level caves for small-scale LWR fuel reprocessing tests. The enclosed shear will retain fission gases released when irradiated fuel rods are cut so that these gases can be collected and analyzed. Measurement of fission gases released during shearing is necessary to obtain mass balances in the small-scale tests, and to provide design data for a plant-scale process.

Fuel shearing is the initial step in the chop-leach process adopted for reprocessing LWR fuel. In small-scale process tests, irradiated fuel rods are sheared before voloxidation and fuel dissolution tests. A nonenclosed shear was previously used to provide 1-inch-long fuel pieces for dissolution tests.[1]

The enclosed shear (Figure 2) is prepared for operation by placing a fuel rod segment (up to 2 feet long) in the shuttle tube and pushing a piston into the tube behind the fuel rod. Pumping air out of the enclosure causes the piston to be drawn through the shuttle tube, which positions the fuel rod underneath the shear. Hydraulic pressure from a pump located outside of the shielded cell forces a 1-inch-wide blade down onto the fuel rod until it shears. The sheared 1-inch-long piece drops into a catch pan beneath the shear (Figure 3), and the shuttle advances the remaining segment of the rod into the shear.

The shear will normally be operated under vacuum. However, other modes of operation are possible because the shuttle can be advanced mechanically or with positive pressure behind the piston.

Fission gases collected inside the enclosed shear are transferred by a series of helium purges into a 55-gallon drum which is part of a recirculating gas analysis system.

After calibration of the shear and off-gas system with radioactive tracer gases, the shear will become an integral part of equipment used in LWR fuel reprocessing tests.

---

1. *Savannah River Laboratory Quarterly Report, Light Water Fuel Recycle, October-December 1976.* USERDA Report DPST-LWR-76-1-4, p. 29.

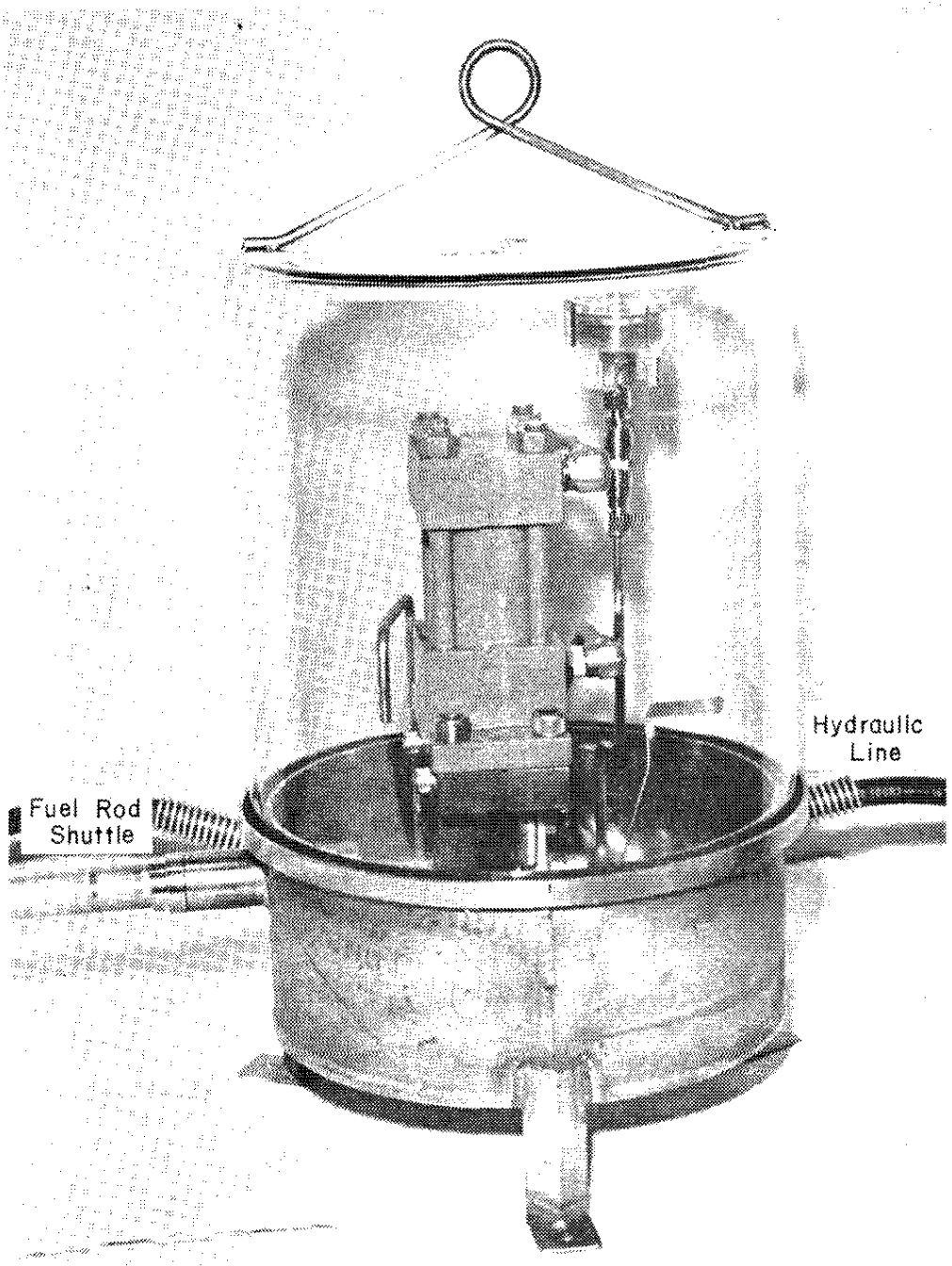

FIGURE 2. Fuel Rod Shear in Gas-Tight Enclosure

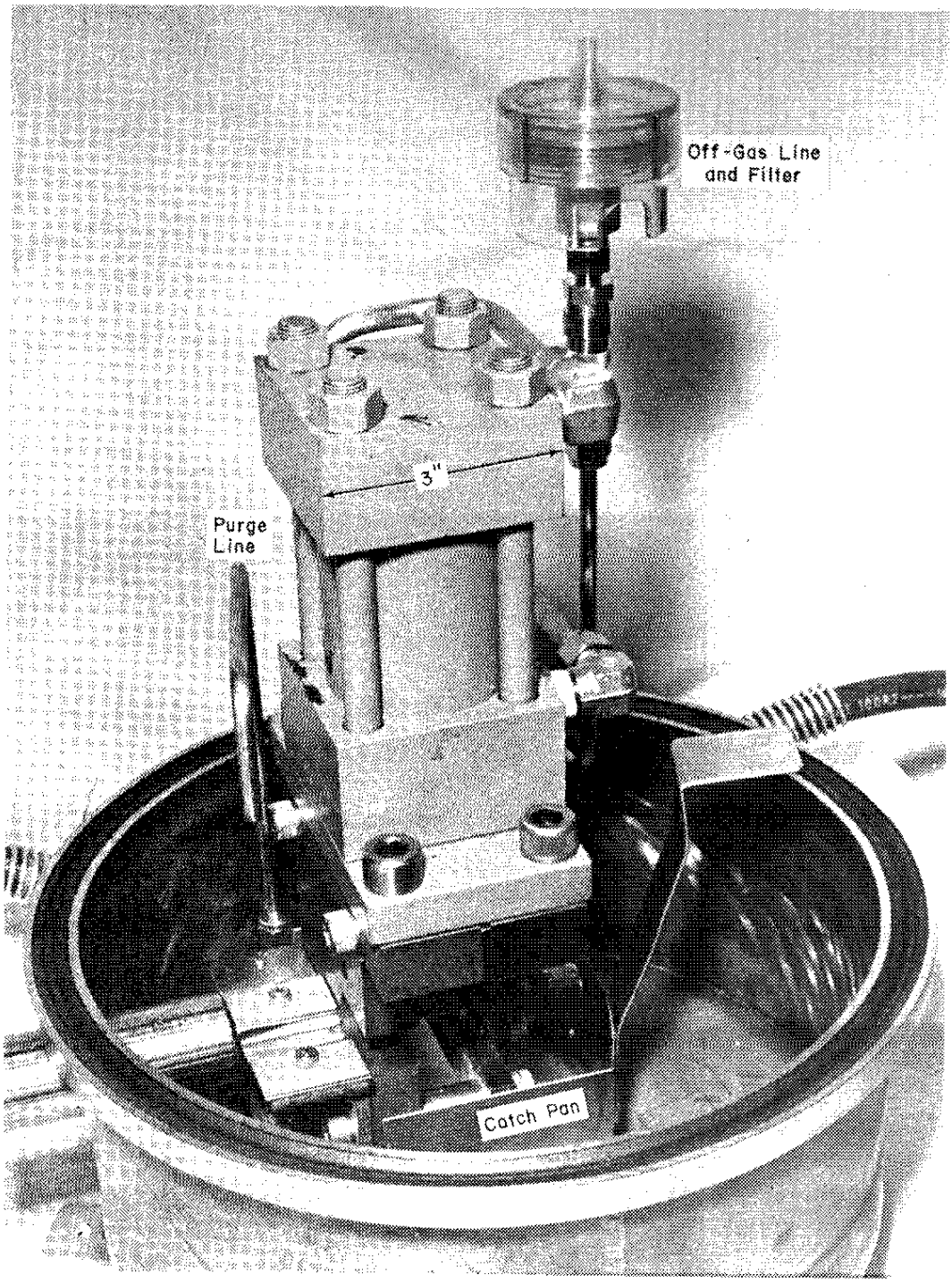

FIGURE 3. Details of Fuel Rod Shear

METALLURGICAL SUPPORT OF CHOP-LEACH PROCESSING

Continuing studies of the effect of chop-leach processing on H. B. Robinson 2 fuel showed that after voloxidation, the Zircaloy-2 cladding was quite ductile and could be flattened without fragmentation to prepare hulls for disposal. Examination of unirradiated UO_2 core material by scanning electron microscopy showed that porosity causes the regions of varied appearance previously reported.[2]

The structure of the UO_2 core, the metallurgical properties of the cladding during chop-leach processing, and the long-term compatibility between the Zircaloy hulls and cement are being evaluated for several types of LWR fuel tubes. This work will (1) characterize irradiated UO_2 cores, (2) help control potential hazards associated with processing Zircaloy (UZr_3 and Zircaloy fines), and (3) evaluate the long-term integrity of the Zircaloy hull-cement waste form. A previous report[2] summarized examination of H. B. Robinson 2 fuel for UZr_3, characterization of the structure of the UO_2 core, evaluating the effect of shearing on the Zircaloy cladding, and qualitative bend tests of the cladding.

Examination of H. B. Robinson 2 fuel will continue when the voloxidation apparatus is available in the high level caves. Meanwhile, fuels from the Vallecitos Boiling Water Reactor and the Saxton Nuclear Experimental Reactor Project are being examined.

Fractography of H. B. Robinson 2 Cladding

Zircaloy-2 cladding from unirradiated and irradiated H. B. Robinson 2 fuel was fractured by flattening ring sections (or bending half-ring sections) cut from the fuel. All fractures occurred at the 180° bends. Fractured cladding was examined by metallographic sectioning and by scanning electron microscopy of fracture surfaces. Cladding from both irradiated and unirradiated fuel was fractured before and after heating to voloxidation temperature. Also, the unirradiated cladding was fractured after an actual voloxidation treatment.

Unirradiated Zircaloy-2 Fractured Before Heating

The fracture surface of unheated, unirradiated cladding exhibited both ductile and cleavage features (Figure 4). The areas of cleavage were generally associated with small secondary

---

2. *Savannah River Laboratory Quarterly Report, Light Water Reactor Fuel Recycle, January-March 1977.* USERDA Report DPST-LWR-77-1-1, p. 19.

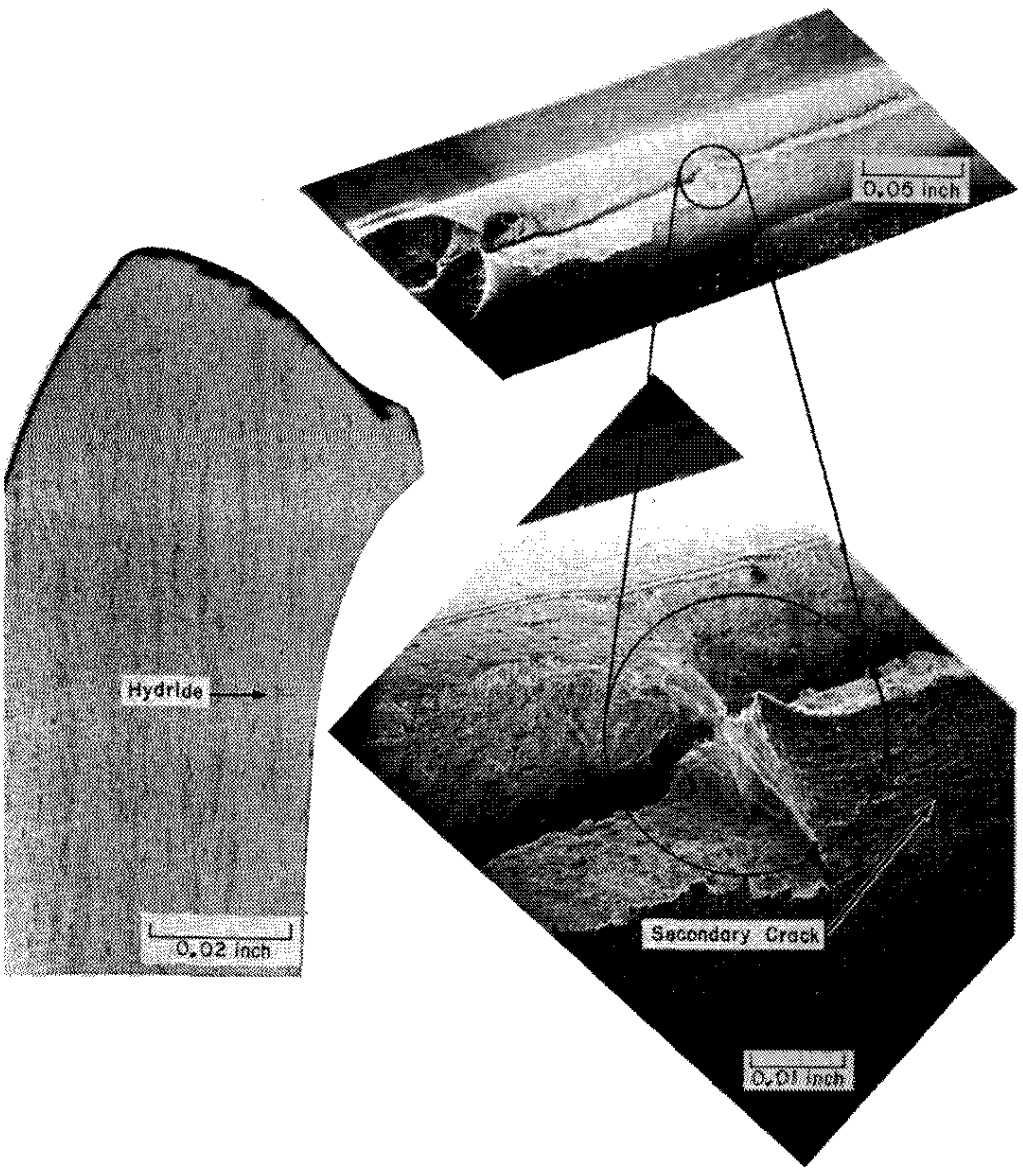

FIGURE 4. Unirradiated Zircaloy-2 Fractured Before Heating

cracks. Hydride platelets, oriented generally in a circumferential direction, were observed metallographically. The cracks occurred at these platelets.

Unirradiated Zircaloy-2 Fractured After Heating

Unirradiated cladding heated at 500°C for three hours in a muffle furnace to simulate voloxidation conditions fractured in a uniformly ductile manner (Figure 5). The heating dissolved the hydrides, and evidently the air cooling prevented reprecipitation.

Similarly, unirradiated cladding that had been through the actual voloxidation step (500°C for four hours with 3-hour cooling) in the SRL voloxidizer fractured in a very ductile, uniform manner as indicated by the fine dimples (Figure 6). This material was so ductile that the main fracture did not extend through the entire cladding thickness. Much smaller hydride particles were found; however, these particles appear to be arranged randomly in contrast to the aligned platelets in the cladding before heating. Apparently the cooling was slow enough to allow the hydrides to reprecipitate. Secondary cracks did not form on these smaller particles.

Irradiated Zircaloy-2 Fractured Before Heating

Unheated, irradiated Zircaloy-2 cladding (Figure 7) fractured like unheated, unirradiated Zircaloy-2 cladding, by ductile fracture and cleavage. The fracture surface, however, contained more pronounced irregularities. A metallographic section through the specimen showed that the unheated, irradiated Zircaloy-2 specimen contained more hydride platelets than the unheated unirradiated specimen, that they were oriented circumferentially, and that fracture had occurred away from the main fracture along the hydride platelets. Fracture in this manner could produce undesired Zircaloy fines.

Irradiated Zircaloy-2 Fractured After Heating

Irradiated cladding that had been heated in a muffle furnace at 500°C for three hours and air cooled also fractured in a uniformly ductile manner (Figure 8). The fracture was similar to that of the heated, unirradiated cladding (Figure 5). No hydride particles were found. Although cladding from voloxidized irradiated fuel was not examined, it is expected to fracture like unirradiated cladding after voloxidation. These fractures appeared to be sufficiently ductile that little, if any, fragmentation is expected either during shearing or during compaction to prepare hulls for disposal.

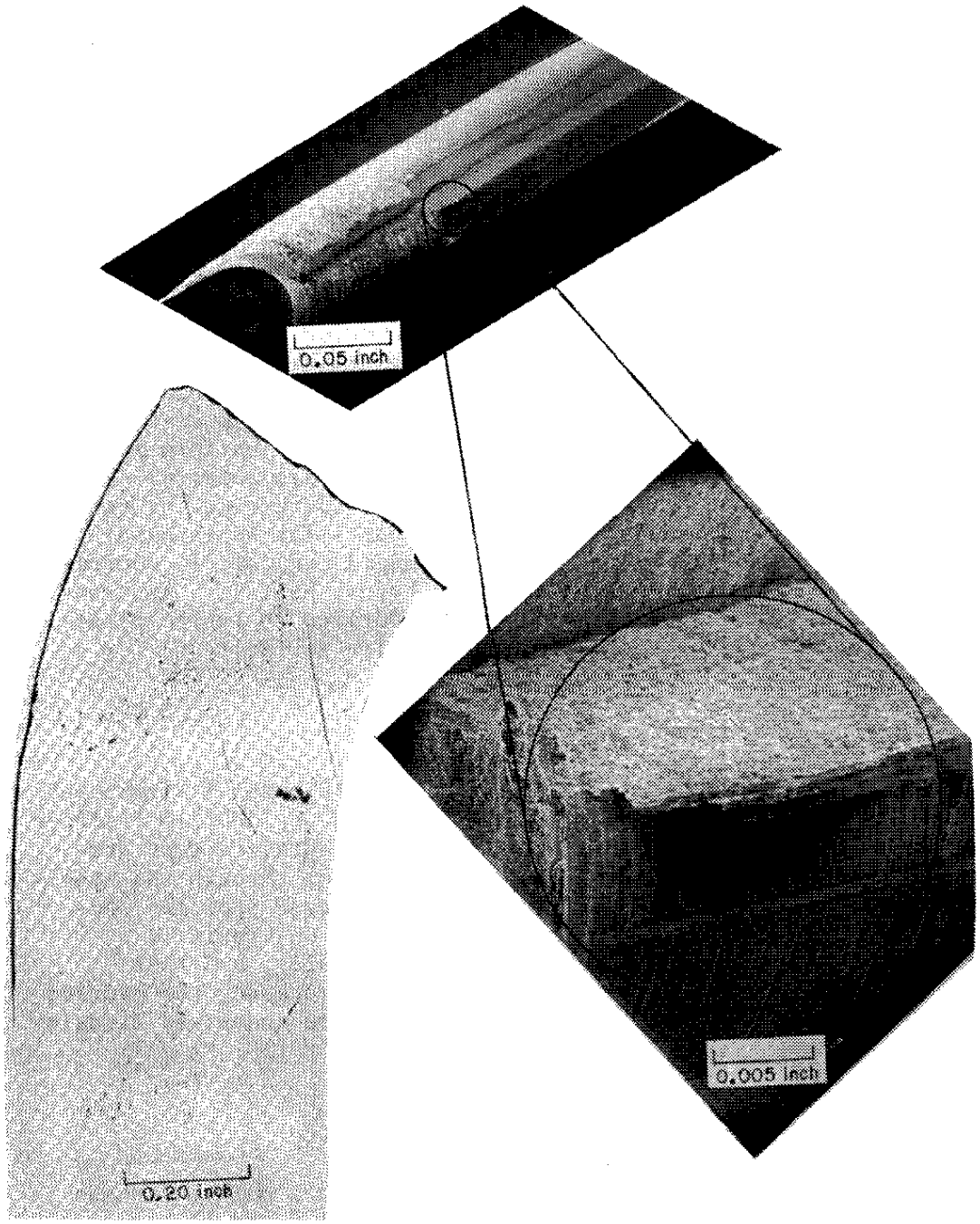

FIGURE 5. Unirradiated Zircaloy-2 Fractured After Heating

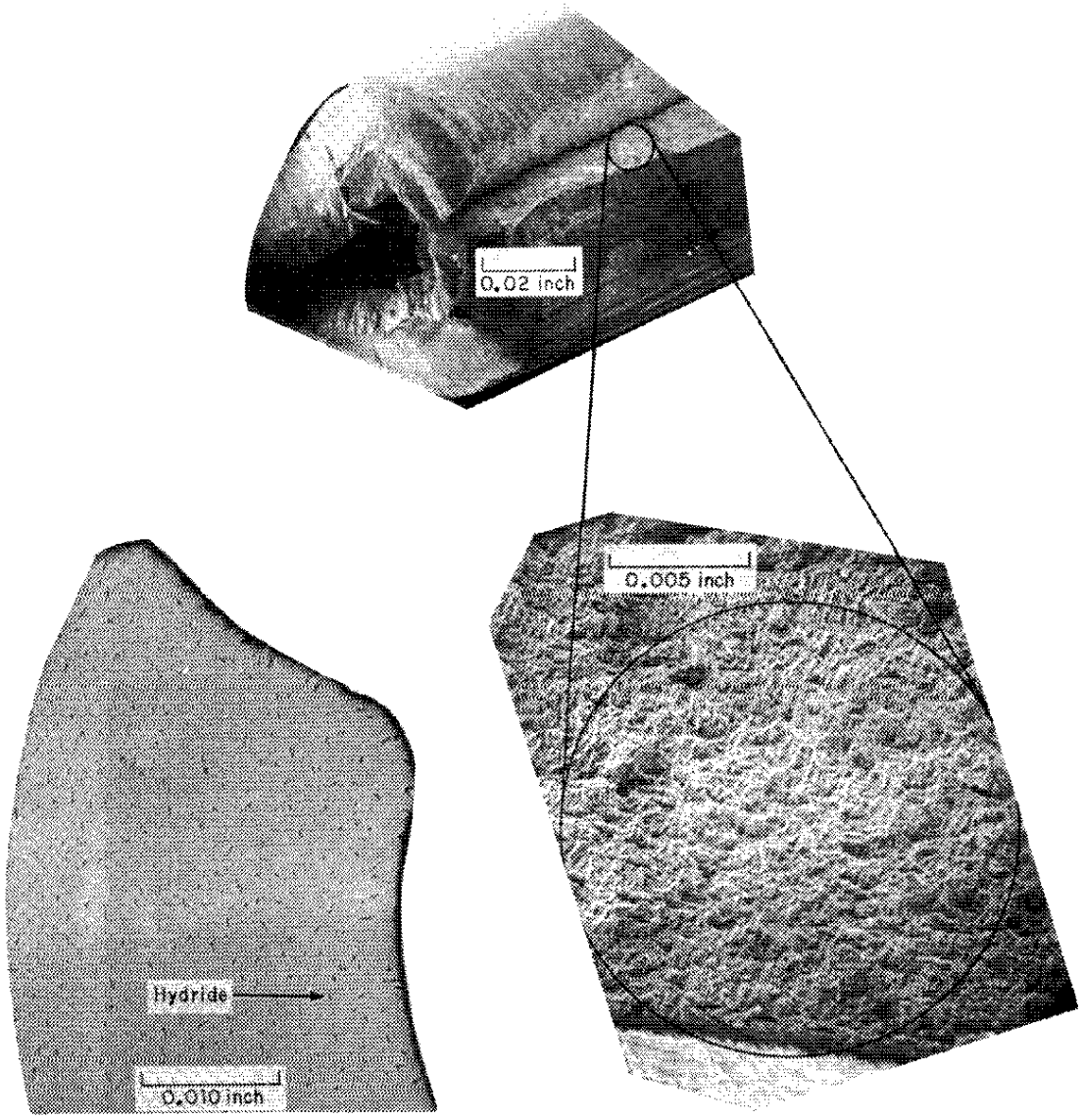

FIGURE 6. Unirradiated Zircaloy-2 Fractured After Voloxidation

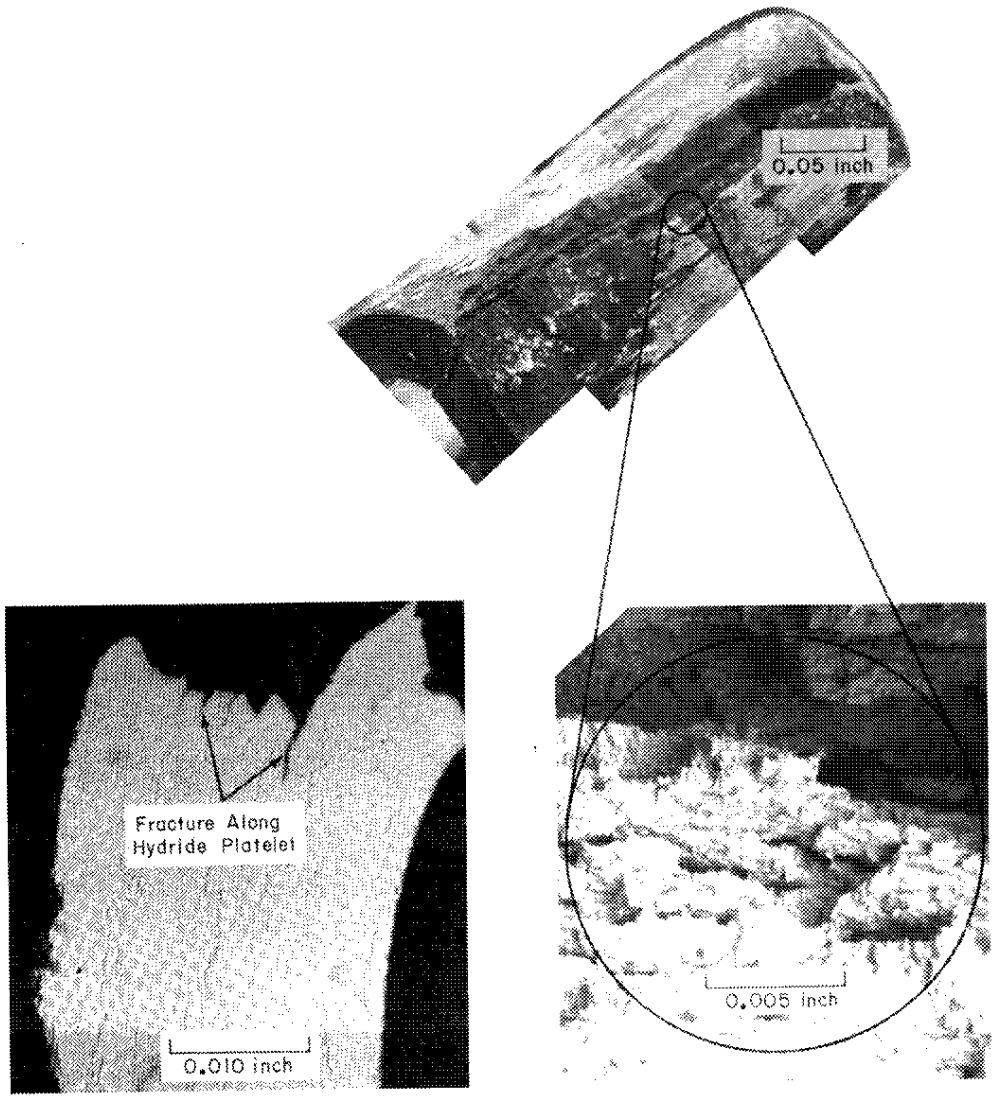

FIGURE 7. Irradiated Zircaloy-2 Fractured Before Heating

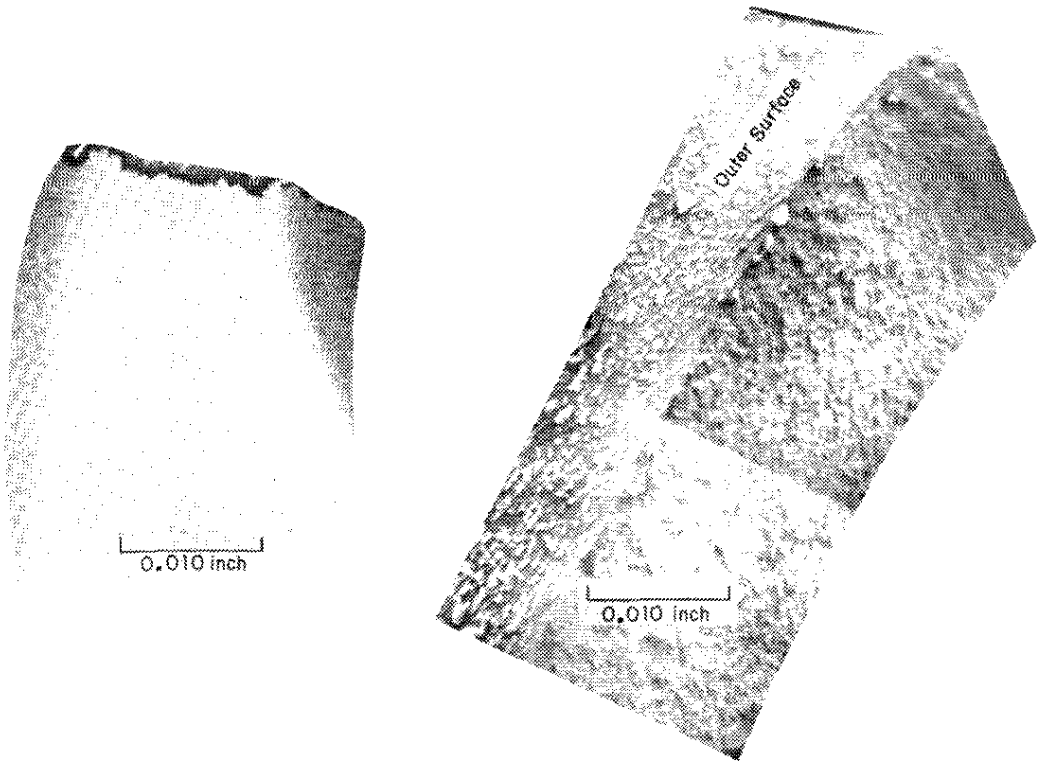

FIGURE 8. Irradiated Zircaloy-2 Fractured After Heating

Structure of the H. B. Robinson 2 UO_2 Core

The UO_2 core of the unirradiated fuel was composed of two different looking regions of approximately equal area. The regions were especially well delineated by polarized light (Figure 9). Only one phase, UO_2, was revealed by x-ray diffraction analysis. Scanning electron microscopy examination showed that the varied appearance is caused by differences in porosity.

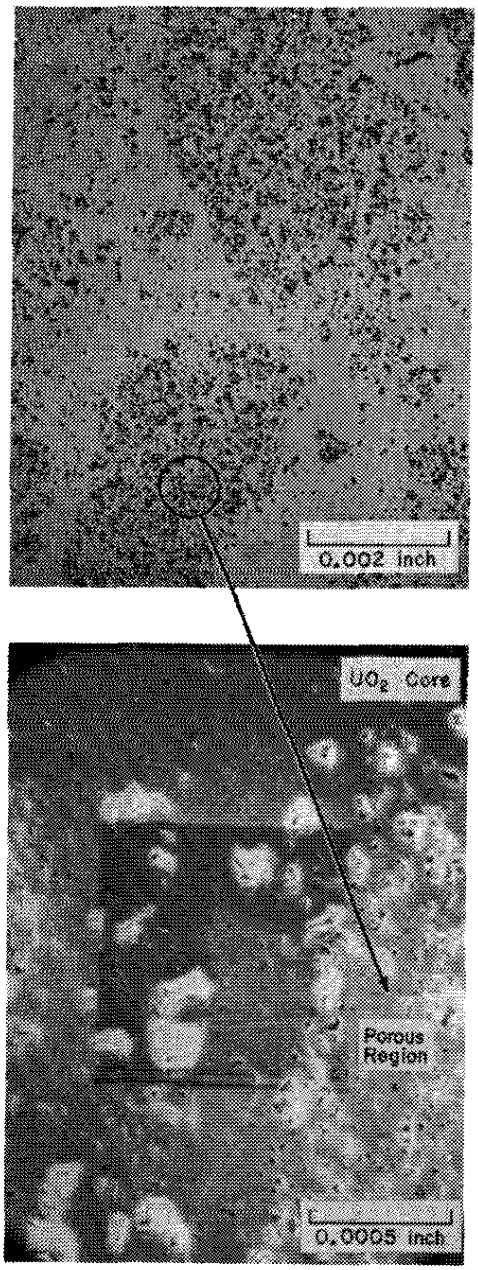

FIGURE 9. Areas in H. B. Robinson 2 Caused by Porosity

VOLOXIDATION TESTS

A voloxidizer-dissolver has been built and installed in the high level caves for small-scale fuel reprocessing tests. The equipment was tested with unirradiated fuel before installation, and with irradiated fuel after installation. With this equipment, sheared pieces of fuel are heated to volatilize tritium and oxidize UO_2 to U_3O_8 and then are dissolved in nitric acid. Fission gases released during voloxidation and dissolution can be measured quantitatively.

Voloxidation is a candidate process for removal of tritium from irradiated power reactor fuel. Preliminary tests at ORNL[3,4] have shown that up to 99% of the tritium remaining in sheared fuel can be removed by voloxidation. As a head-end reprocessing step, voloxidation would permit recovery of tritiated water in concentrated form, thus avoiding isotopic dilution by normal water during dissolution of the fuel. In voloxidation, sheared fuel pieces react with oxygen at about 500°C, to convert UO_2 to U_3O_8. The reaction dislodges fuel from the cladding, greatly increases the surface area of the fuel, and is expected to evolve the tritium quantitatively. Although some iodine and noble gases are also volatilized, voloxidation is considered exclusively as a method of tritium control.

As part of the SRL program,[5] voloxidation will be studied with a variety of fuels and process conditions. In a preliminary test,[6] H. B. Robinson 2 fuel was voloxidized in a laboratory muffle furnace.

---

3. J. H. Goode. *Voloxidation-Removal of Volatile Fission Products from Spent LMFBR Fuels*. USAEC Report ORNL-TM-3723. Oak Ridge National Laboratory, Oak Ridge, TN (1973).

4. *Aqueous Fuel Reprocessing Quarterly Report for Period Ending March 31, 1973*. USAEC Report ORNL-TM-4240, p. 12 (1973).

5. *Savannah River Laboratory Quarterly Report, Light Water Reactor Fuel Recycle, April-June 1976*. USERDA Report DPST-LWR-76-1-2, p. 9.

6. *Savannah River Laboratory Quarterly Report, Light Water Reactor Fuel Recycle, January-March 1977*. USERDA Report DPST-LWR-77-1-1, p. 26.

Voloxidizer-Dissolver Design

Figures 10 and 11 show the assembled voloxidizer-dissolver and the gas control manifold. The voloxidizer-dissolver is suspended from a shaft mounted through two support bearings so that the entire device can be tilted. Three positions are used: vertical for fuel dissolution; tilted 17° above horizontal (Figure 10) for voloxidation; and tilted below horizontal (until the stirring motor touches the tray) to discharge acid and hulls. Electrical service, coolant, and off-gas lines are mounted along the support shafts (Figure 11). The unit was designed to be operated and serviced remotely.

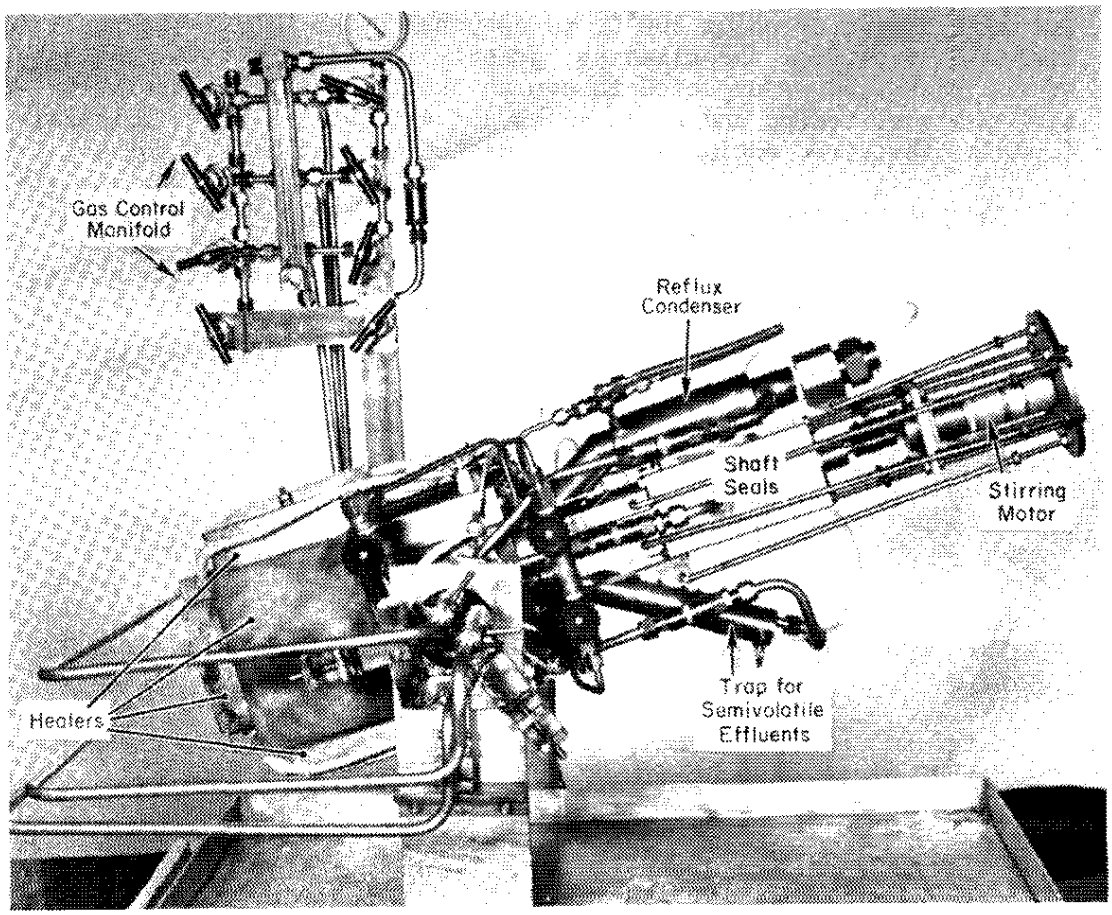

FIGURE 10. Voloxidizer-Dissolver in Tilted Position for Voloxidation -- Front View

Temperature Control

Voloxidation and dissolution will take place in a 4-inch-diameter, 2-liter cavity, which was cut into a 10-inch-long by 6-inch-square stainless steel block. The block and lid contain twelve thermocouple wells so that a complete temperature profile can be obtained. Temperatures are displayed on a 15-point chart recorder.

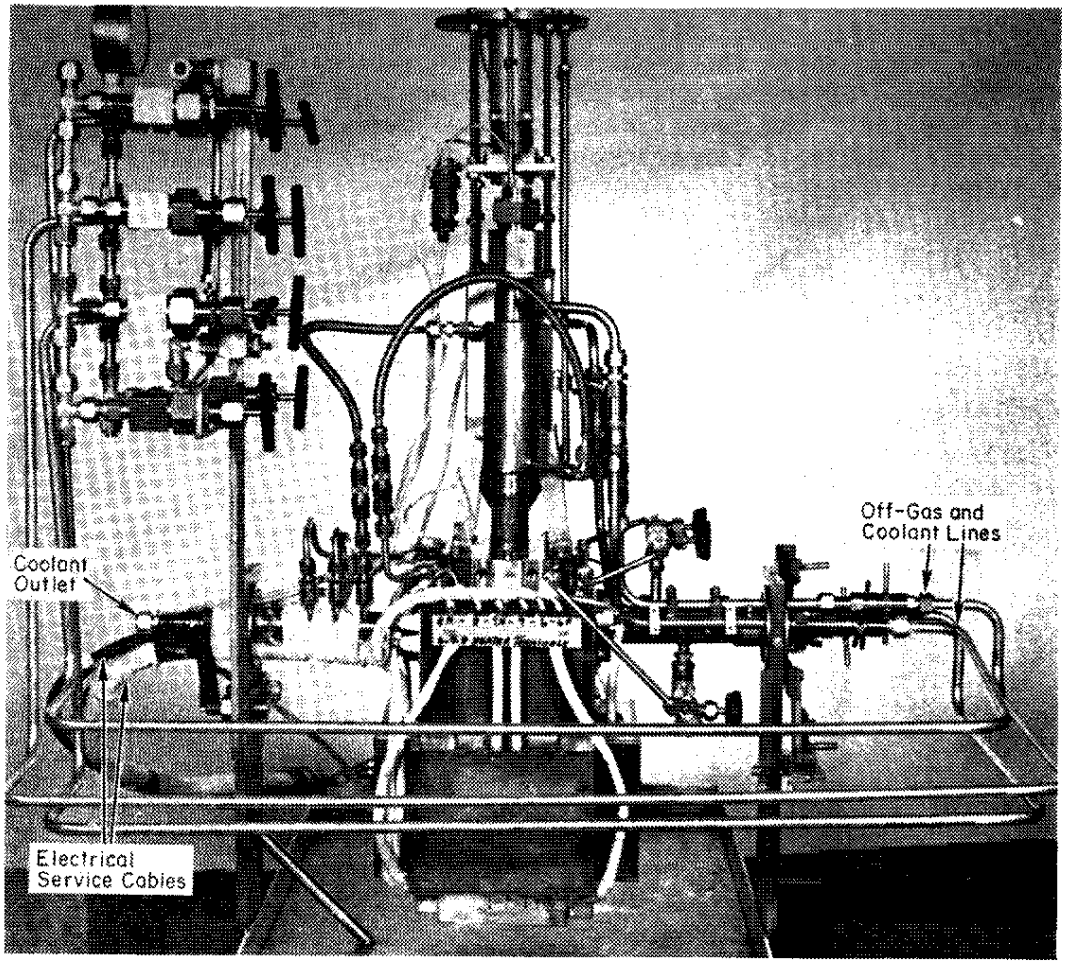

FIGURE 11. Voloxidizer-Dissolver in Vertical Position for Fuel Dissolution — Side View

The bottom of the block is heated by nine electric heaters. Four ring-type electric heaters are mounted on the sides of the block, and a fifth is mounted underneath. These outside heaters (Figure 10) are covered with protective metal shields. Four cylindrical heaters are inserted in holes drilled down in the four corners of the block. About 4 kw (total) of power can be supplied to the nine heaters; about 2 kw will maintain the voloxidizer at 500°C, the nominal voloxidation temperature.

The voloxidizer is cooled by three helical coils around the inside of the 10-inch-deep cavity (Figure 12). The top coil cools the upper 2 inches, the middle coil cools the central 6 inches, and the lower coil cools the bottom 2 inches. Compressed air passing through the upper coil during voloxidation prevents the lid from exceeding about 250°C, to protect the O-ring that seals the lid. The lower coils are used during fuel dissolution to control the acid temperature. Air or water can be used as a coolant.

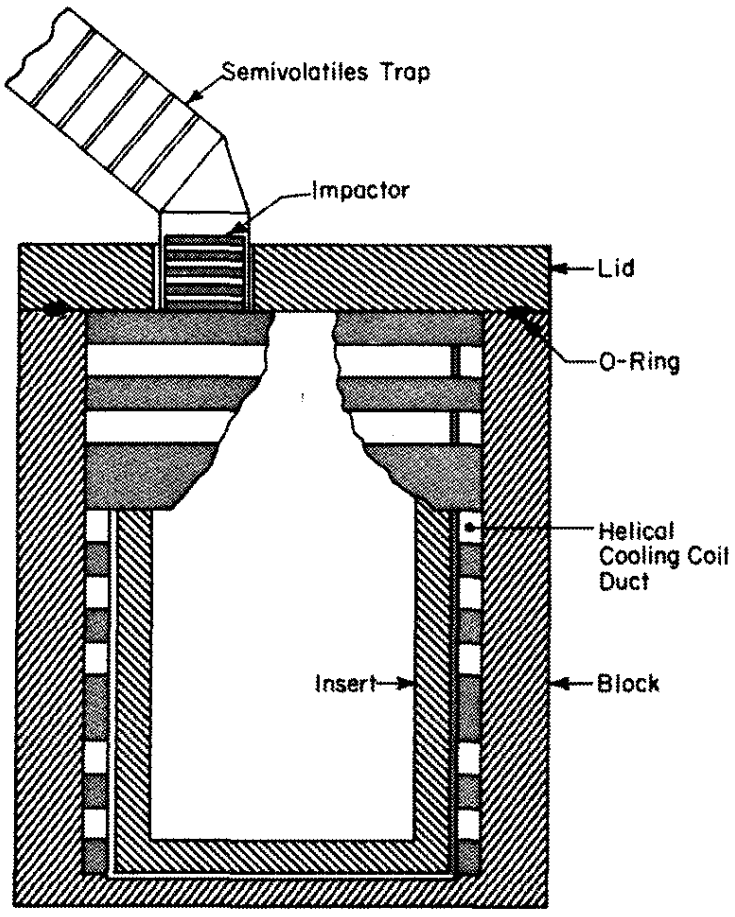

FIGURE 12. Section of Voloxidizer-Dissolver

Fuel Bed Agitation

A typical voloxidation test requires ten fuel rod pieces about 1 inch long and 1/2 inch in diameter. During voloxidation, fuel is dislodged from the cladding so that a heterogeneous bed of powder, fuel pieces, and hulls results. A motor-driven agitator, which has two stirring rods (Figure 13), produces a tumbling action in the bed when the voloxidizer is operating in the tilted position (Figure 10).

Because of the heterogeneity of the bed, the agitator was carefully designed to prevent jamming. Hulls are particularly prone to jam because of their jagged edges produced by shearing the irradiated Zircaloy.[1] To help prevent jamming, the upper parts of the stirring rods were wound into springs to allow the rods to flex past obstructions. If spring action does not clear an obstruction, a current monitor interrupts power to the driver motor. The motor is manually reversed and restarted to clear the obstruction.

The drive motor and shaft seals are well above the heated block (Figure 10) to protect them from overheating.

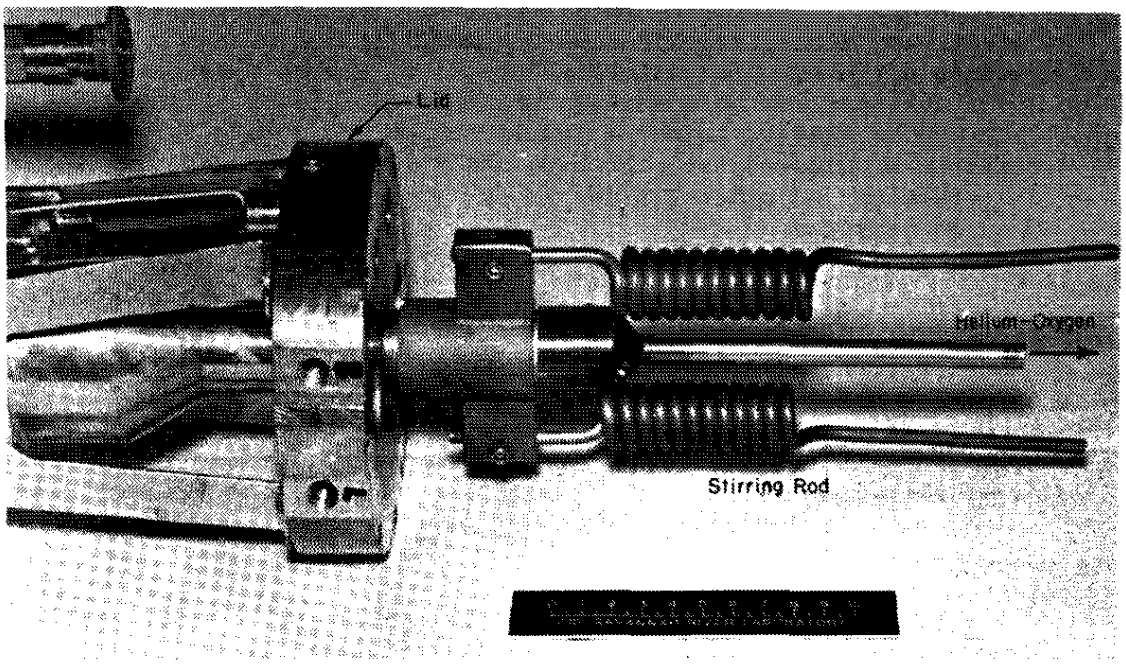

FIGURE 13. Fuel-Bed Agitator

Off-gas Control and Analysis

The voloxidizer-dissolver is part of a closed, recirculating gas-handling system, which also includes the enclosed shear and a series of fission gas traps. The recirculating gas will be typically 80% helium - 20% oxygen. Helium functions both as a carrier for fission gases released during voloxidation and dissolution, and as an inert diluent for oxygen to retard oxidation during voloxidation. Excessively fast oxidation could sinter the UO_2 and inhibit tritium release, or could cause zirconium fines to ignite.

The helium-oxygen mixture enters the voloxidizer through the hollow shaft of the agitator (Figure 13) and flows over the UO_2 bed and out through the semivolatiles trap (Figure 10). During dissolution, off-gas exits through a reflux condenser (Figure 10). A 20-psig pressure relief valve on the condenser prevents the voloxidizer from overpressurizing.

The following devices collect fission gases, semivolatile fission products, and particulates evolved during voloxidation and dissolution.

Voloxidizer Insert. Data from ORNL[4] show that ruthenium volatilized during voloxidation may adhere preferentially to the hottest surfaces. To test this effect, a removable stainless steel cylinder can be inserted into the voloxidizer (Figure 12). Fuel can be charged into the insert and voloxidized. The insert can then be removed, and the U_3O_8 and hulls discharged. The quantity of ruthenium and other fission products deposited in the insert can then be measured.

Semivolatiles Trap. Fission products such as cesium may deposit at lower temperatures than those in the insert. To trap these effluents (Figures 10 and 12), a 1-inch-diameter tube containing a stack of ten 1/2-inch-wide stainless steel rings is mounted on the lid of the voloxidizer. The temperature drops from 200°C at the lid to 70°C at the last ring. After voloxidation, each ring is leached in acid. Analysis of the leachant solutions will determine the amount of each fission product deposited as a function of temperature.

For dissolution tests, the semivolatiles trap is replaced with a connector which allows (1) charging the unit with acid, (2) sparging the U_3O_8-acid mixture, and (3) sampling the mixture. The opening for the semivolatiles trap is also used for charging fuel pieces into the voloxidizer and for discharging hulls and acid without removing the insert.

Impactor. An impactor for trapping particles carried in the off-gas is mounted in the base (hottest part) of the semivolatiles trap (Figure 11). The impactor, a set of stainless steel disks drilled through with various sized holes, will provide data on the quantity and size distribution of particles entrained in the off-gas.

Iodine Traps. Heated silver-zeolite traps for collecting iodine are located (1) immediately downstream from the semivolatiles trap, and (2) on the gas control manifold. The former iodine trap is used during voloxidation, and the latter during dissolution. (Neither of these traps is shown in the photograph.) The silver-zeolite traps must be near the voloxidizer to obtain quantitative iodine release data.

Tritium, Krypton-85, and Carbon-14 Traps. HTO is collected with a molecular-sieve trap in series with either silver-zeolite trap, in the shielded cell containing the voloxidizer. HT, ^{85}Kr, ^{14}CO, and $^{14}CO_2$ are carried in the recirculating helium-oxygen stream to a gas-handling system outside of the shielded cell. HT, ^{14}CO, and $^{14}CO_2$ are collected for analyses in separate molecular-sieve traps. ^{85}Kr is measured by on-line gamma-ray counting of the recirculating stream.

Tests with Unirradiated Fuel

Proper operation of the voloxidizer was verified in bench top tests using clad, unirradiated UO_2 fuel segments. The voloxidizer was heated to 500°C while a mixture of 80% He - 20% O_2 flowed through the unit at 1.5 L/min. The gas was not recirculated. Stirring speed was about 15 rpm. Test results showed that:

- The UO_2 in a bed of ten 1-inch-long by 1/2-inch-diameter fuel segments can be oxidized to U_3O_8 in about four hours.
- When the heater power is set, the voloxidizer temperature will remain steady.
- The agitator will jam occasionally, but it is readily freed by reversing the motor. Jamming will be frequent if the bed contains more than 15 fuel pieces.
- More than 90% of the resulting U_3O_8 particles are 1.5 to 15 microns in diameter (Figure 14).
- Enough U_3O_8 dust was carried in the off-gas to cover the disks in the impactor.
- Voloxidation did not affect the Zircaloy hulls.

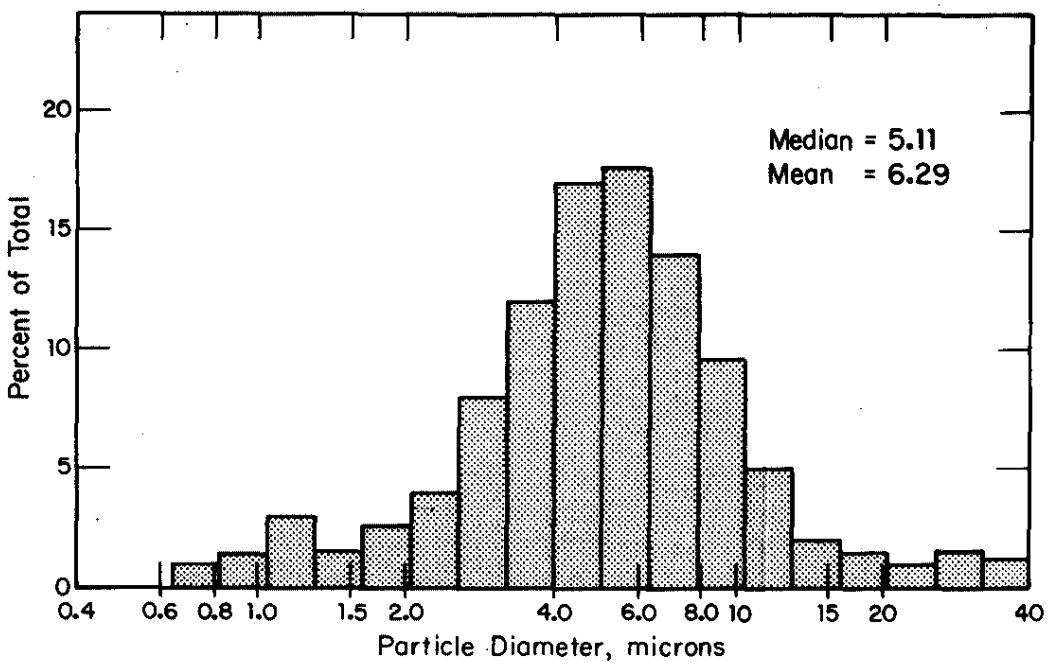

FIGURE 14. U_3O_8 Particle Size Distribution by Coulter Counter

In one test, two hulls each contained a fuel pellet that resisted oxidation. Surface analysis did not reveal why those pellets resisted oxidation. Oxidation resistance is not expected in irradiated pellets because they will be extensively fractured.

Test With Irradiated Fuel

The new voloxidation equipment was operated successfully in the high level caves with irradiated LWR fuel. The first test demonstrated the equipment under actual operating conditions and with previously characterized H. B. Robinson 2 fuel fragments without cladding. Off-gases including tritium were trapped and analyzed. This section summarizes ^{3}H, ^{14}C, and ^{85}Kr evolution and characterization of the U_3O_8 product.

Voloxidizer and Off-Gas Equipment

The voloxidizer is coupled to off-gas handling equipment both inside and outside the shielded cell, as shown schematically

in Figure 15. Helium carrier gas recirculates through the closed system, and oxygen is added as it is consumed in the voloxidation reaction. ^{85}Kr is measured by on-line gamma counting; the other fission gases are collected in a series of molecular-sieve traps for later analyses. Particulates in the off-gas are sorted by particle size and collected on impacter plates[7] at the mouth of the voloxidizer. Semivolatiles such as cesium, antimony, and ruthenium are expected to plate out along a temperature-gradient tube following the impacter. A molecular-sieve trap for HTO and a silver-zeolite trap for iodine are closely coupled to the voloxidizer to ensure quantitative recovery. In a hood outside the shielded cell, other traps collect $^{14}CO_2$, ^{14}CO, and HT; an oxidizing bed of CuO at 300°C is provided to convert the latter two species to collectable forms. Nonradioactive carrier gases are added to the system to promote trapping of each species. Before the first voloxidation with irradiated fuel, the off-gas system was tested and calibrated with tracer amounts of radioactive gases.

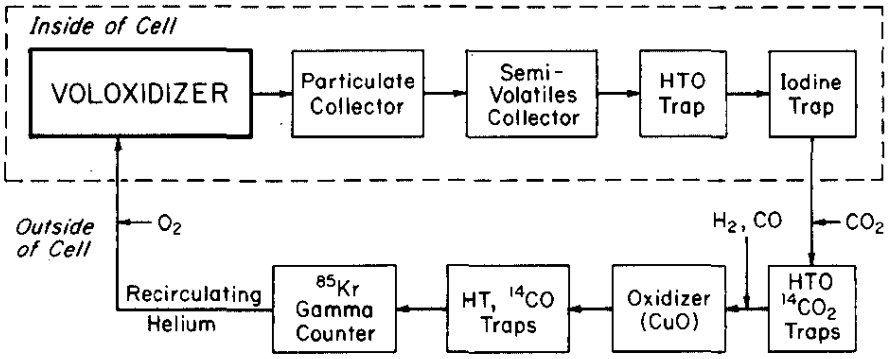

FIGURE 15. Voloxidizer Off-Gas System

Experimental Procedure

For the voloxidation test, 166.5 g of irradiated UO_2 fragments without cladding were charged to the voloxidizer. Properties of the H. B. Robinson 2 fuel have been given previously.[8]

---

7. *Savannah River Laboratory Quarterly Report, Light Water Reactor Fuel Recycle, October-December 1976.* USERDA Report DPST-LWR-76-1-4, p. 31.

8. *Savannah River Laboratory Quarterly Report, Light Water Reactor Fuel Recycle, July-September 1976.* USERDA Report DPST-LWR-76-1-3, p. 32.

The fragments were from Rod A-1 of the B-05 assembly and had ∿31,500 MWD/MTU maximum burnup. Fresh molecular sieves were installed in each off-gas trap. The system was tested for leak-tightness, and then filled with 0.8 atm of helium and 0.2 atm of oxygen. Oxygen content of the recirculating gas was monitored periodically with an in-line oxygen analyzer.

The test was begun by turning on heater power to the voloxidizer and simultaneously starting the various off-gas systems. In about one hour, the voloxidizer reached 490°C and then was held at this temperature for four hours. The rotary agitator operated at 4 rpm throughout the test. When evidence of oxygen comsumption was noted, as the temperature approached 490°C, oxygen was added to the system at 45 mL/min for the remainder of the test. The system was cooled overnight, reheated, and water vapor was introduced to ensure complete trapping of HTO.

At the completion of the test, the voloxidizer was disassembled; the product was removed, examined, and sampled. Product weight, powder density, and particle-size fraction larger than -325 mesh were measured. The molecular-sieve traps, iodine trap, particulate collector, semivolatiles collector, and voloxidizer liner were removed for subsequent analyses.

Off-Gas Analysis

Analyses of the off-gas traps for tritium and ^{14}C and the measurement of ^{85}Kr at maximum buildup are given in Table 15. Table 16 compares these results with results from a similar voloxidation experiment at ORNL,[9] with measurements from dissolution of unvoloxidized fuel at both SRL[8] and ORNL,[10] and with values calculated by the ORIGEN code.[11]

For tritium, the amount evolved is in excellent agreement with the ORNL voloxidation result, but is somewhat lower than the dissolution measurements, which in turn are lower than the calculated values. The differences between the voloxidation and dissolution results may be due to incomplete evolution of tritium during voloxidation or to experimental uncertainties in both types

---

9. *LWR Fuel Reprocessing and Recycle Program. Quarterly Report for Period January 1 to March 31, 1977.* USERDA Report ORNL/TM-5864, p. 2-32 (1977).

10. *LWR Fuel Reprocessing and Recycle Program. Quarterly Report for Period October 1 to December 31, 1976.* USERDA Report ORNL/TM-5760, p. 30, 33 (1977).

11. *ORIGEN - The ORNL Isotope Generation and Depletion Code.* USERDA Report ORNL-4628 (1973).

of measurement. Previous results[6] showed that very little tritium remained in the U_3O_8 product. Tritium lost as HT during fuel rod cutting and storage of the UO_2 fragments, and tritium trapped in the cladding, would not have been measured in the present test.

Total ^{14}C evolved also is in excellent agreement with the ORNL voloxidation results, but is only 28% of the dissolution measurement. Incomplete evolution of ^{14}C during voloxidation appears to be the most probable reason for the difference.

TABLE 15

Tritium, ^{14}C, and ^{85}Kr in Voloxidizer Off-Gas

Nuclide	*Activity, dis/min*
Tritium	4.17×10^{10}
^{14}C	2.15×10^{7}
^{85}Kr	$(5 \pm 3) \times 10^{10}$

TABLE 16

Comparison of Measured Activities in Voloxidizer Off-Gas with Other Measurements and Calculated Values

	Activity, Ci/MTU		
	^{3}H	*^{14}C*	*^{85}Kr*
Voloxidation off-gas			
Present SRL measurement	128	0.066	153 ±92
ORNL measurement[a]	128	0.066	581
Unvoloxidized fuel dissolution			
SRL measurement[a]	242	-	-
ORNL measurement[a]	312	0.24	-
ORIGEN calculation[b]			
From fission	470	-	7082
From activation	450	0.534[c]	-

a. Not adjusted for decay of about 6%/yr for ^{3}H and ^{85}Kr (negligible for ^{14}C).

b. For H. B. Robinson 2 fuel with 30,745 MWD/MTU burnup, cooled 3.1 yr.

c. Typical calculation for 20 ppm ^{14}N, neglecting ^{17}O contribution.

^{85}Kr evolved during voloxidation was ∿2% of the calculated value in the SRL test and 8% in the ORNL test. These results suggest that significant amounts of noble gases may have been lost when the fuel rods were cut and in subsequent handling and storage. Fuel fragments for the SRL test were stored after cutting about a year longer than those used in the ORNL test. Incomplete evolution of ^{85}Kr during voloxidation also is possible.[3]

Test Results

Parameters measured as a function of time during the test are shown in Figure 16. After initial warmup, the temperature of the reaction chamber was held at 490 ±5°C throughout the test. The rate of oxygen addition was sufficient to hold the oxygen content at 4.5% for much of the test. About double the stoichiometric amount of oxygen was consumed; the extra oxygen most likely regenerated the CuO bed. The buildup of ^{85}Kr in the system was easy to measure and provided a convenient method to monitor the course of the reaction. Evolution of ^{85}Kr began during the warmup period and continued throughout the first 3 hours at 490°C; no further evolution of ^{85}Kr was observed in the last hour of heating. The steady-state count rate corresponds to (23 ±14) × 10^{-3} Ci of ^{85}Kr.

Properties of the voloxidized fuel are given in Table 17. As shown in Figure 17, the product is a fine black powder characteristic of complete conversion to U_3O_8. Yield was calculated assuming pure UO_2 starting material; it was not corrected for ∿4% burnup of the uranium. This correction would increase the calculated yield. 99.6% by weight of the product has particle size smaller than 44 μm (-325 mesh). The minimum density of unpacked powder for the voloxidized product is 2.5 g/cm^3, or 30% of the crystallographic density.

TABLE 17

Properties of Voloxidized H. B. Robinson 2 Fuel

	Measured	*Calculated*	*Yield*
UO_2 fuel voloxidized	166.5 g	-	-
Voloxidized product	172.8 g	<173.1 g	>99.8%
Weight gain	6.3 g	<6.6 g	>95%
Larger than -325 mesh	0.7 g	-	0.4%
Powder density of product	2.5 g/cm^3	8.3 g/cm^3	30%

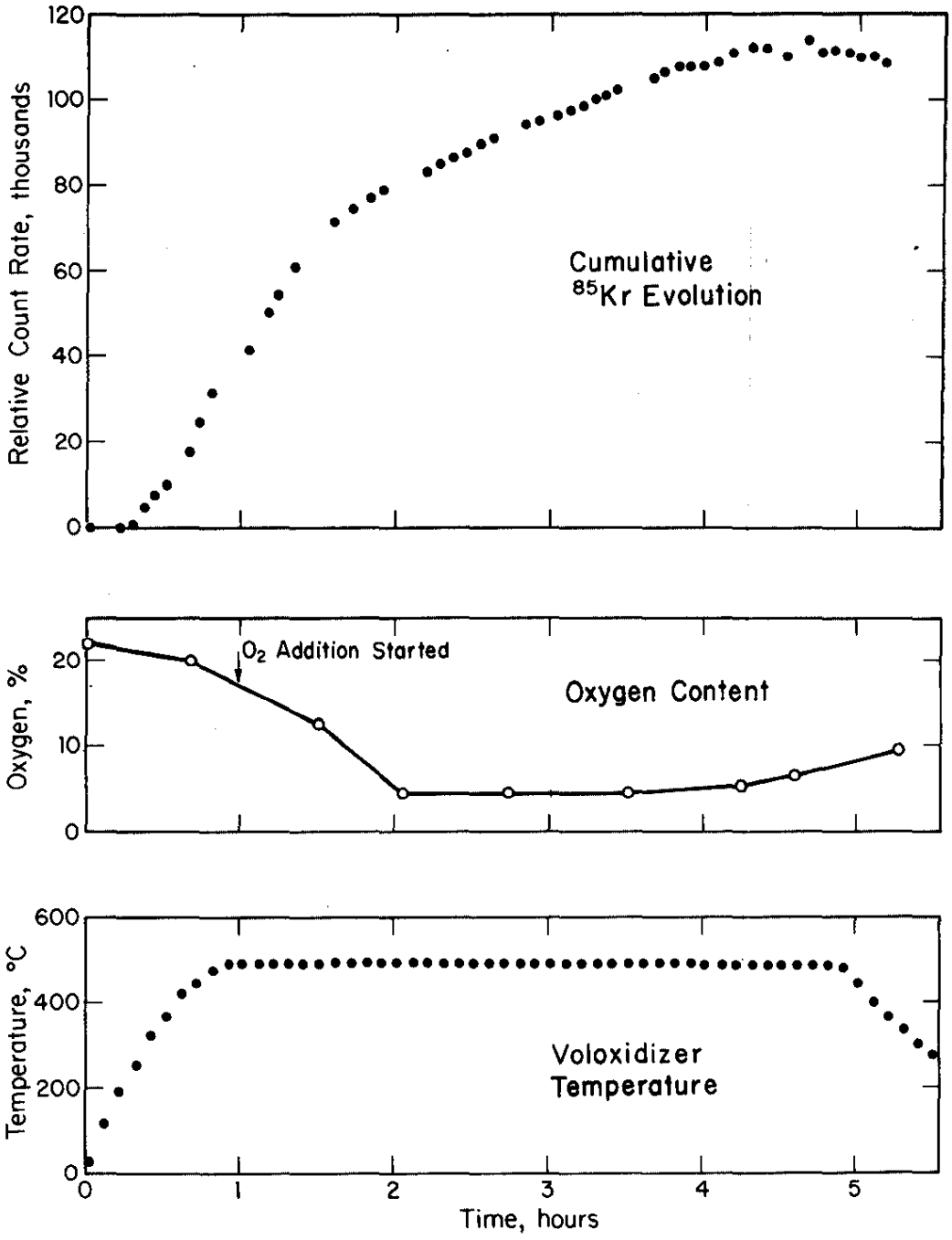

FIGURE 16. Voloxidation Test Measurements

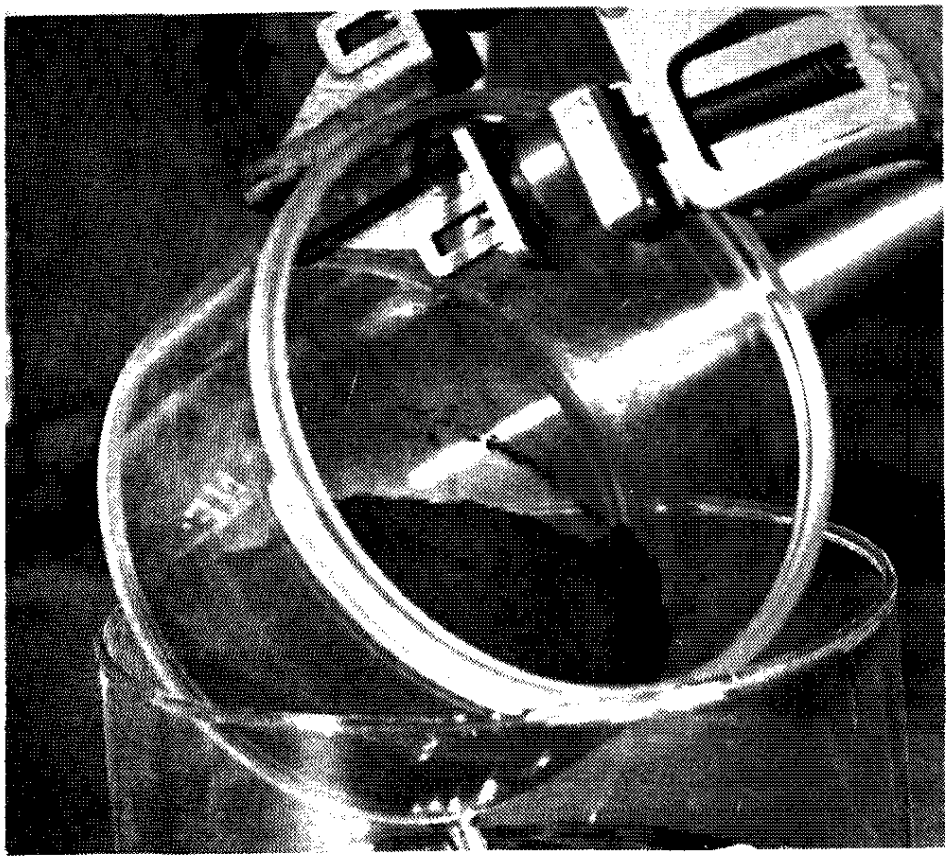

FIGURE 17. Voloxidation Product

Experimental Program

The amount of tritium remaining in the U_3O_8 product is of particular interest. The product will be dissolved to determine ^{3}H, ^{14}C, ^{85}Kr, and ^{129}I remaining after voloxidation. The dissolution will provide a test of the metal equipment in the dissolving mode and will provide additional feed for solvent extraction studies. Laboratory techniques are being developed for removing ^{129}I from silver-zeolite traps for analysis. Ruthenium and other fission products plating out on the semivolatiles collector and the liner are being determined.

Future voloxidation tests will use sheared pieces of clad fuel, initially from the Saxton reactor. Process parameters to be studied include fuel burnup, reaction temperature, oxygen content, effect of agitation, and fuel piece length. New statistical techniques will be applied to optimize experimental design, based on the accumulated data from previous tests.

Continuing Study

The SRL overall experimental program will provide:

- Experience with a wide variety of actual, irradiated LWR fuel.
- Basic chemical data for understanding voloxidation.
- Engineering data to supplement current technical data.

Other data needed to design a plant-scale process will be developed by studies of:

- Release of ruthenium, which could plug filters and provide an unwanted heat source.
- Volume of particulates carried in the off-gas.
- Reactivity of Zircaloy hulls and fines.
- Effect of voloxidation on subsequent reprocessing steps.

Voloxidizer data will be used for a parametric study of tritium release as a function of:

- Fuel Burnup
- Fuel Type
- Reaction Temperature
- Oxygen Concentration
- Bed Agitation
- Fuel Piece Length

EXAMINATION OF LWR FUELS

Metallographic studies of irradiated, Zircaloy-clad LWR fuels showed that high-burnup fuel from the Saxton Nuclear Experimental Reactor* Project contains an unidentified layer, which may be UZr_3, a hazardous unstable intermetallic compound. The presence of UZr_3 would require that this fuel be processed in a HNO_3-HF dissolver rather than the SRP electrolytic dissolver. No evidence of UZr_3 was found in Vallecitos Boiling Water Reactor (VBWR) fuel, which is therefore considered processable in the SRP electrolytic dissolver.

VBWR fuel is slightly enriched uranium as UO_2; Saxton fuel is natural uranium as UO_2 mixed with PuO_2. The VBWR fuel had been irradiated to 5,900 MWD/MTU; the Saxton fuel to 44,800. Both fuels were examined for the epsilon phase of the U-Zr system, UZr_3, which can form in Zircaloy-clad uranium oxide fuels when the core and cladding are in physical contact at temperatures above 350°C. UZr_3 has been known to react vigorously, and even explosively, in HNO_3 solution. UZr_3 is insoluble in HNO_3, but will dissolve in HNO_3 + HF. Thus, hazardous amounts could accumulate in an electrolytic dissolver where fluoride cannot be used because it corrodes the electrodes. In shear-leach dissolver operations, UZr_3 is a potential hazard during shearing, hull handling, and hull disposal.

VBWR fuel was studied to confirm earlier experimental and theoretical studies which show that UZr_3 is not present in the fuel. The required minimum temperature (350°C) for UZr_3 formation was not attained during fabrication, irradiation, or storage. The current study of VBWR fuel is applicable to both the Alternate Fuel Cycle Technologies and the program to determine which fuels stored in the Receiving Basin for Offsite Fuel (RBOF) are processable in SRP equipment. VBWR fuel currently occupies about 2.5 of the storage rows in RBOF.

Saxton fuel was studied because some Saxton assemblies in RBOF with mixed-oxide cores had been irradiated to very high burnups. Mixed-oxide fuels are not proposed for processing at SRP because PuO_2 in these fuels requires fluoride for dissolution, and because electrolytic decladding would be necessary. This study is applicable at SRP only to the extent of indicating whether UZr_3 might be present in the high-burnup, Zircaloy-clad UO_2 fuels in RBOF. This study is also pertinent to reprocessing of LWR and breeder fuels by the shear-leach method (page 28).

---

* Pressurized Water Reactor.

Experimental Method

Short sections (<0.5 inch) of each fuel were mounted and vacuum impregnated with epoxy resin (Figure 18). After grinding and polishing, the samples were examined on the metallograph.

VBWR Results

The VBWR core material was severely cracked, and some oxide fell out when the rod was cut. A section of the oxide is missing from the sample (Figure 18); some of the cracks in the core are wide enough to be visible at low magnification.

The gap between the core and cladding was examined at 500X around the entire core circumference. The gap is continuous and varies from about 1.2 to about 2.5 mils wide (Figure 19). No evidence of any layer on the inner surface of the cladding or on the core was found. The layer of ZrO_2 on the cladding, reported previously,[12] was not found.

Saxton Results

The Saxton UO_2-PuO_2 also had cracks, but a sample was mounted without loss of core material. Under high magnification, the Saxton fuel differed from VBWR fuel. There is a layer of material 0.25 mil thick on the inner surface of the cladding (Figure 20). This layer is composed of two parts. There is not as wide a core-cladding gap in the Saxton fuel as in VBWR fuel.

Studies are continuing to determine whether the layer is UZr_3.

---

12. C. J. Baroch, et al. *Comparative Performance of Zircaloy and Stainless Steel Clad Fuel Rods Operated to 10,000 MWD/T in the VBWR.* USAEC Report GEAP-4849 (1966).

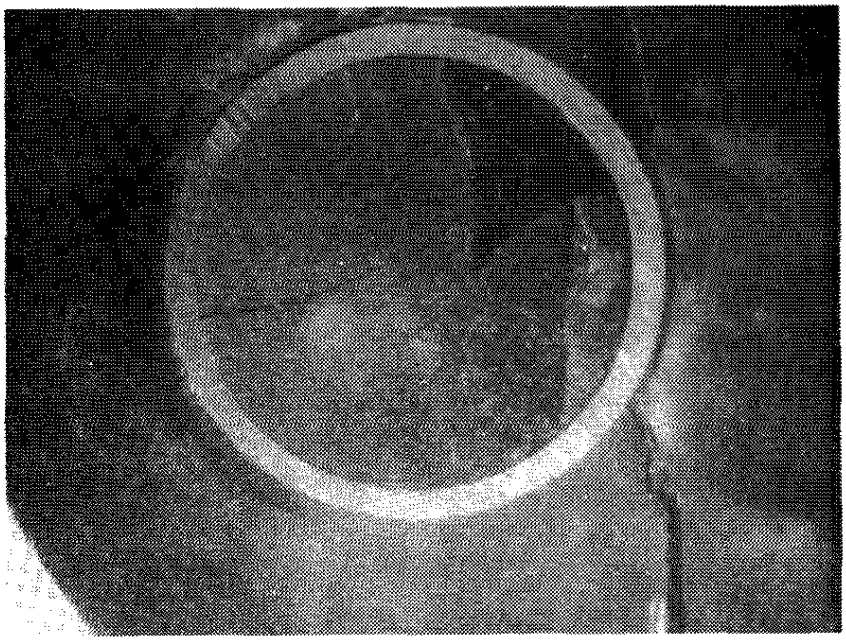

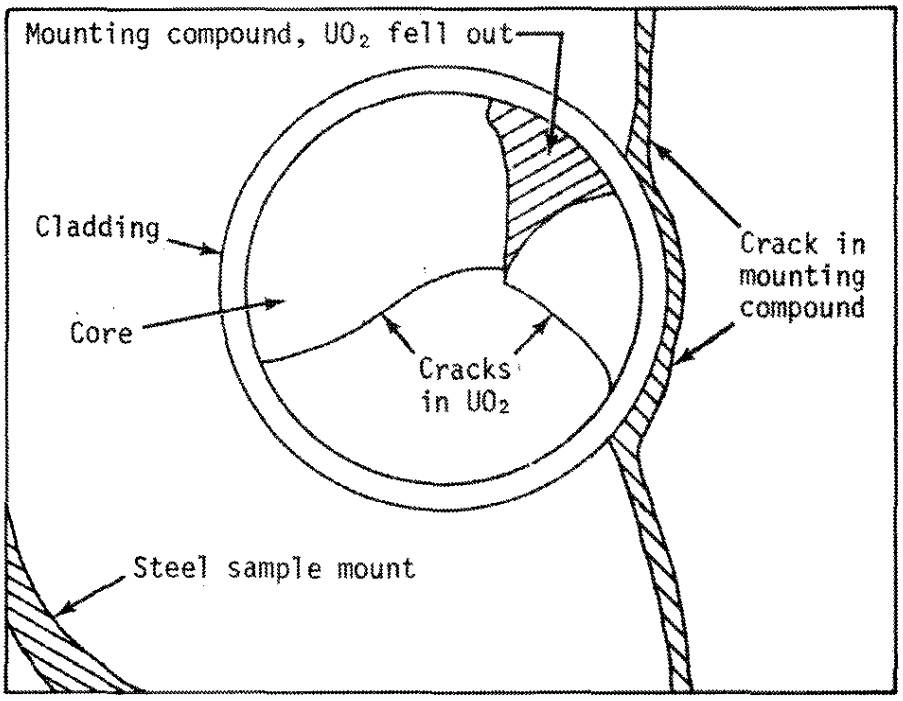

FIGURE 18. Mounted VBWR Specimen
(Magnification: 8X, OD: 0.32 inch)

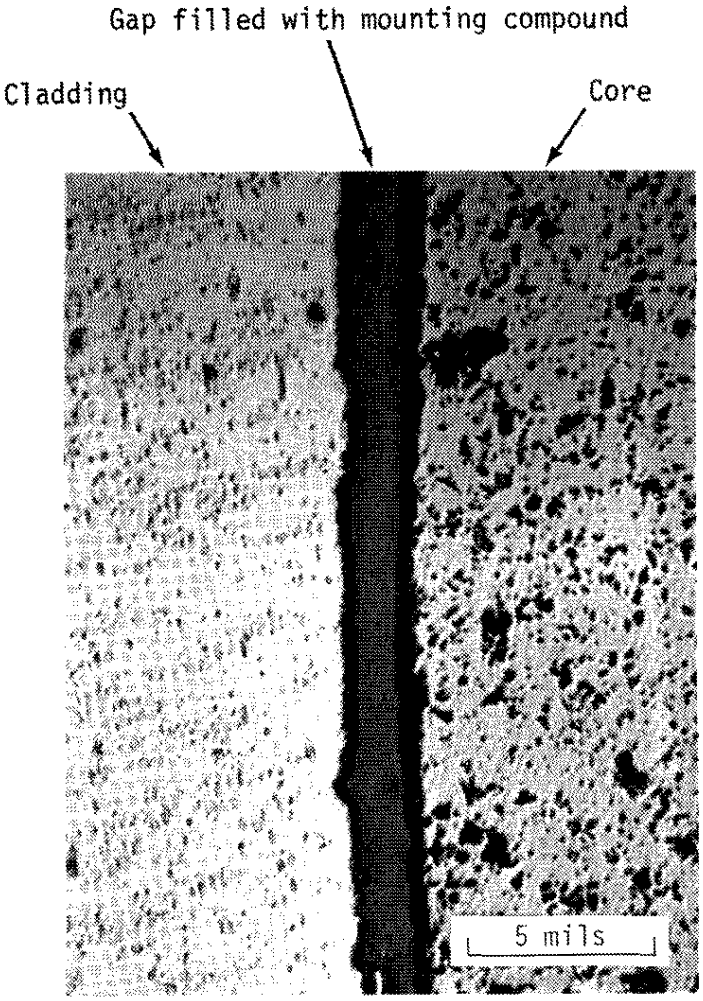

FIGURE 19. VBWR Core-Cladding Interface

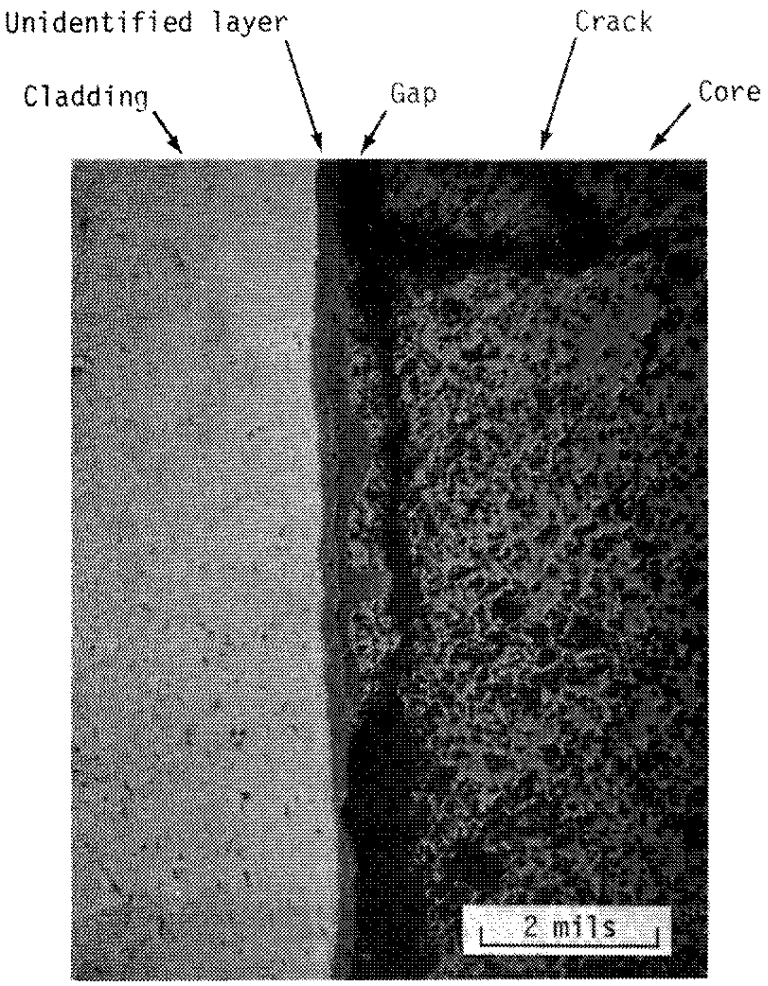

FIGURE 20. Saxton Core-Cladding Layers

DISSOLUTION TESTS WITH OCONEE 1 FUEL

Dissolution tests were continued with Zircaloy-4-clad Oconee 1 reactor fuel to demonstrate dissolution behavior of UO_2 fuel. The Oconee 1 fuel was irradiated to a lower burnup (about 10,000 to 14,000 MWD/MTHM) than the H. B. Robinson 2 fuel (about 19,000 to 28,000 MWD/MTHM) reported previously.[1,6,8] The tests showed that:

- The UO_2 dissolution rate for Oconee fuel is similar to that of Robinson 2 fuel.
- The weight of insoluble fission product residue collected from Oconee 1 and high burnup Robinson 2 fuel dissolutions is approximately proportional to fuel burnup.

Description of Oconee 1 Fuel

A Zircaloy-4-clad Oconee 1 fuel rod was received from Oak Ridge National Laboratory (ORNL) in nine segments, each about 16.5 inches long. Data characterizing the irradiated fuel were supplied by Babcock and Wilcox. The UO_2 fuel rod (No. 47108) was irradiated in Fuel Assembly 1A16 in the Oconee 1 reactor during Cycle 1 operation and discharged in October 1974. Initial uranium enrichment was 2 atom % ^{235}U. A gross gamma scan of a fuel rod in an assembly position symmetric to the received fuel rod was used to determine the peak power position along the rod. Isotopic analysis from a sample taken at that position indicated a peak fuel burnup of 13,900 MWD/MTHM for the Oconee 1 fuel. Total fuel rod length was 150 inches with a fuel column length of 143.1 inches.

Fuel Shearing

A 16.5-inch segment of the fuel rod was sheared to provide fifteen one-inch pieces for fuel dissolution studies. The chosen segment occupied a position measuring from 83.5 to 100 inches from the bottom of the fuel rod as placed in the reactor. The single pin shear equipment has been described previously.[1] The fuel rod was in a vertical position during shearing. Cutting pressures were between 450 and 950 psig. Deformation of the cut ends was minimal (<20% closure).

The total weight of UO_2 was 274 g. About 39% of the UO_2 was dislodged from the cladding during shearing. With Robinson 2

fuel, a similar fraction (~43%) was dislodged. However, the fuel was not dislodged uniformly from each cladding piece; one piece was visually observed to be free of fuel, but all other pieces contained some fuel.

Dissolution Test

Equipment and procedures for the dissolution test have been described previously.[1,6,8] Experimental conditions (Table 18) approximated those in the conceptual process for dissolution. Eleven one-inch pieces containing UO_2 fuel were randomly chosen from the sheared fuel batch. About 25% of the total UO_2 had to be added as unclad fragments to make up the desired weight of UO_2 for the test. The clad pieces were placed in a stainless steel screen basket to facilitate removal of the spent hulls after dissolution. The UO_2 fragments were added to the bottom of the reaction kettle. The metered 10M HNO_3 charge was begun immediately after adding the initial 3M HNO_3 charge to the fuel. The solution was not heated above ambient temperature until ninety minutes after the dissolution procedure was started.

Dissolution Rate

The dissolution rate for the Oconee 1 fuel (Figure 21) is about the same as that for clad UO_2 fuel from the H. B. Robinson 2 reactor (~19,000 MWD/MTHM).[1] Thus, the UO_2 fuel dissolution rates

TABLE 18

Fuel Dissolution Conditions

	Oconee 1	*Robinson 2*[a]
Total Fuel Charge, g[b]	224.0	202.3
UO_2 Charge, g	~185.0	~169
3M HNO_3 Volume, mL	192	170
10M HNO_3 Volume, mL	250	220
10M HNO_3 Meter Rate, L/min per liter of 3M HNO_3 charge	0.019	0.020
Final Solution Volume, mL	~430	~400
Final HNO_3 Concentration, M	3.45	2.63
Final Uranium Concentration, g/L	380	344
Gross Alpha Activity, dis/(min)(mL)	1.0×10^9	2.8×10^9

a. Run 4 in Reference 1, ~19,000 MWD/MTHM burnup.

b. Includes Zircaloy-4 cladding.

were independent of fuel burnup in the range investigated (10,000 to 30,000 MWD/MTHM). The dissolution rate for unclad Robinson 2 UO_2 fuel fragments in one test (Run 3 in Reference 2; ∿28,000 MWD/MTHM) was somewhat higher. However, this was probably because of a higher initial solution temperature (∿45°C) and higher exposed fuel surface area rather than higher fuel burnup.

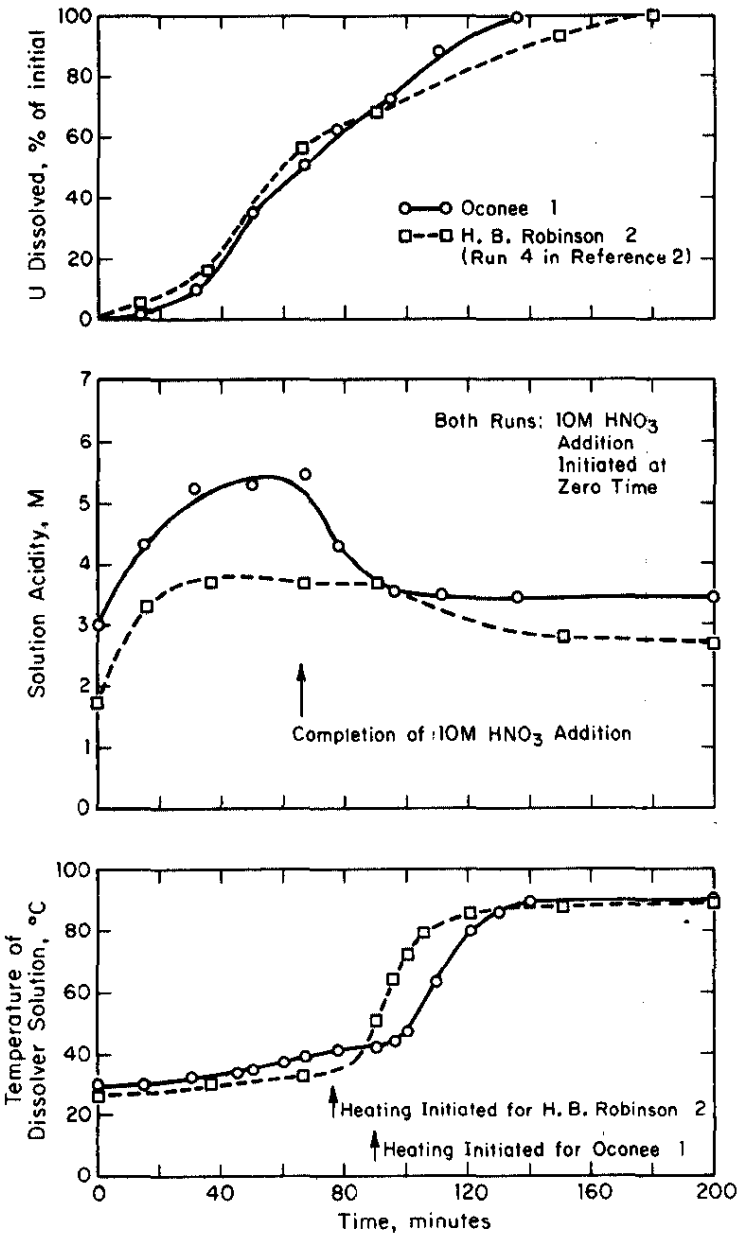

FIGURE 21. Dissolution of Clad UO_2 Fuels

Characterization of Dissolver Solution

Measured transuranic actinide concentrations (Table 19) and uranium and plutonium isotopic distributions (Table 20) are consistent with the reduced Oconee 1 fuel burnup as compared to the H. B. Robinson 2 fuel.[8] GLASS-calculated actinide compositions as a function of fuel exposure for the Oconee 1 fuel are being computed to determine more precisely the average burnup for the dissolved fuel section. The measured uranium concentration (380 g U/L) is in the range calculated for complete fuel dissolution. No undissolved oxide was observed within the one-inch pieces of cladding. The measured plutonium concentration (2.01 g Pu/L) corresponds to 0.53 wt % of the uranium charged to the dissolver.

TABLE 19

Composition of Dissolved Oconee 1 Fuel[a,b]

	Concentration
HNO_3, M	3.45
Total Uranium, g/L	380
Total Plutonium, g/L	2.01
^{241}Am, g/L	0.027
^{242}Cm, g/L	0.000015
^{244}Cm, g/L	0.00022

a. Analyses during May 1977; not corrected for decay.

b. ^{237}Np data incomplete.

TABLE 20

Isotopic Composition of Uranium and Plutonium in Oconee 1 Fuel

Uranium	*Atom %*	*Plutonium*	*Atom %*
^{234}U	0.017	^{238}Pu	0.33
^{235}U	1.15	^{239}Pu	74.15
^{236}U	0.18	^{240}Pu	17.67
^{238}U	98.64	^{241}Pu	6.69
		^{242}Pu	1.16

Measured gamma-emitting fission product concentrations in the dissolver solution and in the first caustic scrubber (Table 21) show that <0.002% of nonvolatile radionuclides are entrained in the off-gas stream. This observation agrees with reported data for the H. B. Robinson 2 fuel.[8] As expected, the fission product concentrations in the Oconee 1 fuel dissolver solution are reduced relative to the Robinson 2 fuel solutions.

TABLE 21

Gamma-Emitting Fission Products in Solutions From Oconee 1 Fuel Dissolution

Fission Product	*Activity, dis/min, in*	
	Dissolver Solution[a]	*NaOH Scrubber*[b]
^{95}Zr	2.1×10^{10}	Not detected
^{95}Nb	1.4×10^{10}	Not detected
^{106}Ru	7.5×10^{12}	9.7×10^{7}
^{137}Cs	1.2×10^{13}	6.9×10^{7}
^{144}Ce	2.4×10^{13}	4.4×10^{7}

a. Solution Volume = 430 mL; 380 g U/L.

b. Solution Volume = 150 mL.

The measured tritium concentration in the dissolved Oconee 1 fuel solution (Table 22) is reduced by a factor of 35 when compared to the measured tritium concentration in the dissolved H. B. Robinson 2 fuel solutions [5.5×10^{8} dis/(min)(g U)].[8] The significantly lower tritium concentration in the Oconee 1 fuel is surprising because fuel burnup differs by only a factor of 2 to 3. Further dissolution studies (including characterization of the spent hulls) are planned, to investigate this observation.

TABLE 22

Iodine and Tritium in Dissolver Solution and Off-Gas Scrubber From Oconee 1 Fuel

	Measured	*% of Total*
^{129}I, mg		
Dissolver Solution	0.052	0.4
First Scrubber	13.4	99.4
Second Scrubber	0.024	0.2
Tritium, dis/(min)(g U)		
Dissolver Solution	1.6×10^{7}	-

Characterization of Dissolver Off-Gas and Insoluble Residue

Analyses for volatile fission products in the caustic scrubbers in the off-gas stream were limited to ^{129}I (Table 22). Most of the ^{129}I was evolved from the dissolver solution by air sparging during dissolution, as it was in previous tests.[8] Less ^{129}I was trapped in the first caustic scrubber than in the Robinson 2 fuel studies (23.5 mg ^{129}I for fuel exposure of ∿28,000 MWD/MTHM), in agreement with the lower burnup of the Oconee 1 fuel.

The dissolved Oconee 1 fuel solution was dark and opaque because of finely divided solids suspended in solution. The solution was clarified by adding 0.12 g of an organic flocculant *(Primafloc C-3*)*[13] as an ∿200 weight ppm solution, followed by centrifuging. The insoluble black residue recovered by this procedure (solution residue) was washed thoroughly and dried; it weighed 0.108 g. Spark-source mass spectrometric analysis of the solution residue found a fairly low carbon content (Table 23), indicating that only a small fraction of the flocculant was present in the solid.

TABLE 23

Analysis of Dissolver Solution and Undissolved Residue by Spark-Source Mass Spectrometry

	Amount in		
Nuclide[a]	*Dissolver Solution, mg/L*	*Solution Residue,*[b] *wt %*	*Rinse Residue,*[c] *wt %*
^{238}U	∿4 × 10^5	<0.04	<0.01
Total Rare Earths (Pm, Nd, Pr, Ce, La)	880	<0.1	<0.1
$^{113,114}Cd$	<20	-	-
^{109}Ag	≤5	6	0.02
$^{105,106,107,108,110}Pd$	40	5	4
^{103}Rh	20	5	5
$^{101,102,104}Ru$	70	26	22
^{99}Tc	30	5	3
$^{95,97,98,100}Mo$	200	27	13
$^{90,91,92,94,96}Zr$	200	0.3	21
^{16}O	-	∿8	∿11
^{12}C	-	∿6	∿3

a. Mass numbers assigned to element with highest calculated concentration by ORIGEN Code.

b. Residue recovered by centrifuging dissolver solution after transfer from reaction kettle and head-end clarification; residue weight = 0.108 g.

c. Residue recovered by centrifuging 3M HNO_3 rinse of reaction kettle; residue weight = 0.026 g.

* Trademark of Rohm and Haas.

13. *Savannah River Laboratory Quarterly Report, Light Water Reactor Fuel Recycle, January-March 1977.* USERDA Report DPST-LWR-77-1-1, p. 39.

The reaction kettle containing the spent hulls was rinsed thoroughly with 3M HNO_3 at ambient temperature. The rinse solution contained traces of insoluble residue (rinse residue), which were recovered by centrifuging without any organic flocculant addition. This residue was washed and dried; it weighed 0.026 g, making the combined solid residue weight 0.134 g. The total insoluble residue corresponding to a fuel burnup of 10,000 to 14,000 MWD/MTHM is about 0.08 wt % of the uranium charged to the dissolver. This is slightly less than half of the corresponding weight for the high burnup H. B. Robinson 2 fuel (0.18 to 0.32 wt % of uranium for ∿28,000 MWD/MTHM). Thus, insoluble residue weight is approximately proportional to fuel burnup. However, the amount of residue recovered will depend in practice on the severity of dissolution conditions, so that deviations from strict linear dependence of residue weight on fuel exposure are expected.

Analyses of both the solution residue and the rinse residue by spark-source mass spectrometry (SSMS) (Table 23) show that the major elemental constituents are ruthenium, molybdenum, palladium, technetium, and rhodium, in agreement with previous determinations for H. B. Robinson 2 fuel.[6,8] However, the rinse residue also has a high composition of natural zirconium (as determined by zirconium isotopic composition), which probably results from cladding fines produced during shearing. These fines most likely have a larger particle size than the fission product residue solids. Thus, they settle more rapidly from solution and remain in the dissolver after transfer of the solution from the dissolver.

A portion of the solution residue (0.098 g) was leached with 10M HNO_3 at 90°C for 6 hours. This procedure dissolved 0.040 g of the residue. The remaining solid was recovered by centrifuging, washing, and drying; then, it was leached with concentrated HCl at 90°C for 6 hours. The HCl leach dissolved 0.041 g of solid leaving 0.017 g of undissolved solid residue. The 10M HNO_3 leach supernate contained <0.002% of the uranium and <0.005% of the plutonium in the dissolver solution. The HCl leach supernate contained <0.001% of the uranium and <0.004% of the plutonium in the dissolver solution. Therefore, the actinides present in the insoluble residue from dissolution of the Oconee 1 fuel represent a very small percentage of the actinides in the initial fuel charge.

The only significant gamma-emitting radionuclide found in either the 10M HNO_3 or the HCl leach supernate was ^{106}Ru (6.9×10^{11} dis/min in the 10M HNO_3 solution and 1.6×10^{12} dis/min in the HCl solution, as compared to a total of 7.5×10^{12} dis/min in the dissolver solution). SSMS data (Table 24) show that the HCl leach solution has a fission product composition approximately equivalent to the solid residue (mostly ruthenium and molybdenum). Thus, the leaching procedure appears to dissolve fission products uniformly from the solid.

The residue remaining after both leach tests (0.017 g solid) also was characterized by SSMS (Table 24). The concentration of natural zirconium in those solids was significantly increased from the initial solution residue characterization (Table 23), indicating that zirconium fines from shearing of the fuel were not dissolved by the leach treatments. The total weight of zirconium fines in the collected residues based on the SSMS data (which has a factor of 2 to 3 accuracy) is <0.1% of the total zirconium cladding weight of the sheared fuel segment (16.5 inches).

TABLE 24

Analysis of HCl Leach Solution of Residue and Leached Residue by Spark-Source Mass Spectrometry[a]

Nuclide	*HCl Leach Solution, mg/mL*[b]	*Leach Residue,*[c] *wt %*
^{109}Ag	0.3	0.1
$^{105,106,107,108,110}Pd$	0.2	8
^{103}Rh	0.4	2
$^{101,102,104}Ru$	1.0	9
^{99}Tc	0.2	3
$^{95,97,98,100}Mo$	0.9	8
$^{90,91,92,94,96}Zr$	<0.03	40
^{16}O	-	~15
^{12}C	-	~1

a. Only fission products with mass number 90 to 110 reported; all other fission products at generally lower concentration.

b. Total volume = 10 mL; 41 mg solid dissolved in HCl.

c. Remaining residue weight = 17 mg.

Continuing Study

Voloxidation of the Oconee 1 fuel will be tested in a static bed to continue determinations of the extent of tritium volatilization during oxidation of clad fuel. Dissolution behavior of the voloxidized fuel will be tested to support previously reported dissolution data for U_3O_8 powder.[6] Dissolution behavior of enriched Saxton UO_2 fuels will be tested in support of a planned parametric test for the voloxidation program.

CLARIFICATION OF DISSOLVER SOLUTIONS

Laboratory tests of the ability of organic flocculants to clarify LWR dissolver solutions continued. Two of the most successful of these tested previously,[14] *Primafloc C-3** and *Percol E-24*,** as well as *Primafloc A-10*,* were added to dissolver solutions in amounts varying from 0.2 to 8300 ppm. At the highest concentrations, *A-10* caused some redispersion of undissolved solids, while *E-24* caused partial flotation; both performed adequately at lower concentrations. *C-3* clarified well at all concentrations. At 190 ppm, *C-3* appeared stable after two weeks in the dissolver solution; after three weeks some degradation was apparent. The flocculated solids contained about 0.02 wt % of the total plutonium and only traces of uranium.

Need for Chemical Clarification

As reported previously, laboratory dissolution of test pieces of irradiated H. B. Robinson 2 UO_2 fuel rods yielded a black, opaque solution. It could not be clarified by filtration through a fine-pore glass frit that could remove particles as small as 5 μ. Even after centrifugation, the solution was gray.[15]

During solvent extraction of the gray solution, black solids collected at the aqueous/organic interface of several mixer-settler stages.[16] These solids could plug mixer-settlers or other equipment. The high ^{106}Ru activity of these solids would hinder decontamination by accelerating radiolytic decomposition of the solvent. Some head-end treatment will be necessary to prevent accumulation of solids during solvent extraction.

Although the usual Purex head-end treatment with MnO_2 clarified the dissolver solution effectively, MnO_2 significantly increased the amount of solid waste and dissolved some of the ruthenium in the black colloidal particles (thereby increasing

---

* Trademark of Rohm and Haas.

** Trademark of Allied Colloids.

14. *Savannah River Laboratory Quarterly Report, Light Water Reactor Fuel Recycle, January-March 1977.* USERDA Report DPST-LWR-77-1-1, p. 42.

15. *Savannah River Laboratory Quarterly Report, Light Water Reactor Fuel Recycle, July-September 1976.* USERDA Report DPST-LWR-76-1-3, p. 40.

16. *Savannah River Laboratory Quarterly Report, Light Water Reactor Fuel Recycle, October-December 1976.* USERDA Report DPST-LWR-76-1-4, p. 45.

the concentration of ^{106}Ru in the clarified solution).[17] Therefore, 40 organic flocculants were tested, several of which appeared promising.[1] Two of these and one other (*A-10*) were selected for further tests reported here.

Settling Tests

The three organic flocculants (*Primafloc C-3*, *Primafloc A-10*, and *Percol E-24*) were added to dissolved H. B. Robinson 2 fuel (350 g U/l in 3.1M HNO_3) in concentrations of 0.19, 1.9, 19, 190, 560, 1700, and 8300 ppm. For all but the highest concentration, 25 ml of dissolver solution was added to 5 ml of the appropriate flocculant concentration. For 8300 ppm samples, 25 ml of 1 wt % flocculant solution was added to 5 ml of dissolver solution.

Within one hour, solids in all the 8300-ppm samples had started to settle. After 1.5 hours, solids in all samples containing 190 ppm or more had started to settle. After two hours, solids in all samples were settling. In general, samples containing *C-3* settled faster than the others.

At 8300 ppm, *C-3* was clearly superior to the other two (Figure 22). *E-24* caused flotation of much of the solids, which could make separation difficult. The sample containing *A-10* separated into three regions: the top of the sample was clarified, some solids settled to the bottom, while some were apparently redispersed in the middle.

At 1700 ppm (Figure 23), both *C-3* and *A-10* clarified the solution acceptably. However, *E-24* again caused much of the solids to float. There was no apparent difference among the flocculants at less than 1700 ppm, except that at a given concentration *C-3* settled solids faster.

Stability in Dissolver Solution

Two samples containing 190 ppm *C-3* were used to evaluate flocculant stability in dissolver solutions. One sample was heated for 6 hours in a water bath at 80 to 90°C, the other was not disturbed. After two weeks, solids in both samples gave no indication of flocculant degradation. After three weeks, a slight amount of redispersion above the solid was apparent in both samples.

---

17. Reference 1, p. 40.

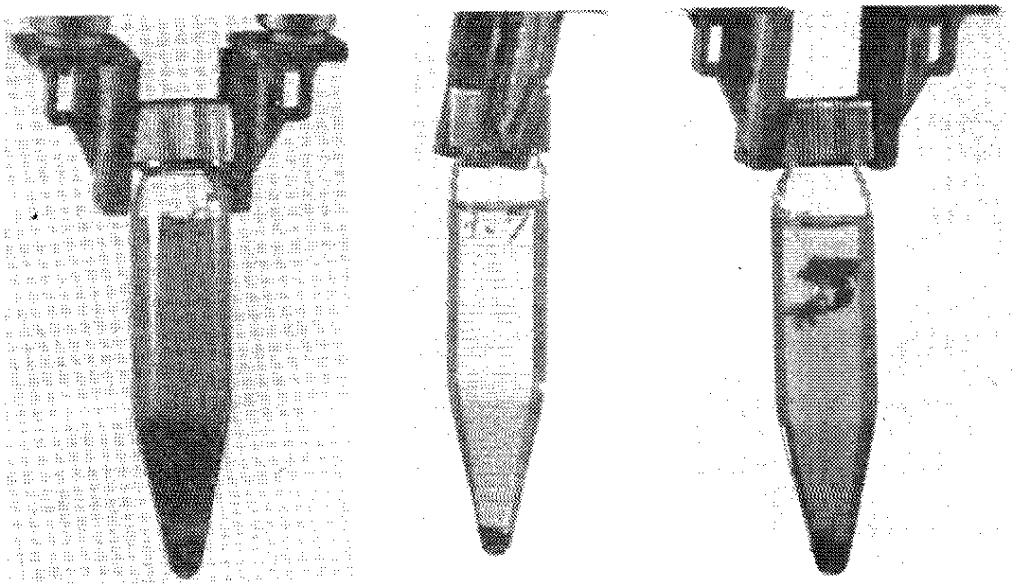

Primafloc A-10 *Primafloc C-3* *Percol E-24*

FIGURE 22. LWR Dissolver Solutions with 8300 ppm Flocculant after Standing Overnight

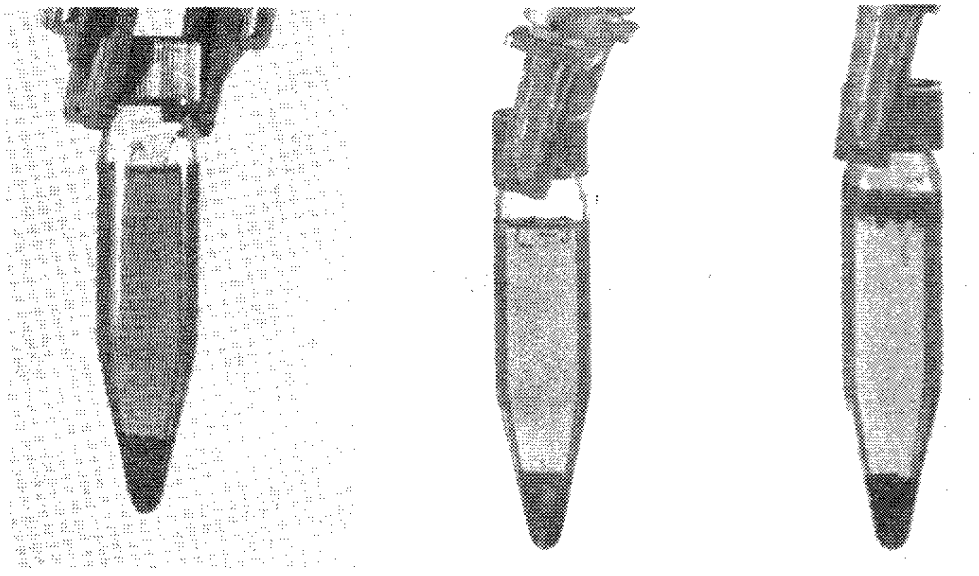

Primafloc A-10 *Primafloc C-3* *Percol E-24*

FIGURE 23. LWR Dissolver Solutions with 1700 ppm Flocculant after Standing Overnight

Analysis of Solids

Solids flocculated by *C-3* and *E-24* were combined, washed five times with 0.5M HNO_3, then dissolved in hot HCl. Analysis of this solution by spark-source mass spectrometry showed that the solids contained about 18% of the total ruthenium and only 0.02% of the plutonium originally present in the dissolver solution. There was too little uranium to be quantitatively determined.

Continuing Study

C-3 will be added to a dissolver solution at 200 ppm to determine whether the flocculant interferes with solvent extraction. Subsequent dissolver experiments will determine whether *C-3* is incompatible with solvent extraction at any higher concentration. Other flocculants will be tested, if needed.

SOLVENT EXTRACTION OF LWR FUELS

Solvent extraction flowsheets for the recovery and purification of uranium and plutonium from irradiated LWR fuel are being developed (Figure 24) from SRP operating experience, theoretical calculations, and tests in miniature mixer-settlers.[1,2] Additional tests were completed with simulated feed and with solutions prepared by dissolution of irradiated H. B. Robinson 2 fuel and irradiated Oconee 1 fuel. The results showed that:

- Increased saturation in both 1A and 1A' banks improved ^{106}Ru decontamination factors for both types of irradiated fuel feed; but ^{95}Zr decontamination factors were lower for Oconee 1 fuel (not measured for Robinson 2 fuel).

- Partitioning of uranium and plutonium from Robinson 2 fuel with hydroxylamine nitrate and hydrazine was improved by adjusting

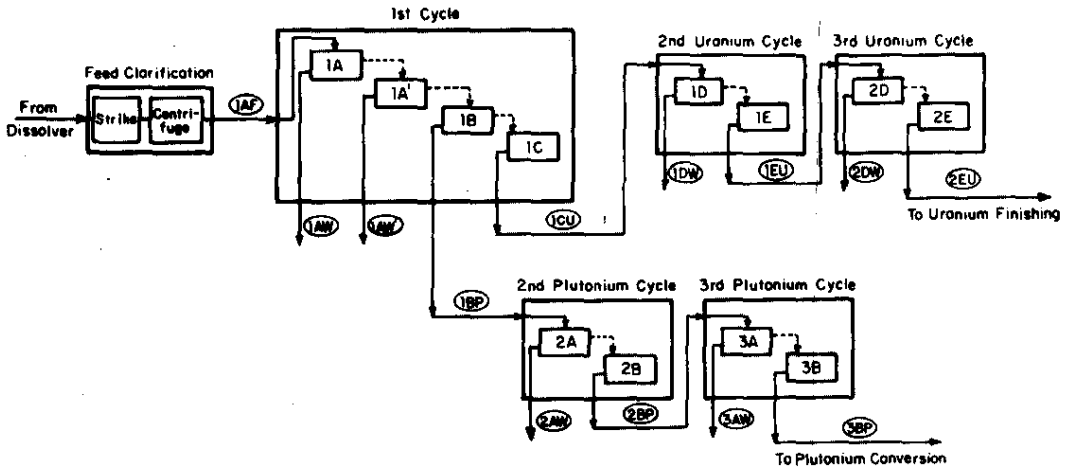

FIGURE 24. Generalized Solvent Extraction Flowsheet

1. *Savannah River Laboratory Quarterly Report, Light Water Reactor Fuel Recycle, October-December 1976.* USERDA Report DPST-LWR-76-1-4, p. 43.
2. *Savannah River Laboratory Quarterly Report, Light Water Reactor Fuel Recycle, January-March 1977.* USERDA Report DPST-LWR-77-1-1, p. 46.

the nitric acid concentration and increasing the hydroxylamine concentration in the 1B bank.

- Partitioning of uranium and plutonium in simulated feed with U(IV) was ineffective: 14% of the plutonium was left in the organic phase with the uranium.

Previous Tests of Uranium and Plutonium Recovery

Four previous tests (LWR-1,2,3,4)[1,2] of the first-cycle solvent extraction flowsheet using dissolved H. B. Robinson 2 fuel showed that:

- Recoveries of uranium and plutonium from solutions of irradiated fuel were good with no prior adjustment of plutonium valence.
- Decontamination was good from all fission products except ruthenium, zirconium, and niobium.
- Neptunium was extracted with uranium and plutonium, and was directed to the 1AW' waste stream.
- Improvement of ruthenium and zirconium-niobium decontamination was marginal with a low-acid 1A' scrub bank.*
- Partitioning with hydroxylamine nitrate as a reducing agent was improved by lowering the acidity in the 1B bank.

Recent Tests of Uranium and Plutonium Recovery

During a fifth test (LWR-5) with dissolved Robinson 2 fuel, losses of uranium and plutonium to the 1AW aqueous waste stream were high (Table 25). These high losses were attributed to saturation of tributyl phosphate (TBP) by uranium in the middle of 1A extraction bank.

TABLE 25

Losses of Uranium and Plutonium

Test[a]	*Source of Irradiated LWR Fuel*	*Number of Extraction Stages in A Bank*	*Loss to 1AW, %*[b]		*Loss to 1AW', %*[b]	
			Uranium	*Plutonium*	*Uranium*	*Plutonium*
LWR-5	Robinson 2	9	0.75	0.89	0.004	0.14
LWR-6	Oconee 1	9	0.02	0.017	0.06	0.032

a. Results of LWR-1,2,3,4 reported in References 1 and 2.

b. Design losses: ≤0.01% for uranium, ≤0.05% for plutonium.

* The primary purpose of the 1A' bank is to remove zirconium.

Conditions for LWR-5 were similar to those for the previous tests, except that the ratio of the 1AX' extractant (30 vol % TBP) flow to the 1AS' scrub (1M HNO_3) flow was increased from 1.5 to 1.6, to decrease the losses of plutonium to the 1AW'. Saturation in the 1A bank varied from 100% at the feed stage (Stage 8) to 88% at Stage 14. Saturation in the 1A' bank was about 100% from Stage 2 through Stage 8. The high saturation in the 1A bank resulted from low TBP concentrations (29.0 to 29.5 vol % TBP) and low organic-to-aqueous flow ratios.

During a sixth test (LWR-6) with dissolved Oconee 1 fuel which had been irradiated to 14,000 MWD/MT, uranium losses were high. Conditions for LWR-6 were similar to those for previous tests. The organic extractant (30 vol % TBP) flow, 1AX, was increased to avoid complete saturation in the 1A bank. The ratio of the 1AX' extractant (30 vol % TBP) flow to the 1AS' scrub (1M HNO_3) flow was increased from 1.6 to 1.65, to decrease plutonium losses to the 1AW'. The flow changes gave acceptably low plutonium losses in both the 1A and 1A' banks. But uranium losses, which should have been lower than plutonium losses, were higher (Table 25). These high losses are as yet unexplained.

Decontamination from Fission Products

Decontamination factors for ruthenium, one of the most difficult fission products to remove, were greatly improved by the increased saturation in both the 1A and 1A' banks during Test LWR-5 (Table 26). Zirconium decontamination factors could not be measured during Test LWR-5 because the zirconium concentration in the feed was too low.

TABLE 26

Decontamination from Ruthenium and Zirconium

Test	*Banks*	*Temp., °C*	*Decontamination Factors*[a] ^{106}Ru	^{95}Zr
LWR-1, LWR-2	1A only	30	410[b]	<260[b]
LWR-3	1A and 1A'	30	315[c]	<1500[c]
LWR-4	1A and 1A'	45	4,000[c]	1300[c]
LWR-5	1A and 1A'	45	260,000[c]	-
LWR-6	1A and 1A'	45	12,000[c]	150[c]

a. See Table 22 of Reference 1 and Tables 10 and 11 of Reference 2 for decontamination factors for ^{95}Nb and other fission products.

b. Average for Tests LWR-1 and LWR-2, Table 19 of Reference 1.

c. Overall decontamination factor = (DF in 1A) × (DF in 1A'); compare with design decontamination factor >1000.

In contrast, previous tests (LWR-1,2,3,4) had indicated good decontamination from all fission products except ruthenium, zirconium, and niobium. However, the very high ^{106}Ru decontamination factor obtained in Test LWR-5 probably cannot be maintained in practice because the degree of saturation during Test LWR-5 is too high for a practical plant process.

Two differences in head-end treatment from previous tests might also account for the very high ^{106}Ru decontamination factor obtained in Test LWR-5. First, fuel for the LWR-5 test was vol-oxidized before dissolution, lowering the ruthenium concentration in the feed. Second, the feed solution was clarified with an organic flocculant, *Primafloc C-3*,* not MnO_2.

The high ^{106}Ru decontamination factor and the unusually low ^{95}Zr decontamination factors measured during Test LWR-6 are inconsistent with results of Test LWR-4. LWR-6 test conditions and saturation were similar to those for LWR-4, except for fuel irradiation and head-end clarification. Although Oconee 1 fuel used in Test LWR-6 had been irradiated about half as much as the Robinson 2 fuel used in Test LWR-4, zirconium activities were about the same, because Robinson 2 fuel had been cooled longer. After dissolution, the Oconee 1 feed for Test LWR-6 was clarified with *Primafloc C-3*, whereas LWR-4 feed had been clarified with MnO_2, a strong oxidant and adsorber for zirconium species. Further study is necessary to determine whether these differences in head-end clarification caused the differences between the decontamination factors observed in Tests LWR-4 and LWR-6.

Partitioning of Uranium and Plutonium

To partition uranium and plutonium, a reducing agent is added in the partitioning bank (1B) to reduce Pu(IV) to Pu(III), allowing plutonium to be stripped into the aqueous phase. SRP uses ferrous sulfamate to reduce Pu(IV). However, the resulting ferric ion increases waste volumes, and sulfamate is converted to sulfate which interferes with fixation of solidified waste in glass forms. Alternative reductants that do not add solids to the waste, such as uranium(IV) and mixtures of hydroxylamine nitrate ($NH_2OH \cdot HNO_3$) and hydrazine (N_2H_4), have been investigated.

---

* Trademark of Rohm and Haas. *Primafloc C-3* was the best of 40 organic flocculants tested recently for their ability to clarify dissolver solutions.

Partitioning with Hydroxylamine Nitrate-Hydrazine

Earlier tests[1,2] with mixtures of $NH_2OH \cdot HNO_3$ and N_2H_4 showed that reducing the acidity in the 1B bank decreased the plutonium loss to the uranium product; at high acid concentrations, $NH_2OH \cdot HNO_3$ is autocatalytically destroyed, so that plutonium can be reoxidized by NO_2^- and thus re-extracted.

Test LWR-5 confirmed that $NH_2OH \cdot HNO_3$ plus N_2H_4 is satisfactory for partitioning uranium and plutonium. Increasing the concentrations of both $NH_2OH \cdot HNO_3$ and HNO_3 reduced the uranium impurity in the plutonium product (Table 27). Since the plutonium impurity in the uranium product remained the same as in Test LWR-4, the increased concentration of $NH_2OH \cdot HNO_3$ compensated for the increased acidity in the 1B bank. There was no indication that plutonium dibutylphosphate (PuDBP) complexes interfered with stripping of plutonium, as had been observed in Test LWR-4.[2]

TABLE 27

Partitioning of Uranium and Plutonium by Hydroxylamine Nitrate + Hydrazine

Test	*Number of Strip Stages in 1B Bank*	*Composition of Aqueous Strip, M*			*U in Pu Product, % of U in Feed*[a]	*Pu in U Product, % of Pu in Feed*[a]
		Max HNO_3	*$NH_2OH \cdot HNO_3$*	*N_2H_4*		
Simulated LWR[b]	8	2.3	0.1	0.2	0.03	15.9
LWR-3[b,c]	8	1.2	0.1	0.2	0.004	1.53
LWR-4[b,c]	10	0.6	0.1	0.2	0.10	0.12
LWR-5[c]	8	0.9	0.4	0.2	<0.002	0.12

a. Design losses: ⩽0.01% for uranium, ⩽0.05% for plutonium.

b. Reference 2, Table 12.

c. Robinson 2 fuel.

Measurement of initial and final concentrations of $NH_2OH \cdot HNO_3$ showed that about 20 times the stoichiometric quantity of $NH_2OH \cdot HNO_3$ was consumed during reduction to Pu(III). This is similar to the excess ferrous sulfamate presently required in SRP operations.

During Test LWR-6, the 1B bank did not partition effectively, and plutonium losses to the 1BU uranium product stream were high. These results are discussed on page 96.

Partitioning with Uranium(IV)

U(IV) is an attractive alternative to ferrous sulfamate because U(IV) would not add any waste, and it has been shown[3] to allow stripping of plutonium from the PuDBP complex. It could be produced electrolytically from a portion of the uranium product stream.

Earlier work[1,4] indicated that large amounts of U(IV) were sometimes consumed during partitioning. The present tests with simulated feed at low acidity, where the rate of reduction of Pu(IV) by U(IV) should be favorable, show that use of U(IV) results in incomplete partitioning of uranium and plutonium (page 96).

Test Conditions

Kinetic studies[5-7] have shown that the rate of reduction of Pu(IV) by U(IV) varies inversely with the square of the acid concentration.[6] There is also a slight inverse dependence on nitrate concentration. Thus lowering the nitric acid concentration should enhance reduction of Pu(IV) and therefore improve partitioning.

---

3. W. Ochsenfeld and H. Schmieder (to Gesellschaft für Kernforschung m.b.H., Karlsruhe, Germany). *Method of Stripping Plutonium from Tributyl Phosphate Solution Which Contains Dibutyl Phosphate-Plutonium Stable Complexes.* U.S. Patent 3,949,049 (April 6, 1976).

4. C. S. Schlea, M. R. Caverly, H. E. Henry, and W. J. Jenkins. *Uranium(IV) Nitrate as a Reducing Agent for Plutonium(IV) in the Purex Process.* USAEC Report DP-808, E. I. du Pont de Nemours and Co., Savannah River Laboratory, Aiken, SC (1963).

5. T. W. Newton. "The Kinetics of the Reaction Between Pu(IV) and U(IV)." *J. Phys. Chem. 63,* 1493 (1959).

6. P. Biddle, J. H. Miles, and M. J. Waterman. "Catalysis in the Reduction of Plutonium(IV) by Uranium(IV)." *J. Inorg. Nucl. Chem. 28,* 1736 (1966).

7. V. I. Marchenko and V. S. Koltunov. "Kinetics of the Reaction of Plutonium Ions with Tetravalent Uranium in Nitric Acid. I. Reduction of Pu(IV)." *Sov. Radiochem. 16,* 477 (1974).

Conditions for testing the effectiveness of U(IV) are summarized in Table 28. Acid concentration in the 1AS stream was lowered from 3.0 to 1.5M, as in a 1A' bank. The 1BX' acidity was lowered from 2.0 to 0.8M; hydroxide formation was not a problem at acid concentrations equal to or greater than 0.1M. U(IV) was present in 10-fold stoichiometric excess. U(IV) solutions were prepared electrolytically; ceric titrations showed that approximately 95% of the total uranium was U(IV). In the presence of Pu(III), the U(IV) normality was taken as the difference between the total reducing normality and the Pu(III) concentration (determined by alpha counting).

TABLE 28

Experimental Conditions for Partitioning Test With U(IV)

Stream	*Composition*	*Stage*	*Flow, mL/min*
1 CAF: Cold Feed to 1A Bank at Start of Test	250 g/L U 2.3M HNO_3	8	0.75
1 HAF: Hot Feed to 1A Bank	250 g/L U 2.3 g/L Pu 2.3M HNO_3	8	0.75
1AX: Extractant to 1A Bank	30 vol % TBP	16	2.14
1AS: Scrub to 1A Bank	1.5M HNO_3	1	0.43
1BF: Feed to 1B Bank	1 AP: product from 1A	8	-
1BS: Scrub to 1B Bank	30 vol % TBP	16	1.09
1BX: Extractant to 1B Bank	0.1M HNO_3 0.2M $N_2H_5NO_3$	1	0.30
1BS': Reductant to 1B Bank	0.2M U(IV) 0.2M $N_2H_5NO_3$ 0.8M HNO_3	9	0.18

The test was run with cold feed for eight hours before hot feed was added. During this time, U(IV) refluxed in the 1B bank and its concentration increased (Figure 25). This provided an additional reservoir of U(IV) to ensure complete reduction of Pu(IV).

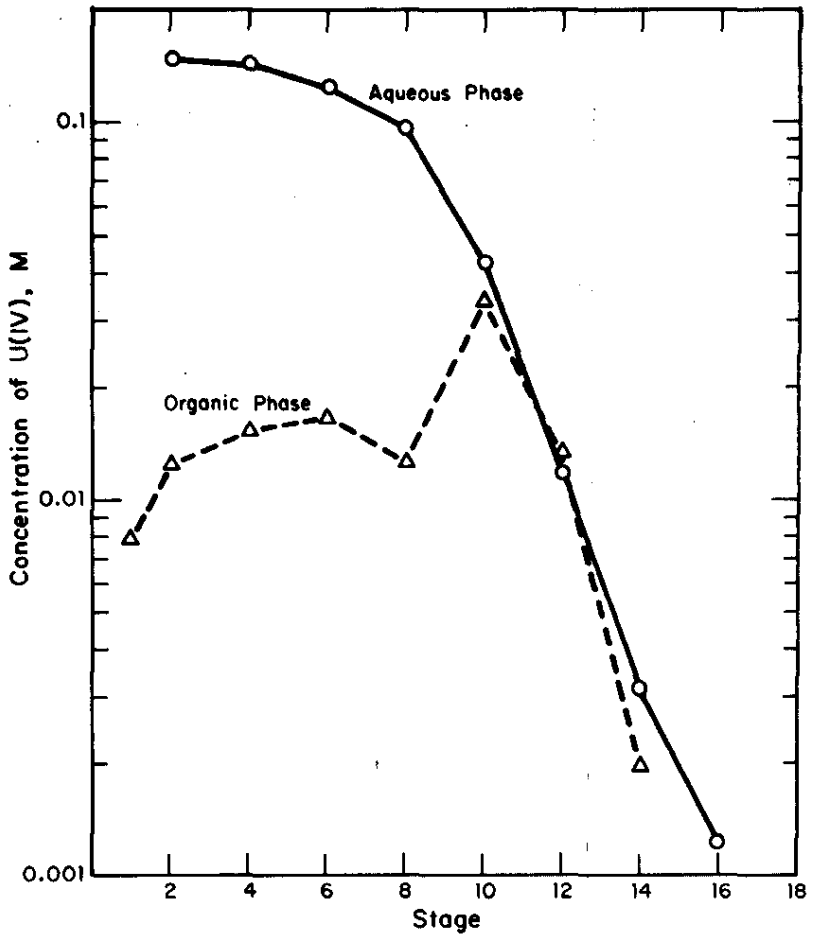

FIGURE 25. Distribution of U(IV) in 1B Bank after Operation for Eight Hours with Cold Feed

Results of Partitioning Test

Uranium(IV) was not effective for partitioning in the 1B bank:

- The plutonium content of the 1BP stream (plutonium product) initially increased to a level corresponding to nearly 100% recovery of plutonium, but then dropped off to 84% after 12 hours.
- The plutonium impurity in the 1BU stream (uranium product) increased steadily; losses were 13.8% by 12 hours (Figure 26).

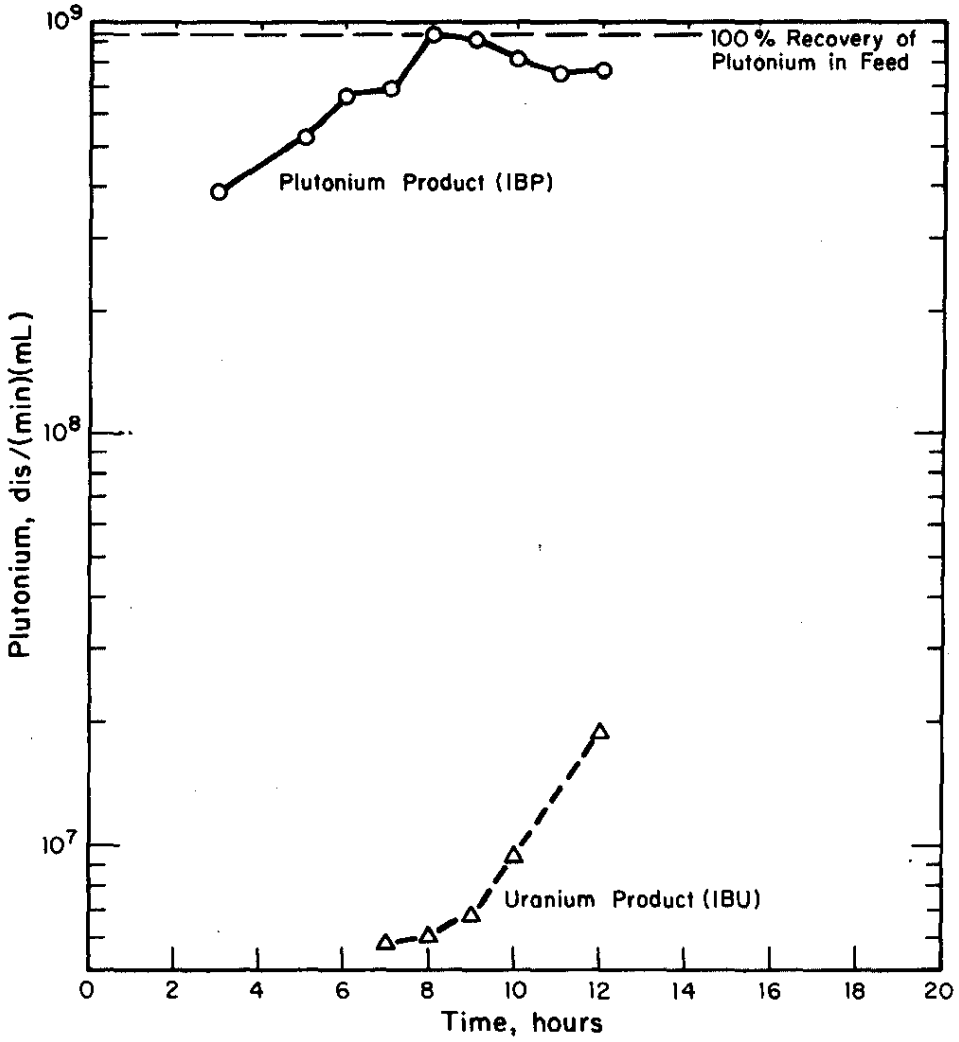

FIGURE 26. Plutonium Activity in Plutonium and Uranium Product Streams from 1B Bank

- The plutonium profile in the 1B bank (Figure 27) shows that some Pu(III) was reoxidized to Pu(IV) which was then extracted into the organic phase.
- The 10-fold excess of U(IV) reductant was almost completely oxidized, even though hydrazine was added as a stabilizer.

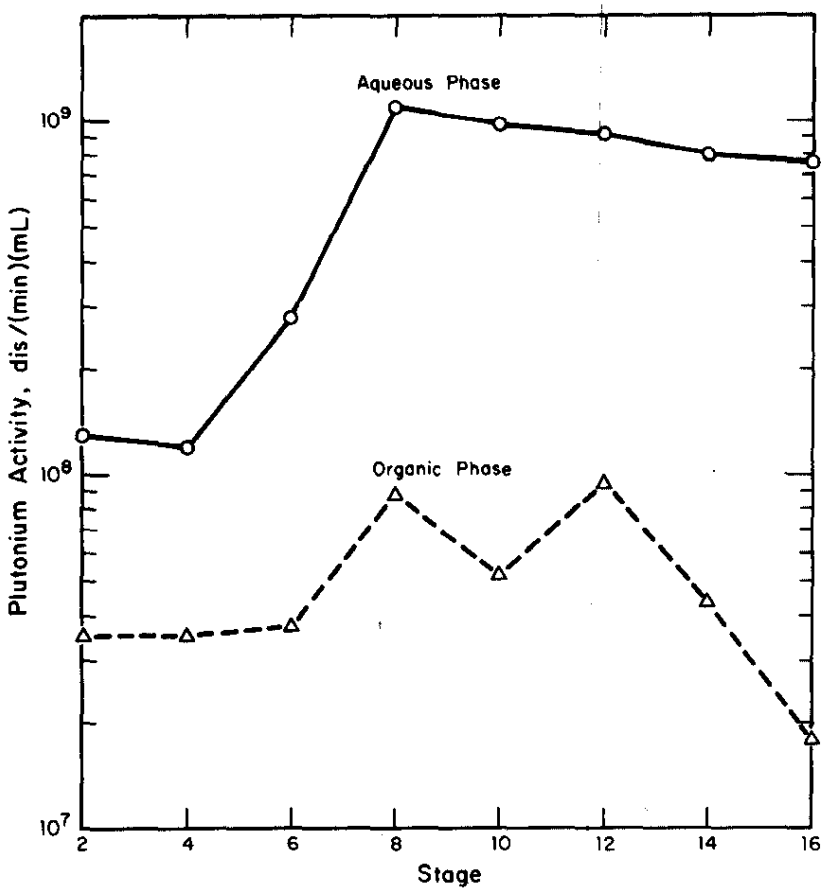

FIGURE 27. Distribution of Plutonium in 1B Bank after Operation for Twelve Hours (End of Run)

The U(IV) color in the 1B bank faded gradually as the run proceeded. No U(IV) was detected in either the 1BP or 1BU streams after four hours. At the end of the run, no U(IV) was detected in the organic phase of the bank stages and very little in the aqueous phase (Figure 28).

Loss of U(IV) occurs only when plutonium is present. When the banks are run under cold conditions, U(IV) is stable for days. Even when a nitrite stream is added, there is no loss of U(IV).

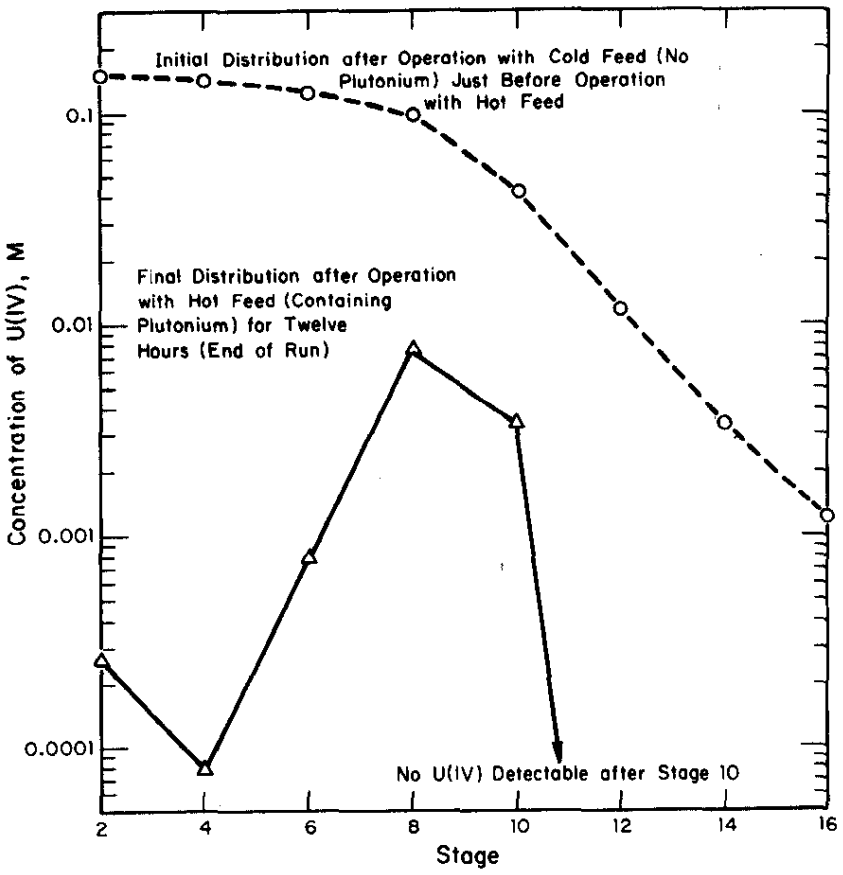

FIGURE 28. Distribution of U(IV) in 1B Bank at Start and End of Operation with Hot Feed

The results of this test are similar to those observed previously.[1] Since the loss of plutonium to the 1BU stream actually increased slightly from 12.3 and 12.4% to 13.8%, the rate of the U(IV)-Pu(IV) reaction apparently does not determine partitioning effectiveness.

Unexplained Oxidation of U(IV)

Although this test indicated that plutonium is involved in the oxidation of excess U(IV), the large consumption of U(IV) cannot be explained in terms of known reactions in the aqueous phase (Table 29). Reactions 1 to 3 form an autocatalytic cycle which could consume large amounts of U(IV). However, addition of hydrazine should interrupt this cycle, because hydrazine reacts very rapidly with nitrite.[8] Relative reaction rates in Table 30, calculated for concentrations similar to those in the 1B bank, show that the hydrazine reaction is much faster than any of the others. The hydrazine is present in high concentration and should consume all of the nitrite in the aqueous phase, thereby preventing reoxidation of Pu(III).

The observed loss of U(IV) thus cannot be explained in terms of these aqueous phase reactions. Organic phase reactions may be involved, but they are poorly defined and almost no rate data are available. Investigation is continuing to discover why U(IV) and Pu(III) are oxidized, and to determine conditions under which U(IV) would be effective for partitioning.

Continuing Study

- Tests will be conducted to improve decontamination factors for ruthenium, zirconium, and niobium.
- Tests will determine the effects of organic flocculants on the solvent-extraction flowsheet.

8. J. R. Perrott and G. Stedman. "The Kinetics of Nitrite Scavenging by Hydrazine and Hydrazoic Acids at High Acidities." *J. Inorg. Nucl. Chem. 39*, 325 (1977).

TABLE 29

Aqueous-Phase Reactions in Mixer-Settler

$$Pu^{3+} + NO_2^- + 2H^+ \rightarrow Pu^{4+} + NO + H_2O \quad (1)$$

$$U^{4+} + 2Pu^{4+} + 2H_2O \rightarrow UO_2^{2+} + 2Pu^{3+} + 4H^+ \quad (2)$$

$$2NO + NO_3^- + H_2O \rightarrow 3NO_2^- + 2H^+ \quad (3)$$

$$U^{4+} + 2NO_2^- \rightarrow UO_2^{2+} + 2NO \quad (4)$$

$$N_2H_5^+ + NO_2^- \rightarrow HN_3 + 2H_2O \quad (5)$$

TABLE 30

Relative Rates of Aqueous-Phase Reactions

		1M HNO_3		*2M HNO_3*	
Reaction	*Reference*	*Rate Constant*	*Relative[a] Rate*	*Rate Constant*	*Relative[a] Rate*
Pu^{3+}/NO_2^-	9	1.7[b]	1	3.17[b]	1
	10	90 [c]	5	360 [c]	10
U^{4+}/Pu^{4+}	6	7600[b]	2000	1900[b]	250
U^{4+}/NO_2^-	11	∿0.05[c]	0.1	∿0.025[c]	0.04
$N_2H_5^+/NO_2^-$	8	100,000[b]	70,000	200,000[b]	70,000

a. Calculated assuming flows in Table 28, 25°C, and $[U(IV)] = [N_2H_4] = 0.2M$, $[Pu(IV)] = [Pu(III)] = [NO_2^-] = 0.01M$.

b. In units of $(M^{-\frac{1}{2}})(min^{-1})$.

c. In units of $(M^{-1})(min^{-1})$.

9. V. S. Kiltunov and V. I. Marchenko. "Reaction Between Plutonium(III) and Nitrous Acid. II. Kinetics of Forward Reaction." *Sov. Radiochem. 15,* 787 (1973).

10. E. K. Dukes. "Kinetics and Mechanism for the Oxidation of Trivalent Plutonium by Nitrous Acid." *J. Amer. Chem. Soc. 82,* 9 (1960).

11. V. S. Kiltunov and V. I. Marchenko. "Kinetics of Oxidation of U(IV) by Nitrous Acid Catalyzed by Ferric Ions." *Sov. Radiochem. 15,* 77 (1973).

COPROCESSING OF URANIUM AND PLUTONIUM BY SOLVENT EXTRACTION

Coprocessing plutonium with part of the uranium is easily accomplished by changing the operation of the B bank of the solvent extraction process. Several flowsheets were evaluated by computer calculations. Miniature mixer-settler tests of the most promising flowsheet demonstrated the feasibility of coprocessing over a range of plutonium concentration factors of 6 to 28.

To reduce the potential for unauthorized diversion of plutonium, the solvent-extraction flowsheet for recovery and purification of LWR fuels is being altered to eliminate streams containing pure plutonium. One method of eliminating pure plutonium streams (coprocessing) will partially separate uranium and plutonium to yield a pure uranium stream and a mixed uranium-plutonium stream. Extreme coprocessing, with no uranium-plutonium separation at all, has been shown to be economically unattractive.[12]

Possible Coprocessing Flowsheets

A flowsheet suitable for coprocessing is shown in Figure 29. This flowsheet has two advantages. First, no further processing of the uranium-plutonium stream is required after partial partitioning in the 2B bank; consequently, there would be no alteration of the plutonium/uranium ratio by subsequent solvent-extraction cycles. Second, three fewer contactors and two fewer solvent-purification systems would be needed than in the reference solvent-extraction flowsheet (Figure 24).

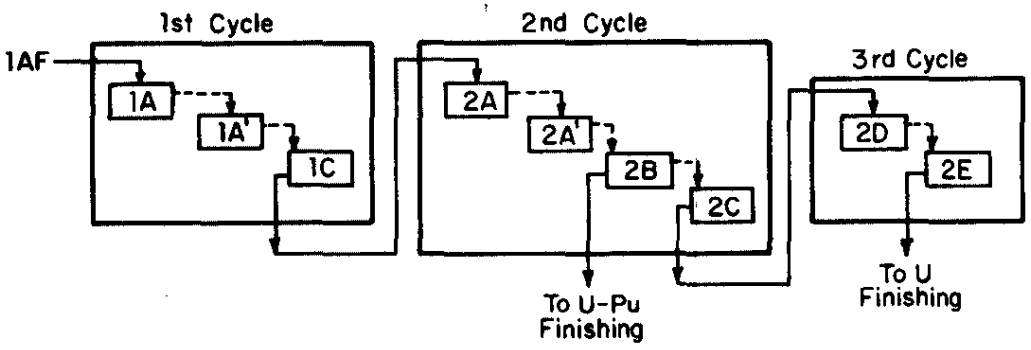

FIGURE 29. Alternative Coprocessing Flowsheet

12. *Savannah River Laboratory Quarterly Report, Light Water Reactor Fuel Recycle, July-September 1976.* USERDA Report DPST-LWR-76-1-3, p. 44.

A possible disadvantage is that a third cycle of solvent extraction of the pure uranium stream might be insufficient to achieve a plutonium decontamination factor of 2×10^8 to 4×10^8, which is needed to meet the proposed specification of 25 to 50 alpha dis/(min)(g U). Although substitution of a cation-exchange column for the third-cycle solvent extraction might yield the required decontamination factor, such a column would slowly accumulate plutonium that would have to be returned to an earlier cycle. This much pure plutonium might not be acceptable.

Feasibility of Coprocessing

Of the several flowsheets examined, the one most likely to work changes the operation of the 1B bank in the reference process (Figure 24) and changes the second and third cycles to extract and strip uranium and plutonium together. Leaving some uranium with the plutonium would not be a drastic change from present Purex operation; SRP could produce a uranium-plutonium stream almost immediately by reducing the organic scrub flow (1BS) to the 1B bank.* In fact, it is more difficult to obtain a pure plutonium stream than to leave some uranium with plutonium. The difficulty with coprocessing is precisely controlling the uranium concentration in the uranium-plutonium product to obtain a desired reactivity for fuel fabrication and reirradiation. This difficulty could be overcome by obtaining product at a higher plutonium concentration than desired for fuel fabrication and diluting with uranium to the precise concentration desired.

Figure 30 shows alternative ways of operating the B bank to obtain uranium-plutonium mixtures. Coprocessing is technically feasible for any mixture of uranium and plutonium, so the concentration of plutonium must be specified before a process can be designed. The upper limit will be determined by the requirement that the concentration of plutonium be too low for direct use in a nuclear weapon. This limit is presumed to be 11.7% plutonium in uranium, because 11.7% total Pu (60% ^{239}Pu, 25% ^{240}Pu, 15% ^{241}Pu) in natural uranium has been calculated to have the same reactivity as uranium enriched to 20% ^{235}U, the most highly enriched uranium that ERDA allows to be shipped without safeguards restrictions.[13] The lower limit will be about 5%, the concentration of plutonium necessary to make mixed-oxide (MOX) fuel for power reactors.

---

* In what follows, it is convenient to refer simply to the "B bank," because the calculations apply equally well to the 1B bank (Figure 24) or the 2B bank (Figure 29), i.e., to whichever cycle in which partitioning occurs.

13. *Physical Protection of Unclassified Special Nuclear Materials.* ERDA Manual 2405-0502.

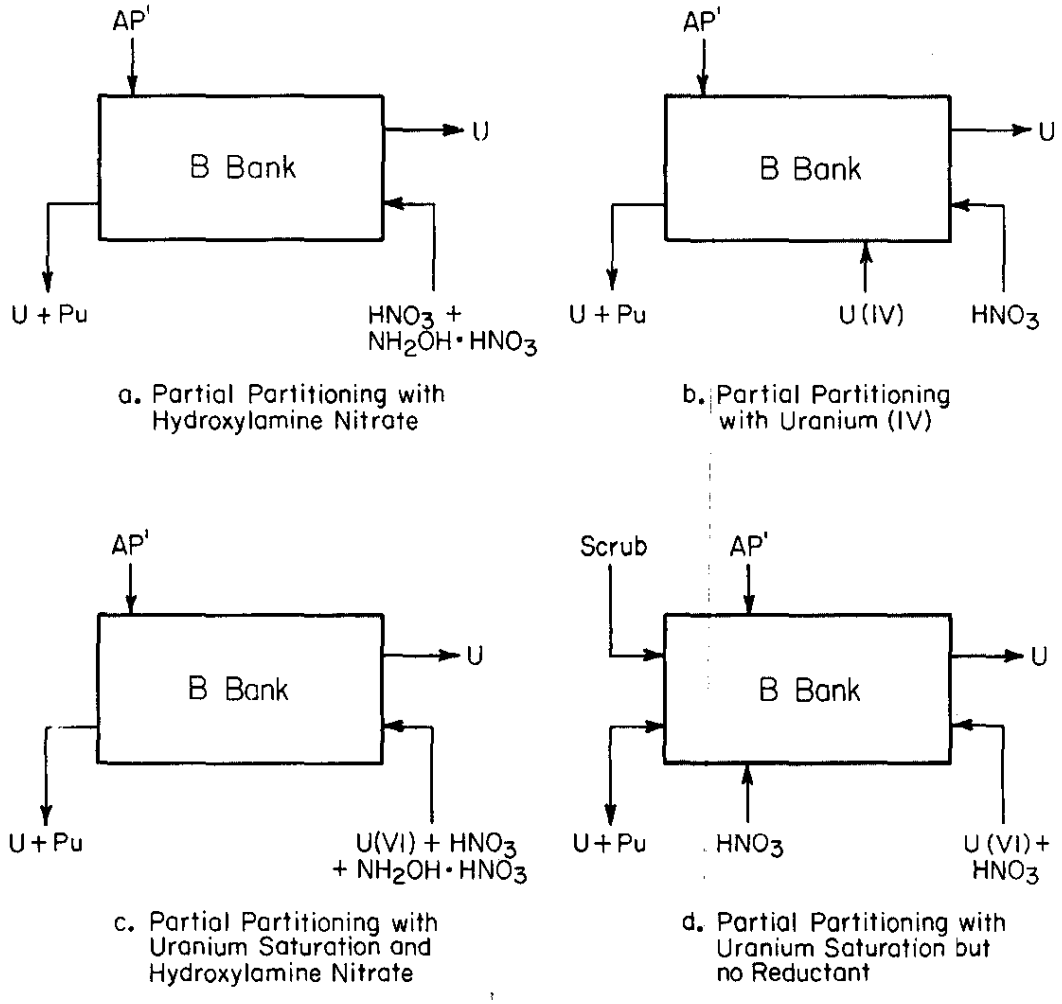

FIGURE 30. Alternative Operational Modes for Coprocessing Uranium and Plutonium in B Bank

Operating Modes

Figure 30a shows the preferred method of operating the B bank to ensure that uranium is present in the plutonium product. Eliminating the organic scrub stream would allow the uranium concentration in the aqueous product to be determined by the distribution of uranium between the organic and aqueous phases in the first stage (product exit). Since the uranium distribution depends on

nitric acid and total nitrate concentrations, the uranium concentration could be controlled by adjusting acidity and nitrate in the strip solution. Increasing the acidity and nitrate would decrease the uranium concentration in the product. Other factors, such as flow rates, temperature, and TBP concentration, will also affect the uranium concentration.

A reductant is needed to ensure complete stripping of plutonium. Hydroxylamine is suitable because it becomes less effective as the acidity increases[1,4,14] and would therefore limit the plutonium content of the product. Also, waste volumes from solvent extraction would be minimized, because hydroxylamine nitrate is converted to gases and water when destroyed by nitrous acid or boiling in nitric acid.[15] Since there is no organic scrub, reoxidation of plutonium by nitrite and re-extraction in the scrub section would not be a problem, and hydrazine would not be required to destroy nitrite. When hydrazine is absent, handling hydrazoic acid or azides is eliminated.

Figure 30b shows B bank operation with U(IV) reductant. Uranium(IV) strips plutonium better than other reductants because U(IV) can replace any Pu(IV) complexed by dibutyl phosphate.[3] Like hydroxylamine, U(IV) does not increase waste volumes, but does require stabilization with hydrazine. Reduction with U(IV) is less dependent on acidity than reduction with hydroxylamine, so that reduction with U(IV) could yield a product with a higher plutonium content.

Uranium(IV) could be produced electrolytically from a portion of the uranium product stream (1CU, Figure 24, or 2CU, Figure 29). However, recycling uranium would complicate accountability, because either uranium must be added or an inventory of uranium must be maintained. Furthermore, operation with U(IV) would require more feed streams to the contactor, complicating operation.

Figure 30c shows B bank operation with uranium saturation and some reductant. Uranium would be recycled from the 1CU (or 2CU) stream to saturate the organic phase with uranium and reduce the Pu(IV) distribution coefficient, so that Pu(IV) would be stripped without reduction. A low concentration of hydroxylamine nitrate would reduce any residual Pu(IV) to Pu(III), to complete

---

14. J. M. McKibben and J. E. Bercaw. *Hydroxylamine Nitrate as a Plutonium Reductant in the Purex Solvent Extraction Process.* USAEC Report DP-1248 (1971).

15. *LMFBR Fuel Reprocessing Program Progress Report for Period October 1 to December 31, 1976.* USERDA Report ORNL/TM-5768, pp. 3-22 (1977).

the stripping of plutonium. This mode of operation would ensure uranium in the plutonium and minimize added chemicals. However, computer calculations have shown that the product would contain too little plutonium (no more than 2%) for recycling as reactor fuel.

Figure 30d shows B bank operation with uranium saturation but no reductant. This variation of the previous mode would allow better control of plutonium and uranium in the product. However, Rosen and Zel'venskii evaluated this type of operation for complete partitioning of uranium and plutonium, and concluded that control would be difficult because small changes in solution flows or concentrations cause large changes in product concentrations.[16] Calculations at SRL reveal the same problem when the process is modified to yield a uranium-plutonium stream. These results are expected because operation at saturation means operation in a metastable state, where small changes in conditions can cause large changes in product concentrations.

The last two cases (Figures 30c and 30d) will not be studied further. The most promising case (Figure 30a) was investigated in more detail by computer studies and mini mixer-settler tests with simulated feed.

Computer Studies of Partial Partitioning with Hydroxylamine Nitrate

The effects of the different process variables for the most promising flowsheet (Figure 30a) were calculated with a modification of the SEPHIS program.[17] This program, which is based on the distribution coefficients of UO_2^{2+}, Pu^{4+}, and HNO_3, gives a good indication of those results that depend upon flow rates, concentrations, and temperature. However, the program does not allow for chemical reactions or the rate of Pu(IV) reduction. Pu(IV) reduction is simulated by entering a negative plutonium term and calculated as instantaneous and irreversible. Therefore, SEPHIS cannot predict the effect of different reductant concentrations; as far as SEPHIS is concerned, the main effect of hydroxylamine nitrate is to add inextractable nitrate.

---

16. A. M. Rozen and M. Ya. Zel'venskii. "Mathematical Simulation of Processes in the Extractive Reprocessing of Nuclear Fuel 4. Separation of Uranium and Plutonium by the Method of Displacement Re-extraction." *Sov. At. Ener. 41*, 91 (1976).

17. S. B. Watson and R. H. Rainey. *Modifications of the SEPHIS Computer Code for Calculating the Purex Solvent Extraction System.* USERDA Report ORNL-TM-5123 (1975).

Calculational Technique

Computer results were evaluated in terms of the increase in the amount of plutonium as a fraction of the total heavy metal (uranium + plutonium) concentration in the product stream relative to the feed. This was calculated for the B bank only, assuming a constant feed from the A or A' bank. Since the amount of plutonium in the feed will vary with different fuels, the relative increase in plutonium is more informative than the absolute value of the final concentration. A concentration factor (CF) was defined as

$$CF = \frac{\text{\% Pu in Total Heavy Metal in Product}}{\text{\% Pu in Total Heavy Metal in Feed}}$$

Based on the initial plutonium concentration, the concentration factor can be chosen to yield the desired product composition.

The importance of ten process variables in controlling the concentration factor was evaluated by a Plackett-Burman statistical screening design.[18] An "effect"* was calculated for each variable. The magnitude of each effect indicates the relative importance of the corresponding variable; those with effects greater than the minimum significant effect** are statistically significant in determining the concentration factor. The sign of the effect indicates whether the concentration factor increases or decreases as that variable increases.

Although there is no experimental error with computer calculations, the system is very complex. With a twenty-run design, the variation in concentration factor with random arrangements of the variables was very high. This variation was decreased considerably by using a 40-run design.

---

18. *Strategy of Experimentation,* p. 29. E. I. du Pont de Nemours & Co., Wilmington, DE (October 1975).

* In this design, each independent variable (e.g., nitrate concentration) is assigned either a high or low input value. The dependent variable (CF) is calculated for different combinations of high and low values for the variables.

$$\text{Effect} = \frac{\Sigma(\text{CF's when variable was high}) - \Sigma(\text{CF's when variable was low})}{\text{Number of cases for which independent variable was high}}$$

** The minimum significant effect at the 95% confidence level is estimated by calculating the effect as above, but with a random arrangement of high and low levels of independent variables.

Predicted Importance of Process Parameters

Variables tested included flow rates, concentrations, temperature, and number of stages. Ranges were chosen to reflect reasonable operating conditions. Variables are ranked in Table 31 according to the magnitude of their effects on the concentration factor. The three most important variables are inextractable nitrate concentration, % TBP in the BF organic feed to the B bank from the A or A' bank, and the BX aqueous extractant (hydroxylamine nitrate + nitric acid) flow rate. Uranium concentration in the BF stream, the BF flow rate, and temperature are also important. Plutonium concentration and acidity of the BF stream, acidity of the BX stream, and the number of mixer-settler stages are without significant effect.

In practice, the % TBP, temperature, and probably the uranium concentration will be held constant. The concentration factor will then be controlled by varying the flow rates and the nitrate concentration in the BX stream. The flow ratio and nitrate concentration necessary to yield the desired concentration factor can be determined from plots such as Figure 31.

TABLE 31

Effect of Process Variables in B Bank

Variable	*Range*	*Effect*
Significant		
Nitrate in BX	0.2 to 1.5M	+21.9
TBP in BF	25 to 35%	+14.5
BX Flow Rate	0.35 to 1.0 mL/min	-13.3
Uranium in BF	60 to 95 g/L	- 8.9
BF Flow Rate	2.0 to 3.5 mL/min	+ 8.2
Temperature	30 to 50°C	- 7.4
Not Significant[a]		
Plutonium in BF	0.4 to 1.0 g/L	- 4.3
Acidity of BF	0.04 to 0.15M	+ 3.7
Number of Stages	12 to 20	- 2.1
Acidity of BX	0.2 to 0.75M	+ 1.0

a. Minimum significant effect = ±4.5.

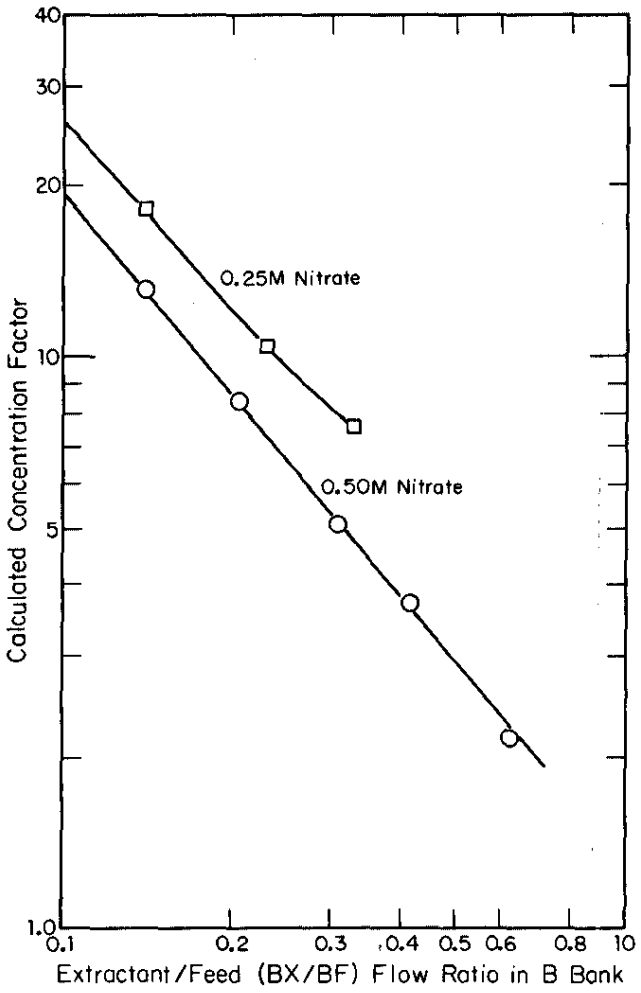

FIGURE 31. Plutonium Concentration Factors Calculated by SEPHIS

Although the acidity of the BX and BF, the plutonium content, and the number of stages are not statistically significant, they may still have some effect because of interactions with other variables. Additional calculations holding the other parameters constant at an intermediate level show that the concentration factor increases slightly with increasing acidity and decreases with increasing plutonium concentration. However, as expected, the changes are small.

The BX acid concentration is least important, but its range is limited by other considerations. The acidity must not be less than 0.1M, to avoid formation of plutonium hydroxide polymer.[19]

19. V. L. Schuelein. *Parameters for Plutonium Polymer Formation in Nitric Acid.* USERDA Report ARH-SA-233 (1975).

Once formed, the polymer is very stable and would result in large plutonium losses during further processing. The diminished stability of hydroxylamine and the slower rate of Pu(IV) reduction at high acidity sets an upper limit on the concentration of nitric acid in the BX stream.

Mixer-Settler Tests with Simulated Feed

Mixer-settler tests with simulated feed demonstrated plutonium concentration factors ranging from 6 to 28. The B bank operated effectively with less than 0.03% loss of plutonium to the BU stream. The conditions derived from SEPHIS calculations were adequate for predicting the concentration factors for these tests.

Conditions for a range of plutonium concentration factors were calculated by SEPHIS. The actual concentration factor needed to yield a given plutonium/uranium ratio in the product will vary with the initial plutonium concentration. The availability of a range of concentration factors will allow coprocessing of fuel of any composition to the desired plutonium/uranium ratio.

Experimental Technique

Three tests were run in the mini mixer-settlers, with target concentration factors of 5, 13, and 26. The same feed was used in all tests (Table 32). The plutonium content was 0.9% of the total heavy metal content, typical of LWR fuel. Before each test, the feed was sparged with air to remove NO_x species and minimize possible reoxidation of plutonium by nitrite. The tests were run for 10 to 12 hours for two consecutive days. Test conditions are summarized in Tables 32 and 33.

A-bank conditions were identical for the three tests. Analysis of the AP product stream indicated effective A-bank operation; uranium, plutonium, and acid concentrations were very close to those predicted by SEPHIS calculations. Feed compositions used to calculate B-bank conditions were therefore very close to actual conditions. Losses to the AW waste stream were low, although slightly higher than design values. Since the objective of the tests was to evaluate B-bank operation, A-bank conditions were not adjusted.

In all three tests, a large excess of hydroxylamine nitrate was used. This amount of reductant should not be necessary to ensure complete reduction of plutonium in this flowsheet. There is no scrub section and reoxidation of plutonium should not be as serious a problem as in the usual Purex process. However, because

hydroxylamine nitrate also serves as a source of inextractable nitrate, its concentration is critical. To obtain concentration factors in the range of 5 to 25, the concentration of inextractable nitrate should range from 0.5 to 0.75M, which corresponds to a 20- to 45-fold excess of hydroxylamine nitrate, depending on the flow rates. Therefore, the amount of hydroxylamine nitrate was determined primarily by the need for nitrate salt rather than for reductant.

TABLE 32

A-Bank Operating Conditions for All Tests With Simulated Feed

Stream	*Composition*	*Stage*	*Flow, mL/min*
CAF	250 g/L U 2.3M HNO_3	8	0.75
HAF	250 g/L U 2.3 g/L Pu 2.3M HNO_3	8	0.75
AX	30% TBP	16	2.14
AS	1.0M HNO_3	1	0.40

TABLE 33

Calculated and Observed Concentration Factors

Test	*BX Composition, M* $NH_2OH \cdot HNO_3$	HNO_3	*BX Flow, mL/min*	*Concentration Factor* Observed	Calculated	*Obs-Calc, % Difference*
1	0.50	0.20	0.65	6.1	5.2	17
2	0.50	0.20	0.30	17.6	13.1	34
3	0.75	0.50	0.21	27.4	26.0	5

Comparison of Test Results with SEPHIS Calculations

Measured concentration factors for all three tests were 5% to 34% higher than predicted by SEPHIS calculations (Table 33). These differences are due to slight deviations in actual test conditions from those specified for the calculations, and to the failure of the calculational model to duplicate the real system.

The two test conditions in which deviations are most likely to have caused the large differences in the concentration factor here are (1) TBP concentration, and (2) BX flow rate. The TBP concentration actually used was high (31%). Since the % TBP has a large positive effect on the concentration factor (Table 31), observed concentration factors would be expected to be higher than calculated.

Table 31 shows that the concentration factor is also sensitive to the BX flow rate. Figure 32 shows that at low flow rates, slight changes in flow rate cause significant changes in the concentration factor. This effect is greater for Tests 2 and 3 than for Test 1. However, the difference between calculated and observed concentration factors is less for Test 3 than for Test 2, despite the lower BX flow rate for Test 3 (steeper part of curve). An additional factor in Test 2 was the large variation in BP uranium content; the uranium concentration in samples taken after equilibrium had been reached varied as much as 13%, whereas the variation was less than 5% for Tests 1 and 3. This trend agrees with SEPHIS calculations, which indicated that the uranium variability would be higher at low nitrate concentrations and high concentration factors, as in Test 2.

Although SEPHIS predicts concentration factors reasonably well, it does not predict uranium and acid concentration profiles in the bank. The SEPHIS plutonium profile is meaningless because of the artificial way in which plutonium reduction is treated. Therefore, the program cannot be relied on to duplicate the real system. SEPHIS calculations are useful as a first approximation of the conditions needed to produce a given concentration factor, but exact conditions will have to be determined by experiment.

In all three tests, equilibrium was reached within about six hours, and after that the banks were stable. The plutonium concentration in the BP and BU streams leveled off (Figure 33). Analyses showed that the BP accounted for 95 to 99% of the plutonium in the feed. Allowing for dilution effects and experimental error, this is equivalent to total plutonium recovery. Plutonium losses to the BU did not exceed 0.03%.

Because of the low plutonium losses to the BU, the plutonium decontamination factors for the uranium stream were high (Table 34). However, this degree of decontamination would be insufficient to allow coprocessing by the flowsheet shown in Figure 29 if an overall decontamination factor of 2×10^8 to 4×10^8 is required. Achievement of such an overall decontamination factor would probably require two additional uranium-purification cycles. Consequently, the most likely candidate is still the flowsheet shown in Figure 24, with a modified 1B bank.

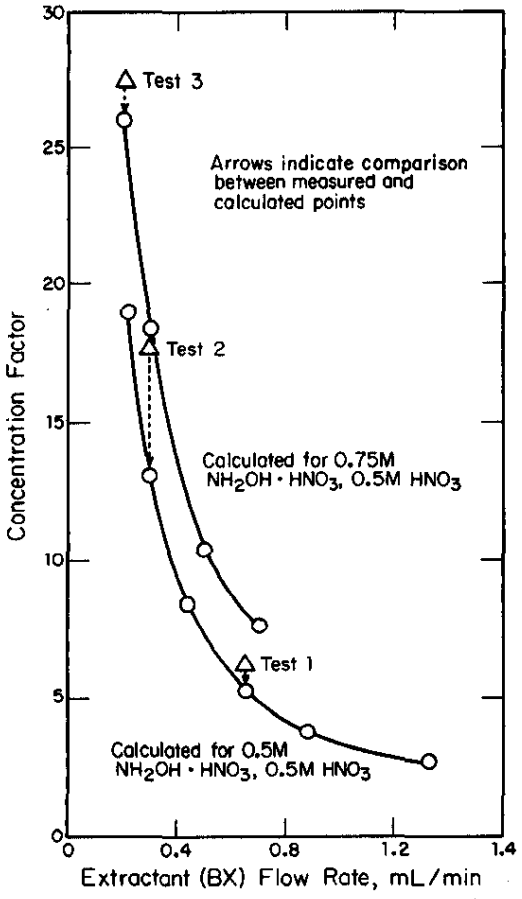

FIGURE 32. Effect of Extractant Flow Rate on Plutonium Concentration Factor in B bank

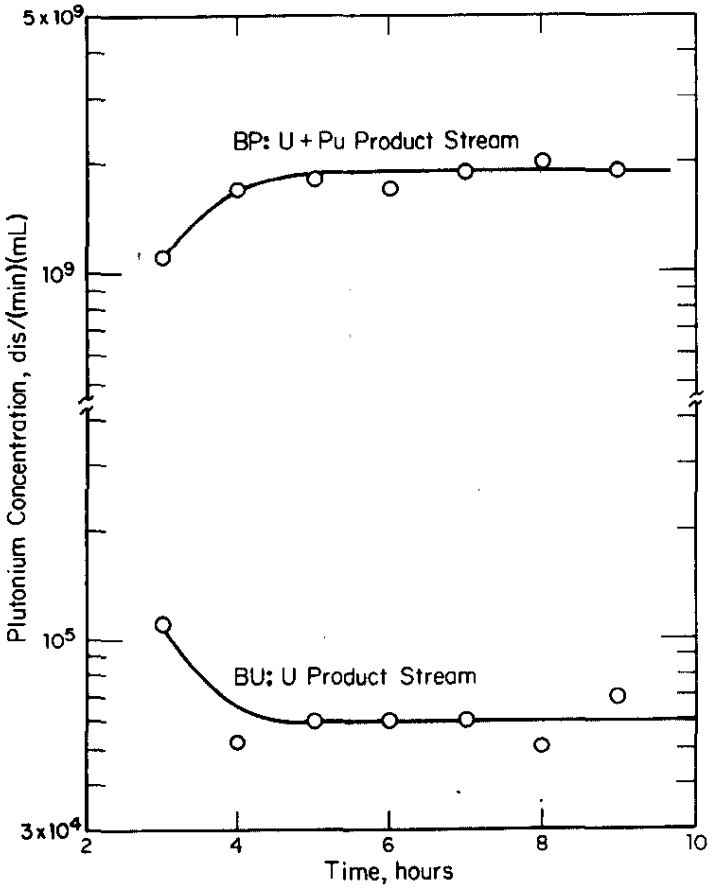

FIGURE 33. Observed Equilibration of Plutonium in B-Bank Product Streams

TABLE 34

Decontamination of Uranium Product from Plutonium

Test	*Plutonium Decontamination Factor*
1	3×10^3
2	8×10^3
3	4×10^3

Partitioning During Test LWR-6

As noted on page 75, the B bank did not partition effectively during Test LWR-6, and plutonium losses to the BU uranium product stream were high.

Conditions were chosen to achieve a plutonium concentration of 20% of the heavy metal content in the BP. Since the initial plutonium concentration was 0.56%, a concentration factor of 36 was required. Under the conditions necessary to obtain this concentration factor, hydroxylamine nitrate did not effectively reduce the plutonium, causing high losses.

The BX extractant flow was 0.30 mL/min; composition was 0.5M $NH_2OH \cdot HNO_3$ (a 60-fold stoichiometric excess) and 1.0M HNO_3. The feed was not air-sparged before the test. Analysis of the A and A' product streams indicates that no plutonium losses occurred there.

The plutonium concentration in the BP leveled off after about six hours. However, plutonium losses to the BU increased steadily to a maximum of 27% at the end of the test (Table 35). At the end, nearly 100% of the total plutonium in the feed was appearing in the BP and BU streams, indicating that equilibrium had probably been reached. The B-bank plutonium profile of Test LWR-6 is compared to that of Test 2 in Figure 34. The concentration buildup shows that plutonium is refluxing in the bank, which explains why attainment of equilibrium was slow.

The high plutonium losses cannot be explained by reoxidation of Pu(III). The reducing normality of the BP indicated that 60% of the $NH_2OH \cdot HNO_3$ was still present, which should have been sufficient to prevent reoxidation of Pu(III). However, the acid concentration in the aqueous phase of the latter B-bank stages was 1.6 to 1.7M; at this acidity, reduction is much slower and only part of the plutonium may have been reduced. These conditions then represent an upper limit for the acid concentration in the BX if hydroxylamine nitrate is the reductant.

TABLE 35

Plutonium Content of the BP and BU Product Streams During the LWR-6 Test

Time, hours	*% of Plutonium in the Feed Appearing in*		
	BP	*BU*	*BP + BU*
4	52.2	1.1	53.3
5	58.9	7.0	65.9
6	64.4	12.4	76.8
7	64.4	11.5	75.9
8	69.3	14.8	84.1
9	69.3	27.2	96.5

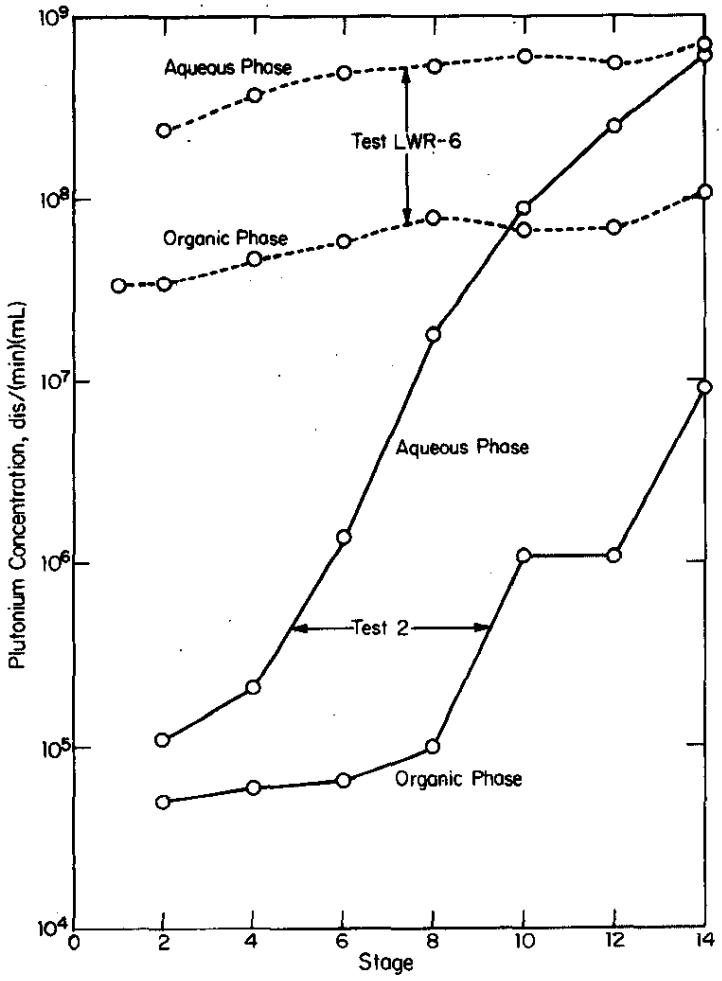

FIGURE 34. Plutonium Profiles in B Bank During Test LWR-6 and Test 2

Continuing Study

- Partial-partitioning tests with hydroxylamine nitrate and uranium(IV) + hydrazine reductants will be continued.
- The nature and rates of reactions in the organic phase during partial partitioning will be investigated.

ELECTROLYTIC REDUCTION OF URANIUM TO U(IV)

A FORTRAN program has been written to model the electrolytic reduction of U(VI) in nitric acid solution at a platinum electrode. Calculated rate-time curves, which are consistent with experimental measurements, have been generated with this mathematical model of the U(VI):U(IV) electrochemical system. If combined with a mathematical model of the electrolytic cell, the reduction model can be used to calculate U(IV) production rates and aid in the conceptual design of a plant-scale cell.

In principle, uranium(IV) can be substituted for ferrous sulfamate in the 1B bank of the solvent extraction process,[20] which would significantly reduce the amount of waste generated (about 20% for SRP; about 10% for a plant processing light water reactor fuels). In addition, elimination of ferrous sulfamate, which forms ferric sulfate, would simplify waste management, because sulfate interferes with conversion of waste to glass forms. Previous studies of U(IV) preparation were summarized in the June 1976 report.[21]

Theoretical Basis

The model is based on the presence of a partial monolayer of hydrolyzed U(IV) on the electrode surface. The reduction rate of uranyl ion is assumed to be different on the platinum surface covered with $U(OH)_4$ than on the bare platinum surface.

The $U(OH)_4$ results from the hydrolysis of U(IV) in the diffusion layer. It is assumed that adsorption of $U(OH)_4$ follows the Langmuir isotherm, so that the adsorption equilibrium constant ψ is given by

$$\psi C_4(0,t) = \frac{\Gamma}{\Gamma_s - \Gamma} [C_H(0,t)]^4 \qquad (1)$$

where

$C_4(0,t)$ = concentration of U(IV) at the electrode surface at time t, moles/cm^3

$C_H(0,t)$ = concentration of H^+ at the electrode surface at time t, moles/cm^3

---

20. *Savannah River Laboratory Quarterly Report, Light Water Reactor Fuel Recycle, October-December 1976.* USERDA Report DPST-LWR-76-1-4, p. 49.

21. *Savannah River Laboratory Quarterly Report, Light Water Reactor Fuel Recycle, July-September 1976.* USERDA Report DPST-LWR-76-1-3, p. 46..

Γ = concentration of $U(OH)_4$ on the electrode surface when the surface is partially covered by a monolayer, moles/cm^2

Γ_s = concentration of $U(OH)_4$ on the electrode surface if the surface is completely covered by a monolayer, moles/cm^2 ($\Gamma_s \geq \Gamma$)

Reduction of UO_2^{2+} is assumed to be irreversible. The reaction rate of UO_2^{2+} on $U(OH)_4$ is proportional to the area of the electrode covered with $U(OH)_4$; the reaction rate of UO_2^{2+} on platinum is proportional to the bare area of the electrode. The electrolytic current i (amp) is then given by

$$i = nFA\left[\frac{\Gamma_s - \Gamma}{\Gamma_s} k_{Pt} + \frac{\Gamma}{\Gamma_s} k_{UOH}\right] C_6(0,t) e^{-\alpha nF(E-E_c^\circ)/RT} \qquad (2)$$

where

n = number of electrons transferred per UO_2^{2+} ion reduced

F = Faraday constant, 96500 (amp)(sec)/mole

A = total area of electrode, cm^2

k_{Pt} = heterogeneous rate constant on bare Pt surface, cm/sec

k_{UOH} = heterogeneous rate constant on Pt covered by $U(OH)_4$, cm/sec

$C_6(0,t)$ = concentration of U(VI) at the electrode surface at time t, moles/cm^3

α = symmetry factor, dimensionless ($0 \leq \alpha \leq 1$)

E = applied electrolysis potential, volts

E_c° = standard electrode potential for irreversible reduction of UO_2^{2+} to U(IV), volts

R = gas constant, 8.314 joules/(degree)(mole)

T = temperature, °K

Since the amount of adsorbed uranium is negligible compared to the bulk concentrations, the above equations can be combined with the corresponding equations for the flux in a stirred solution to give

$$C_6(0,t) = \frac{C_6(\infty,t)}{1 + \frac{\delta}{D_U}\left[k_{Pt} + \frac{\Gamma}{\Gamma_s}(k_{UOH} - k_{Pt})\right] e^{-\alpha nF(E-E_c^\circ)/RT}} \qquad (3)$$

$$\psi[C_U^* - C_6(0,t)] = \frac{\Gamma}{\Gamma_s - \Gamma}\left[C_H^* - 4C_U^* + 4C_6(\infty,t) - \frac{4D_U}{D_H}\{C_6(\infty,t) - C_6(0,t)\}\right]^4 \quad (4)$$

and

$$\frac{dC_6(\infty,t)}{dt} = \frac{-\frac{A}{V}\left[k_{Pt} + \frac{\Gamma}{\Gamma_s}(k_{UOH} - k_{Pt})\right] C_6(\infty,t) e^{-\alpha nF(E-E_c^\circ)/RT}}{1 + \frac{\delta}{D_U}\left[k_{Pt} + \frac{\Gamma}{\Gamma_s}(k_{UOH} - k_{Pt})\right] e^{-\alpha nF(E-E_c^\circ)/RT}} \quad (5)$$

where

$C_6(\infty,t)$ = concentration of U(VI) in the bulk of the solution at time t, moles/cm^3

δ = thickness of diffusion layer, cm

D_U = diffusion coefficient for UO_2^{2+}, cm^2/sec

D_H = diffusion coefficient for H^+, cm^2/sec

C_U^* = initial concentration of UO_2^{2+} in the bulk of the solution, moles/cm^3

C_H^* = initial concentration of H^+ in the bulk of the solution, moles/cm^3

V = volume of electrolytic cell, cm^3.

The OREBA Program

The FORTRAN code OREBA solves these equations to provide rate-time curves.

Because of the fourth-power term in Equation 4, a numerical method (subroutine INTPL) is used to eliminate $C_6(0,t)$ from Equations 3 and 4 and to solve for Γ in terms of $C_6(\infty,t)$. Equation 5 is then solved for $C_6(\infty,t)$ by Runge-Kutta numerical integration.

OREBA calculates and prints the electrolysis current i, the bulk concentration of uranyl ion $C_6(\infty,t)$, and the surface coverage Γ, all as functions of time. In addition to this tabular output, the program plots calculated electrolysis current vs. time for rapid comparison with experimental data. Other calculated quantities can also be plotted as desired.

ALTERNATIVES FOR STORAGE OF HIGH-LEVEL LIQUID WASTE

Alternative methods for interim storage of high-level liquid waste (HLLW) from processing spent LWR fuel were evaluated. Objectives were to minimize capital and operating costs, and to improve the safety of large inventories of HLLW in storage. This study indicates that:

- Prompt solidification of HLLW and storage of the waste canisters in water-cooled basins saves at least $92 million in capital costs compared to the other alternatives that were evaluated. Also prompt solidification is probably the safest method of handling nuclear waste because more waste would be in an immobile, nonleachable form, and current technology can be used for cooling waste canisters in water-cooled basins.

- Separation of cesium and strontium from HLLW before interim storage has no advantage unless there is a firm long-term requirement for fission-product heat sources to justify the additional processing costs.

- Enlarging the storage basin to increase the decay time of spent fuel from one year between reactor discharge and processing to five years significantly reduces the specific power of the HLLW. But the additional basin capacity for storing the spent fuel would require a capital investment of about $100 million more than would prompt solidification of waste decayed only one year. Furthermore, an inventory charge would probably have to be added for the fuel value of uranium and plutonium that would be unavailable for use during the extra storage period before processing.*

Alternative Methods Evaluated

The following methods for storing HLLW from processing spent LWR fuel at a rate of 10 metric tons of uranium (MTU) per day were analyzed:

---

* An annual interest charge of $40 million can be associated with 12,000 MTU of fuel in the basin.

Method 1. Reprocess LWR fuel after a decay period of at least one year after reactor discharge, and store acidic HLLW in cooled stainless-steel tanks about four years before solidification and vitrification in a form suitable for terminal waste storage. Then, store canisters of solidified waste onsite about five years before shipping to a terminal storage facility.

Method 2. Like Method 1, except separate cesium and strontium from HLLW before transfer to tank storage. Solidify and package cesium and strontium for possible sale as fission-product heat sources. If cesium and strontium cannot be sold, recombine with other solidified waste for vitrification.

Method 3. Reprocess LWR fuel after a decay period of at least one year after reactor discharge. Store HLLW for minimum period before solidification and vitrification. Store waste canisters for about 9 years in a water-cooled basin before sealing within outer canisters (double containment, "overpacking") for shipment to a terminal waste storage facility.

Method 4. Reprocess LWR fuel about five years after reactor discharge. Store a four-year inventory of LWR fuel at the reprocessing plant. Store HLLW for a minimum period before solidification and vitrification of the waste products. Store waste canisters for about five years before overpacking and shipment to a terminal waste storage facility.

Technical features of the four methods are summarized in Table 36, capital costs are presented in Table 37, and the schedules for each method are given in Table 38.

Technical Features

Decay Heat

The total decay heat in spent fuel and waste at the LWR reprocessing complex is about 80 MW for all methods analyzed. However, as shown in Table 36 the distribution of power differs among the options. In Method 1, most of the power is generated in the liquid waste, but in Methods 3 and 4, the power is generated in either solidified waste or fuel assemblies.

The power decay of waste associated with one metric ton of LWR fuel is shown as the major curve in Figure 35 for 30 MW/MTU power and 30,000 MWD/MTU (nominal goal for fuel from pressurized water reactors). Actual power decay will vary with the power history of

TABLE 36

Comparison of Methods for Storing High Level Liquid Waste (HLLW) from Processing Spent LWR Fuel

	Method 1: Store HLLW	*Method 2: Separate Cs/Sr*	*Method 3: Store Canisters*	*Method 4: Store Fuel*
Fuel Storage Basin, MTU	850	850	850	12,850
Fuel Storage Basin Area, ft^2	4,000	4,000	4,000	64,000
Fuel Storage Basin Volume, gal × 10^6	3.5	3.5	3.5	32
Stored Volume of HLLW, gal × 10^6	1.8	1.8	0.3	0.1
Volume Waste Tank, gal × 10^6	0.3	0.3	0.15	0.1
Number of Waste Tanks (One spare assumed)	7	7	4	3
Waste Containers in Plant Storage	4,680	4,680	8,800[a]	5,000[a]
Waste Storage Basin Area, ft^2	18,700	18,700	35,200	20,000
Waste Storage Basin Volume, gal × 10^6	4.3	4.3	7.0	4.5
Total Basin Volume, gal × 10^6	7.8	7.8	10.5	36.5
Power in LWR Spent Fuel and Waste at Reprocessing Plant, MW, in:				
Stored Fuel	10	10	10	62
Stored HLLW	52	27	11	1
Stored Solid Waste	20	20	61	19
Stored Cs/Sr	0	0-25[b]	0	0
Total	82	57-82	82	82
Maximum Adiabatic Temperature Rise of Coolant, °C/hr, in:				
HLLW Tanks	8-13[c]	8-9[c]	8-14[c]	2
Storage Basin	0.9	1.6	1.5	0.4
Minimum Time to Start to Boil Coolant, hours				
HLLW Tanks	5	5	5	5
Basin	46	25	26	90
Time Interval for HLLW Level to Decrease One Foot, hours	3.6	3.6	3.5	>10
Water Makeup Necessary to Maintain HLLW Tank Level if Boiling Occurs, gpm				
Maximum Tank	80	80	40	5
All Tanks	360	200	80	10

a. An additional allowance for about 10% more waste containers was made for Methods 3 and 4 because the smaller HLLW tank holdup may lead to less uniform power generation per container than in Method 1.

b. Range depends on amount of cesium and strontium sold for isotopic heat sources.

c. The higher temperature rise would be encountered if the HLLW were concentrated to 150 gal/MTU as generated (see Table 39).

the fuel reprocessed; for example fuel from boiling water reactors is forecast to be discharged at 27,500 MWD/MTU after a lower-power history. The effect of lower exposure is shown in Figure 35 (squares vs. circles).

The effect of removing cesium and strontium on waste power generation is also shown in Figure 35, for use in evaluating Method 2.

TABLE 37

Comparison of Capital Costs of Methods for Storing HLLW

	Capital Costs, millions of FY-1977 dollars			
Variable Cost Item	*Method 1: Store HLLW*	*Method 2: Separate Cs/Sr*	*Method 3: Store Canisters*	*Method 4: Store Fuel*
Fuel Basin	25	25	25	194 (221[a])
Waste Basin plus Auxiliaries (from Table 19)	13	24	39	20
HLLW Tanks	166	154	50	20
Waste Tank Services	33	31	10	4
Off-Gas System				
Spray Drier and Ru Off-Gas	-	-	15	-
Separation of Cs and Sr	-	50	-	-
Total	237	284	139	231
Difference	98	145	-	92

a. The higher estimate of basin cost is based on the general cost relationship up to 4000 MTU extended to the 12,850 MTU requirement.

TABLE 38

Schedule for Methods for Storing HLLW

	Time Required, years			
	Method 1: Store HLLW	*Method 2: Separate Cs/Sr*	*Method 3: Store Canisters*	*Method 4: Store Fuel*
Fuel Decay Before Reprocessing, after discharge from LWR	1	1	1	5
Interval for HLLW Storage	4	4	0.4	0.2
Interval for Solid Waste Storage Before Shipment to Permanent Storage	5.2	5.2	8.8	5.0
Total	10.2	10.2	10.2	10.2
Fuel Decay at Waste Solidification	5	5	1.4	5.2
Total Time Fuel and Waste are at Plant	9.2	9.2	9.2	9.2

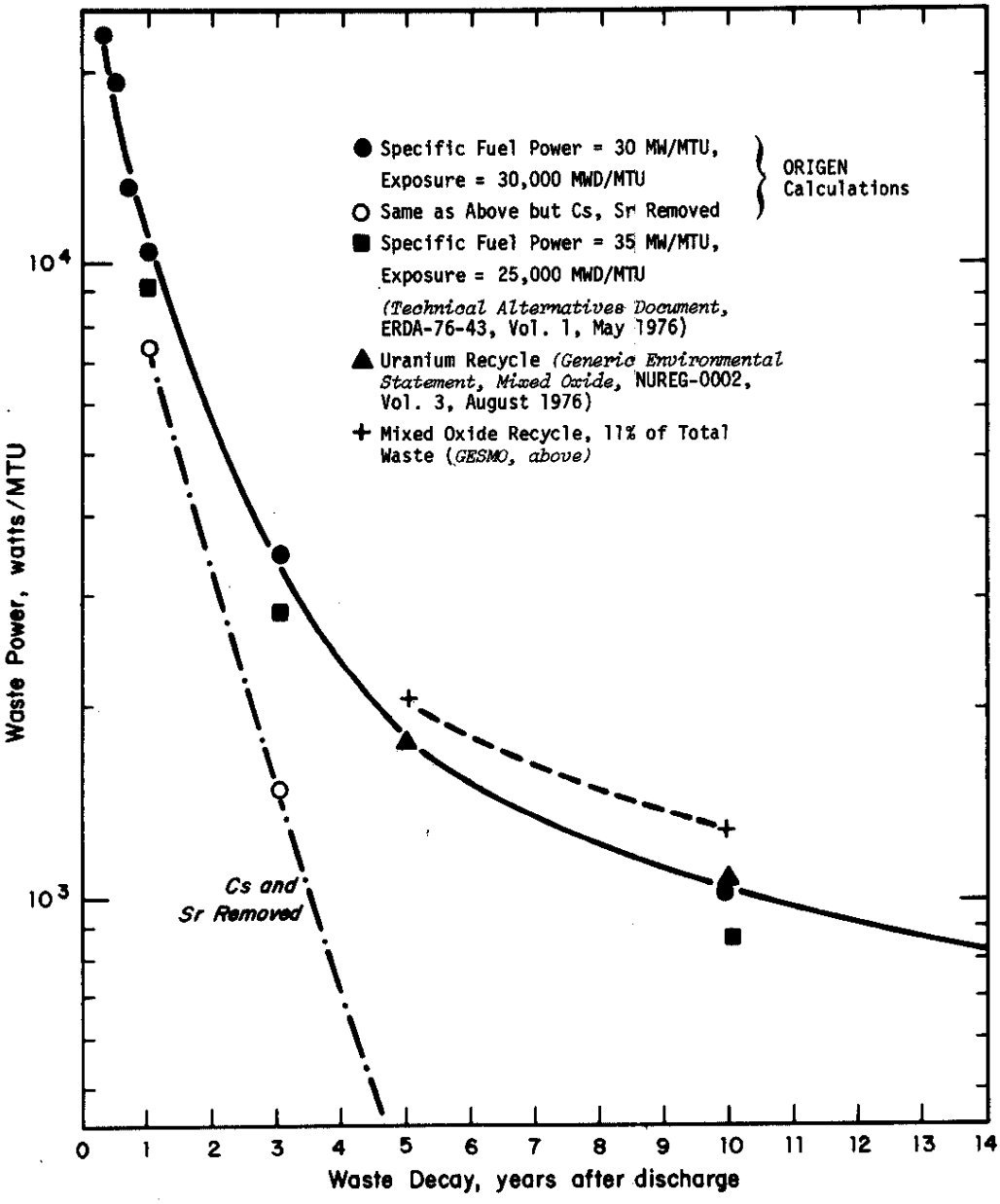

FIGURE 35. Power Generation in LWR Waste

The effect of reprocessing mixed-oxide (MOX) fuel on the waste power decay, also illustrated in Figure 35, is small. Reprocessing MOX would not be anticipated until years after reprocessing plant startup. Scheduling of MOX reprocessing so that MOX wastes are mixed with waste from fuel with lower power generation might be a feasible method to reduce further the effects of the slower power decay in MOX fuel.

HLLW Waste Tanks

Waste tank requirements for storage of HLLW from reprocessing fuel by each method are summarized in Table 39. For each method, heat removal requirements for each tank are based on 150 gal of HLLW/MTU, with no liquid transfer between tanks. Method 1 requires from 4 to 17 MW of tank cooling. However, it would be less expensive to avoid maximum tank cooling requirements by adjusting the concentration of HLLW and allowing transfer of waste among tanks as it decays, as planned by Allied-General Nuclear Services for the Barnwell Nuclear Fuel Plant. For example, as shown in Table 39 for Method 1, three tanks could be provided with less cooling capacity. As the waste in any one of the lower-cooling-capacity tanks is removed for solidification, the waste in one of the higher-cooling-capacity tanks could be pumped into the emptied tank, and then the just emptied high-cooling-capacity tank would be available to receive fresh waste.

With 11 MW generated in 300,000 gallons of HLLW at 60°C, a maximum adiabatic heating rate of 8°C/hour is equivalent to a 5-hour interval without cooling before restoring normal heat removal to prevent boiling in a waste tank. The same heat-up rates were used for the other methods shown in Table 39.

Solid Waste Canisters

For all four methods, solid wastes are assumed to be vitrified in canisters with a nominal 12-inch inside diameter and an active height of 7.1 ft (7.2 ft with fins). The dimensions of the waste canister are not variables because the size is based on the limitations of emplacement in salt after 10 years of decay (250°C surface temperature). Waste canisters described in terminal heat transfer studies are frequently one foot in diameter by 10 feet long, but length has little effect on terminal waste canister temperatures. Some estimates of finned canister temperatures (Table 40) indicate that the maximum temperature of glass waste will be about 300°C (surface temperature 250°C plus centerline-to-surface temperature difference at 60°C) if waste decays 10 years before vitrification.

TABLE 39

HLLW Tank Data

	Tank 1	*Tank 2*	*Tank 3*	*Tank 4*	*Tank 5*	*Tank 6*
Method 1[a]						
If Waste Rate = 150 gal/MTU:						
Decay Heat in Tank, MW	17.4	11.6	8.3	5.6	5.0	4.0
Adiabatic Heating Rate, °C/hr	13.2	8.8	6.3	4.2	3.8	3.0
Time to Boil (from 40°C), hr	3	4.5	6.3	9.4	10.5	13.2
If Tank Cooling Capacity = 11 MW:						
Decay Heat in Tank, MW	11	11	11	8.0	5.0	4.6
Waste Rate, gal/MTU	250	188	136	130	130	130
Days of Storage	120	160	220	230	230	230
Adiabatic Heat Rate, °C/hr	8.2	8.2	8.2	6	4.5	3.5
Time to Boil, hr	4.8	4.8	4.8	6.5	9	11
Method 2[a]						
If Waste Rate = 150 gal/MTU						
Tank Decay Heat, MW	11.6	6.8	4.0	2.4	1.5	1.0
Adiabatic Heat Rate, °C/hr	8.8	5.2	30.	1.8	1.1	0.8
Time to Boil, hr	4.5	7.7	13.2	22	35	52
If Tank Cooling Capacity = 11 MW:						
Decay Heat in Tank, MW	11	6.1	4.6	2	1.5	1.5
Waste Rate, gal/MTU	158	165	130	180	150	125
Days of Storage	190	180	230	160	200	240
Adiabatic Heat Rate, °C/hr	8.2	4.7	3.5	1.5	1.1	0.9
Time to Boil, hr	4.8	8	12	26	35	44
Method 3[b]						
If Waste Rate = 150 gal/MTU						
Tank Decay Heat, MW	9.6	7.8	-			
Adiabatic Heat Rate, °C/hr	19.6	11.9	-			
Time to Boil, hr	2.7	3.4	-			
Days of Storage,[c] maximum	100	100	-			
If Tank Cooling Capacity ≤6 MW:						
Decay Heat in Tank, MW	5.5	5.8	5.8			
Waste Rate, gal/MTU	270	240	215			
Adiabatic Heat Rate, °C/hr	8.5	8.8	9.0			
Time to Boil, hr	4.7	4.5	4.4			
Days of storage						
Maximum	55	62	70			
Typical[c]	28	60	35			
Method 4[d]						
If Waste Rate = 150 gal/MTU:						
Decay Heat in Tank, MW	1.0	1.0				
Adiabatic Heat Rate, °C/hr	2.4	2.4				
Time to Boil, hr	16.8	16.8				
Days of Storage						
Maximum	66	66				
Typical[e]	33	33				

a. Each of the six tanks, typically 54 feet in diameter and 20 feet high, would hold 300,000 gallons when 88% full.

b. Either two or three tanks are used for Method 3. Each tank, typically 38 feet in diameter and 20 feet high, would hold 150,000 gallons when 88% full.

c. Waste tank power is shown for full tanks. With 120 days storage, the HLLW power inventory is reduced to 11 MW, and minor upsets in front end operations or waste solidification can be accommodated in the surge volumes of the HLLW tanks.

d. Each of the two tanks, typically 31 feet in diameter and 20 feet high, would hold 100,000 gallons when 88% full.

e. Tanks half full.

TABLE 40

Temperatures of Air-Cooled Waste Canisters

Waste Decay, years:			*1.0*	*1.5*	*2.0*	*5.0*	*9.0*	*10*	*13*
Waste Power, kW/MTU:			*10.50*	*7.70*	*5.80*	*1.77*	*1.11*	*1.04*	*0.90*
Canister									
Diam; ft	*Glass Height, ft*	*Fins ?*	*Centerline to Surface ΔT, °C*						
1	7.1	No	1242	911	680	209	131	123	101
		Yes	620	455	340	105	65	60	50
1	10.0	No	882	647	483	-	-	-	-
		Yes	441	323	242	-	-	-	-
0.83	10.0	No	860	630	470	-	-	-	-
		Yes	430	315	235	-	-	-	-
			Surface to Air ΔT, °C						
1	7	Either	~1000	-	-	340	240	-	-
			Power Generation in Canister, kW						
1	7	Either	35	-	-	5.9	3.7	-	-

In Method 3, the waste is solidified as soon as possible after reprocessing and then stored. The canister design assumes a maximum glass temperature of about 500°C for single-wall canister storage in a water-cooled basin (decay time of 1.5 years). Several options are evaluated in Table 40 to modify the canister design for waste solidification after decay for as little as one year. If glass temperatures over 500°C are undesirable, the diameter might be reduced from 12 to 10 inches, or the waste might be diluted by increasing the canister length from 7.2 to 10 feet. Higher glass temperatures might also be permitted by further refinement of fin design; fins accelerate melting of the glass frit, but they also reduce core temperatures during storage.

Initial plant processing with aged fuel will permit equipment shakedown and a gradual approach to shorter decay periods for waste before vitrification and consequent higher heat generation in glass cores.

Devitrification of glass waste increases its leachability. Devitrification may occur if glass is reheated to 500°C after initial solidification. The effect of high heat generation in the waste during vitrification is to add to the furnace heat in forming the melt and then to extend the annealing time for the core as the glass solidifies. Therefore, glass formed with waste and aged only one year may be no more leachable than glass containing aged waste.

Costs

Basin Costs

Characteristics of fuel storage basins are summarized in Table 41. The variable costs** for each method are given in Table 42. Some of the basin cost (such as cask unloading facilities) is associated with plant throughput, which is constant for all methods. Costs of fuel storage basins range from $25 million (850 MTU) to $221 million (12,850 MTU), estimated from a $50 million cost for 2000 MTU by assuming cost is proportional to (capacity)$^{0.8}$.

However, Table 42 shows that a breakdown of basin costs for Method 4 would predict a total cost of only $194 million, $27 million less than the scaled cost of $221 million.

With waste canisters stored in the basin, the costs of higher basin coolant requirements are estimated from the itemized costs shown in Table 42. The added costs of larger basins, waste

TABLE 41

Basin Characteristics

	Method 1: Store HLLW	*Method 2: Separate Cs/Sr*	*Method 3: Store Canisters*	*Method 4: Store Fuel*
Fuel Storage Basin				
Capacity, MTU	850	850	850	12,850
Volume, gal × 10^6	3.5 (1.7)[b]	3.5 (1.7)[b]	3.5 (1.7)[b]	32.0 (30.4)[b]
Fuel Power, MW	10	10	10	62
Circulation Rate,[a] gpm	1,900	1,900	1,900	12,000
Heat Exchanger Area,[a] ft^2	19,000	19,000	19,000	120,000
Basin Turnover, hr	31	31	31	43
Waste Basin				
Volume, gal × 10^6	4.3	4.3	7.0	4.5
Waste Power, MW	20	45[c]	61	19
Total Power (Fuel + Waste)	30	55	71	71
Total Basin Volume,[d] gal × 10^6	7.8	7.8	10.5	36.5
Circulation Rate,[a] gpm	5,700	5,700	13,500	13,500
Heat Exchanger Area,[a] ft^2	57,000	57,000	135,000	135,000
Basin Turnover, hr	23	23	13	45

a. Assuming maximum basin water temperature = 60°C and cooling water inlet temperature - 30°C.

b. Total volume for fuel storage plus volume needed for auxiliary equipment; value in parenthesis is for fuel storage only.

c. If all Cs-Sr could be sold, power would be 20 MW.

d. Combined fuel storage plus water storage.

** All costs in FY-1977 dollars.

TABLE 42

Storage Basin and HLLW Tank[a]

Storage Basin Costs	*Method 1: Store HLLW*	*Method 2: Separate Cs/Sr*	*Method 3: Store Canisters*	*Method 4: Store Fuel*
Fuel Storage Basin Cost, estimated by scaling[b]	25	25	25	221
Fuel Storage Basin Cost by Direct Calculation of Individual Costs				
Building	10	10	10	60
Containers	6	6	6	95
Deionizer Exchange System	3	3	3	18
Services	3	3	3	18
Cask Unloading	3	3	3	3
Total	25	25	25	194
Additional Costs for Enlarged Waste Storage Basin				
Building	4	4	9	4
Waste Canister Racks[c]	5	5	9	5
Expanded Heat Transfer System	3	14	18	3
Services	1	1	3	1
Subtotal	13	24	39	13
HLLW Tanks				
Cost of Tank with High Cooling Capacity, millions of dollars	25	25	-	-
Cooling Capacity, MW	11	11	-	-
Volume, gallons	300,000	300,000	-	-
Number Needed	4[d]	2[d]		
Cost of these Tanks, millions of dollars	100	50	-	-
Cost of Tank with Intermediate Cooling Capacity, millions of dollars	22	22	12.5	-
Volume, gallons	150,000	150,000	150,000	-
Number Needed	3	2	4[d]	-
Cost of these Tanks, millions of dollars	66	44	50	-
Cost of Tank with Low Cooling Capacity, millions of dollars	-	20	-	6.7
Volume, gallons	-	100,000	-	100,000
Number Needed	-	3	-	3[d]
Cost of these Tanks, millions of dollars	-	60		20
Total Cost of All Tanks, millions of dollars	166	154	50	20

a. All costs in 1977 dollars.

b. Fuel basin cost = $50 \times \left(\frac{\text{Fuel Capacity, MTU}}{2000}\right)^{0.8}$

c. Waste container racks are estimated to cost $1000 per container.

d. Including one spare tank.

racks, and heat removal equipment are estimated (Table 42) to range from $13 million (Method 1 and Method 4) to $39 million (Method 3).

HLLW Tank Costs

HLLW tank costs are summarized in Table 42. Variable costs for services (such as cooling systems, off-gas condensate, emergency power, and instruments) are estimated as an additional 20% of the base waste tank costs listed above.

Special Costs

Method 2. ^{137}Cs and ^{90}Sr are assumed to be removed from HLLW by precipitation procedures based on Hanford processes. Cesium is precipitated by ferrocyanide and further purified in zeolite columns. However, ferrocyanide has an adverse effect on glass (similar to fluoride); therefore, some development work would probably be needed to adapt the process to the LWR plant.

Strontium is precipitated with $PbSO_4$ carrier and purified by cation exchange. However, sulfate is not compatible with a low-leachable glass waste, and sulfate in HLLW should be minimized.

Costs for strontium and cesium separation equipment are estimated at $50 million. The separated strontium and cesium would presumably be stored in canisters in a basin until customers for heat sources take shipment. Revenue from sale of heat sources would offset the higher cost of the separation. If no customers for strontium and cesium were found, this solid waste would be recombined with other wastes and made into glass.

Method 3. Solidification of waste increases the flow of HLLW to spray dryer(s) from 1500 gal/day (nominal, Method 1) to 2150 gal/day† (10 MTU/day times 215 gal waste/MTU) for the example shown in Table 39. If HLLW has aged about 3 years before solidification, the flow can be reduced to 1500 gal/day. An allowance of $5 million is made in Method 3 for the added drying capacity.

^{106}Ru in off-gas from the vitrification system is increased by a factor of 16 because HLLW is decayed less in Method 3 than in method 1. Total ruthenium is not affected because radioactive ^{106}Ru is only 7% of the total ruthenium after aging one year.

---

† If the HLLW inventory in Method 3 were minimized as in Method 4, the spray dryer feed would be about 2500 gal/day.

Thus, the size of the ruthenium retention system is not increased in Method 3; however, the ruthenium decontamination factor must be 10 to 20 times higher in Method 3 for equal confinement of ruthenium in the two modes. An allowance of $10 million is provided for added stages of ruthenium removal in Method 3.

Operating Costs

The differences in operating cost among all methods are minor, because operating costs depend mainly on plant throughput (10 MTU/day in all cases). Waste monitoring and basin operations are not a major fraction of total plant operating cost. Fixed charges on capital are estimated to be the dominant costs in a fuel reprocessing plant.

The large inventory of fuel in Method 4 represents an added economic penalty because a utility with fuel in storage must replace the fuel value in the irradiated fuel with new fuel. Because of the greater fuel value in inventory by Method 4 as compared to the other methods, Method 4 bears an annual penalty of about $40 million.

Safety Comparison

A preliminary review of safety features in the methods was made to identify any major differences.

Safe storage of HLLW in cooled tanks requires reliable equipment and monitoring. Waste tanks would normally be cooled by circulating water through coils in the tank and then to a cooling pond or cooling tower. Coolant circulation systems would be normally powered by purchased power with diesel (and/or battery) backup for periods of interrupted electricity supply. Off-gas systems from HLLW tanks would be designed with a large capability to condense moisture, and might serve as another backup cooling system if HLLW temperatures rose above 60°C. A source of makeup water for normal coolant would be included to replace water that evaporates in the cooling pond or cooling tower. The final backup source of emergency cooling would probably involve direct addition of water to the HLLW. Response time for such action would be about 5 hours.

Onset of HLLW boiling should not release any activity; a modest makeup would maintain the level of HLLW in the tank even if boiling proceeded. As shown in Table 36, the makeup for all HLLW tanks decreases from about 400 gpm (Method 1) to 200 gpm (Method 2) to 80 gpm (Method 3) as the waste heat in inventory

is redistributed from HLLW storage tanks to solid waste. Sources for such low flow rates would be a cooling pond, nearby streams, or wells; a fire engine could serve as another backup pump. Make-up rates for a single HLLW tank would be accordingly lower; in Method 4, a makeup rate of 10 gpm would be required until normal cooling could be restored. For Methods 1 and 2, the amount of stored HLLW is significantly larger than for Methods 3 and 4.

Cooling of solidified waste containers in water-cooled basins is based on current technology. Glass waste containers might survive complete loss of basin water. The amount of solidified HLLW is significantly higher for Method 3 than for the other methods.

Safeguards considerations are similar for all methods, except for the greater amount of fuel inventory available for diversion in Method 4.

Environmental effects of all methods are equal if the additional ruthenium filtration capability allowed for in Method 3 reduces the releases to the same levels as for Methods 1 and 4.

TANK STORAGE OF HIGH-LEVEL LIQUID WASTE

A process description and technical data summary for interim tank storage of LWR high-level liquid waste (HLLW) was prepared for design and cost studies of the back end of the commercial nuclear fuel cycle. In the proposed process, concentrated acidic HLLW is temporarily stored in a double-walled stainless steel tank before conversion to a borosilicate glass product. The process description describes a typical HLLW tank and required auxiliary facilities. The technical data summary provides data that can be used to design tanks of almost any size, such as small run tanks to hold liquid for a few months before vitrification, or large tanks in a tank farm to store liquid as long as five years before vitrification.

HLLW Storage Technology

The tank storage of HLLW from various sources in the U.S. and elsewhere is reviewed in the March 1976 report.[1] The status of this technology was summarized with respect to such factors as heat load, acidic vs. alkaline storage, single-wall vs. double-wall containment, agitation, and cooling.

HLLW from a nuclear fuel reprocessing plant consists principally of waste streams from the solvent-extraction process. Almost all fission products and actinides other than uranium and plutonium are contained in the HLLW. Before transferring HLLW to an interim storage tank, the waste is concentrated to ~150 gal per metric ton of heavy metal, to minimize storage and handling requirements and to recover some of the nitric acid.

Tank Construction

The acidic HLLW is stored in double-walled stainless steel tanks (Figure 36). The tanks consist of a primary stainless steel container encased in a stainless steel liner to the full height of liquid fill. Both containers are supported by and located inside a reinforced concrete vault. The HLLW is retrievable and the tank is designed for eventual decommissioning. To avoid possible corrosion and tank decontamination problems, the design eliminates obstructions on the tank bottom by supporting all internal structures from the tank top.

---

1. *Savannah River Laboratory Quarterly Report, Light Water Reactor Fuel Recycle, January-March 1976.* USERDA Report DPST-LWR-76-1-1, p. 26.

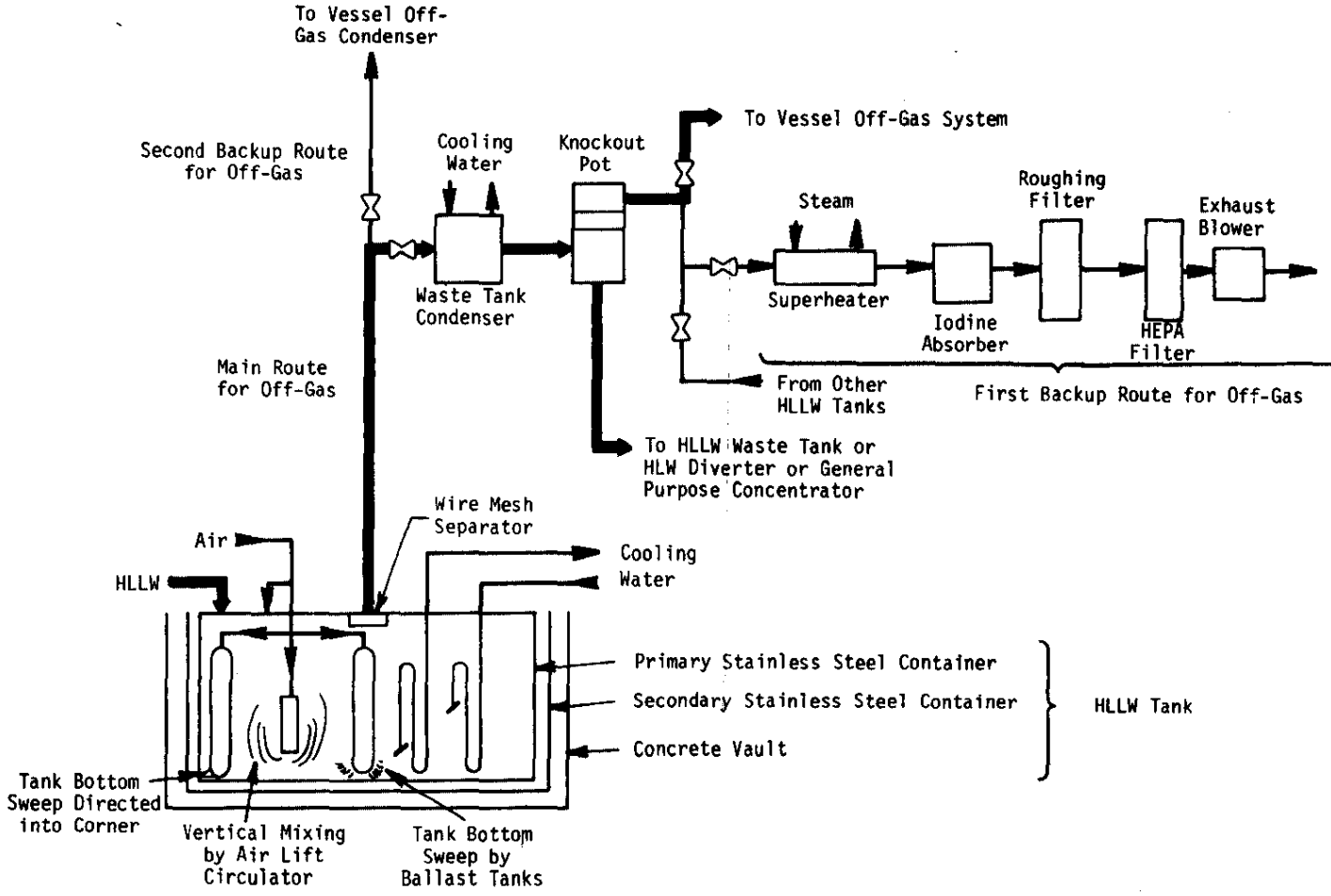

FIGURE 36. HLLW Storage Tank and Off-Gas Systems

Cooling

Internal cooling coils remove radioactive decay heat and maintain the waste temperature below 140°F. The coils are arranged in parallel banks, so that if any one of the coils develops a leak, that bank can be valved off; the remaining banks are capable of removing the design heat load.

Three separate cooling water systems (Figure 37) provide sufficient cooling during all credible events. The primary system is a closed loop with a cooling tower; during normal operation, heat from the closed primary-coolant loop is rejected through heat exchangers to a closed cooling-tower loop. The first backup system supplies well water to the heat exchangers on a single-pass basis. In the second backup system, cooling water from a pond is recycled directly through the coils, by-passing the heat exchangers.

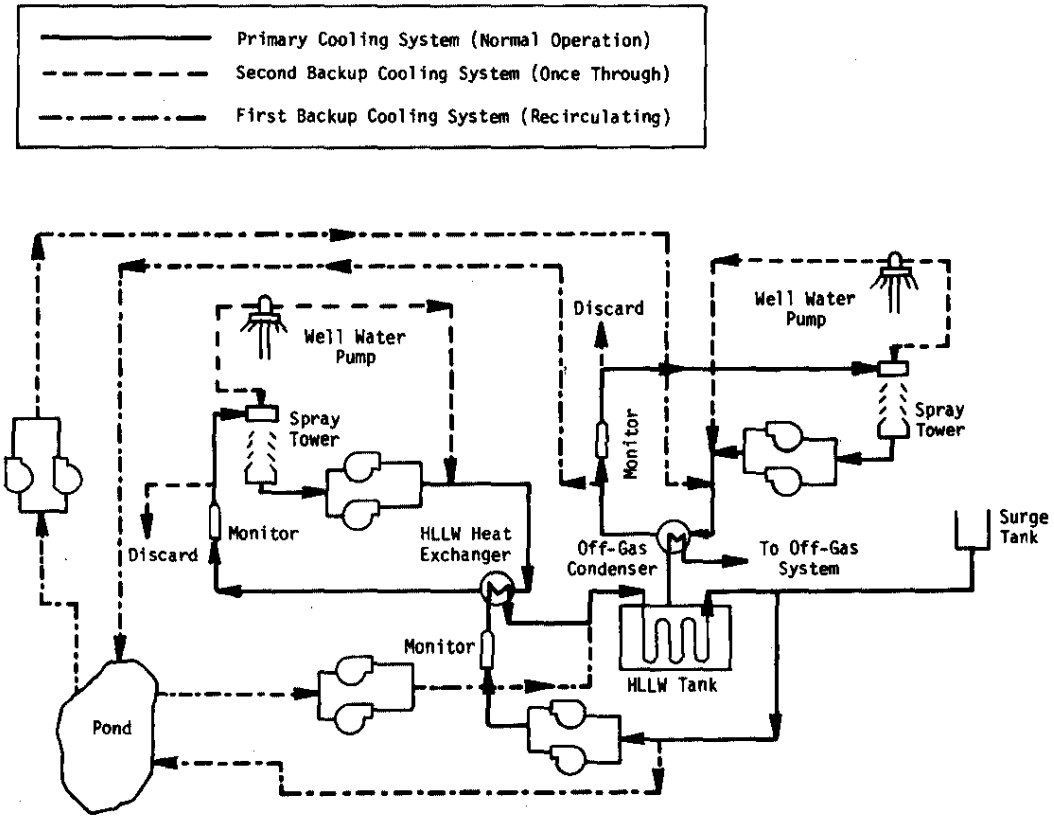

FIGURE 37. Cooling Systems for HLLW Storage Tank

Agitation and Ventilation

High-level acidic wastes will contain insoluble material and, unless means are provided for adequate agitation, local "hot spots" where solids accumulate can accelerate corrosion of the primary container. Air-lift circulators for continuous vertical mixing and ballast tanks to intermittently sweep the tank bottom will keep solids from settling. These techniques are used effectively by the British[2,3] and have been incorporated into the design of BNFP waste tanks.[4]

This agitation system also supplies air to the tank vapor space to dilute radiolytic hydrogen and organic vapors below their explosive limits. The air supply from the agitation system is supplemented by a direct air purge as necessary.

A waste tank off-gas system removes entrained activity and radioiodine from all purge air. Water and nitric acid are condensed from the off-gas and returned to the tank to maintain the desired volume of liquid in the tank. The off-gas system provides three flow patterns for flexible handling of off-gas from each tank (Figure 36). During normal operation, waste tank off-gas is passed through the tank's own condenser and knockout pot,* combined with off-gases from other tanks, and then routed collectively to the vessel off-gas system in the separations facility. If the vessel off-gas system is not operating, the air flow from the knockout pots is routed through a common superheater, iodine absorber, roughing filter, and HEPA filter before being discharged to the sand filter and stack. The third flow pattern provides for

---

* The knockout pot separates the two-phase vapor/gas mixture from the waste tank condenser into gas (overheads) and liquid (bottoms).

2. D. W. Clelland. "High-Level Radioactive Waste Management in the United Kingdom." *Proceedings of the Symposium on the Management of Radioactive Wastes from Fuel Reprocessing, Paris, Nov. 27-Dec. 1, 1972.* Organization for Economic Cooperation Development, Washington, DC (1973).

3. B. F. Warner, A. S. Davidson, M. J. Larkin, and A. Naylor. "Operational Experience in the Evaporation and Storage of Highly-Active Fission Product Wastes at Windscale." *Proceedings of the Symposium on the Management of Radioactive Wastes from Fuel Reprocessing, Paris, Nov. 27-Dec. 1, 1972.* Organization for Economic Cooperation Development, Washington, DC (1973).

4. *Barnwell Nuclear Fuel Plant, Final Safety Analysis Report.* Allied-General Nuclear Services, Barnwell, SC. USNRC Docket-50332, Sections 8 and 9 (October 10, 1973).

direct routing of air flow to the vessel off-gas condenser in the main separations facility, bypassing the tank condensers and knock-out pots.

Monitoring

The HLLW tank and auxiliaries are equipped with an adequate number of highly reliable monitoring systems to ensure operation of the facility within specified limits. Critical monitoring systems are of such integrity and/or redundance that the probability of loss of surveillance is very low.

The integrity of both the primary and secondary containers can be assessed by surveillance. The space between the primary and secondary containers is monitored continuously to determine the condition of the primary container. Collecting channels are installed behind all the welds in the secondary container, and a remote monitoring space is provided under the floor liner. This allows assessment of the integrity of the welds in the secondary container at any time as well as detection of any waste that might pass the secondary container.

LIQUID WASTE EVAPORATION AND ACID RECOVERY

A process description and technical data summary for liquid waste evaporation and acid recovery was prepared for design and cost studies of the back end of the commercial nuclear fuel cycle. In the proposed process, high-level liquid waste (HLLW) and intermediate-level liquid waste (ILLW) are evaporated to minimize storage requirements. The overheads from these evaporation steps are processed further to recover nitric acid and water for reuse and to produce overheads suitable for disposal to the environment. Throughput of the proposed process is equivalent to 10 metric tons of heavy metal per day.

The Waste Streams

A spent-fuel reprocessing facility generates a variety of liquid waste streams containing varying quantities of radioactive constituents. For this study, these wastes are categorized according to the customary usage in the commercial nuclear power industry:*

- *High-Level Liquid Waste (HLLW).* Aqueous waste that contains almost all (more than 99%) of the fission products, plus some uranium and plutonium that is lost during reprocessing.
- *Intermediate-Level Liquid Waste (ILLW).* Aqueous wastes that contain much lower concentrations of fission products than HLLW and no appreciable amounts of uranium and plutonium.
- *Low-Level Liquid Waste (LLLW).* Overheads from ILLW evaporators. LLLW may require some treatment before release to the environment.

HLLW is further subdivided into *High-Activity Waste (HAW)* and *Low-Activity Waste (LAW)*, an arbitrary classification used to indicate the relative activities and the most probable method and facility

---

* These categories are not to be confused with the categories defined by ERDA for defense waste:

- *High-Level Liquid Waste (HLLW).* Aqueous waste that contains sufficient radioactivity to require either storage or further treatment rather than release to the environment.
- *Low-Level Liquid Waste (LLLW).* Aqueous low-level waste (LLW) that may be released to the environment pursuant to ERDAM-0524. ["Standards for Radiation Protection." ERDA Manual, Chapter 0524 (1975).]

There is no intermediate-level liquid waste category for defense waste.

in which these wastes will receive subsequent treatment. There is no singular radionuclide concentration in the waste above which the waste is classified as "high activity" or below which the waste is classified as "low activity." The dividing line depends upon the particular facility or process from which the waste originated.

For this study, HAW from reprocessing spent LWR fuels consists of the raffinate from the first solvent-extraction cycle and off-gas scrubber solution from the HLLW Solidification Module. LAW includes the raffinates from all solvent-extraction cycles except the first cycle, the aqueous solvent wash wastes from the plutonium cycles, and plutonium evaporator overheads. HAW contains more than 99% of the activity of the HLLW, and LAW contains less than 1%. Typical ILLW streams include aqueous solvent wash wastes from the uranium cycles, overheads from the uranium evaporators in solvent extraction, decontamination solutions, laboratory wastes, and laundry wastes.

Waste Evaporator Systems

The HLLW streams are concentrated in either the HAW evaporators or the LAW evaporators (Figure 38). Concentrate from the first stage LAW evaporator is passed through an agitated anion-exchange column to recover plutonium. The acidic concentrated bottoms from the first-stage HAW evaporator and the raffinate from the primary recovery column are combined with the slurry of solids from the feed clarification step in solvent extraction and are stored in the HLLW tanks.

Overheads from the second-stage HAW evaporator are combined with those from the first-stage LAW evaporator and are fed to the second-stage LAW evaporator. Overheads from the second-stage LAW evaporator are transferred to the acid recovery unit to recover nitric acid for reuse in the process. Condensate from the acid recovery unit is either reused as process water or superheated and discharged to the stack, depending on process water requirements.

ILLW streams are concentrated by one of three evaporator systems (Figure 38) according to the origin of ILLW:

- The *General Purpose Evaporator* concentrates ILLW streams associated with or generated by spent fuel reprocessing, such as wastes from the uranium evaporator overheads in solvent extraction and the aqueous solvent-wash wastes from the uranium cycles. These waste streams are concentrated in the as-received acidic condition.

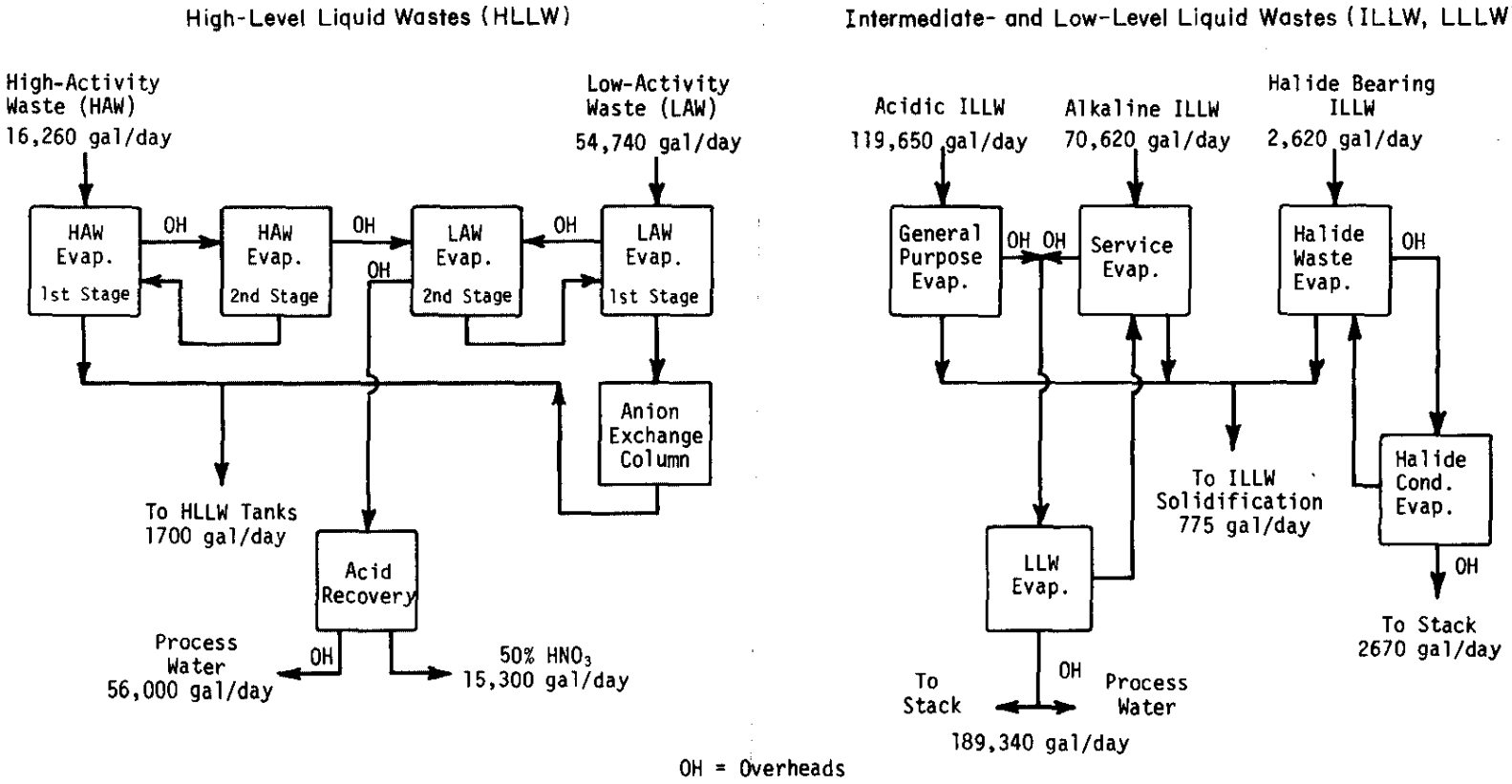

FIGURE 38. Waste Evaporation and Acid Recovery System

- The *Service Evaporator* concentrates ILLW streams associated with or generated by both process and process-support functions. Typical waste streams include decontamination solutions, laundry wastes, wastes from all building floor drains not located in a high radiation area, and fuel storage pool wastes. These wastes are neutralized before evaporation.

- The *Halide Waste Evaporator* concentrates waste streams containing appreciable quantities of chloride and fluoride. Such wastes include laboratory waste, raffinate from the solvent-extraction cycle in the Mixed Oxide Module, and raffinate from the plutonium ion-exchange recovery column in the Plutonium Conversion Module. These wastes are also neutralized before evaporation.

The concentrated bottoms from all ILLW evaporators are combined and sent to ILLW solidification. Overheads from the general purpose and service evaporators are routed to the low-level waste (LLW) evaporator, while those from the halide waste evaporator are re-evaporated in the halide condensate evaporator before being superheated and discharged to the sand filter and stack.

LLLW consists of condensed overheads from the general purpose and service evaporators. LLLW streams are concentrated in the LLW evaporator. The concentrated bottoms are recycled to the service evaporator, and the overheads are either superheated and discharged to the stack or condensed for reuse as process water.

DOSE RATE CALCULATIONS FOR SOLVENT EXTRACTION STREAMS

Radiation dose rates were calculated for the dissolver feed into the solvent extraction cycles of a plant for reprocessing LWR fuels and for the product streams from the first and second plutonium extraction cycles. These rates will be used to evaluate increasing the fission product content of the plutonium product stream as a deterrent to diversion.

The ORIGEN[1] code was used to calculate fission product and actinide contents for two types of LWR fuel: (1) fuel for the equilibrium uranium cycle and (2) MOX fuel with plutonium that had been recycled four times. A reactor exposure of 33,000 MWD/MTHM at a specific power of 30 MW/MTHM followed by a one-year decay period was assumed. The fission product and actinide contents in the solvent extraction product streams were reduced by the decontamination factors given in Table 43. The values in this table represent the fraction of each isotope that remains after the listed solvent extraction cycle. The ORIGEN code was then applied again to obtain the radiation sources.

TABLE 43

Solvent Extraction Decontamination Factors

Solvent Extraction Cycle	*Product/Feed Stream*	*U*	*Pu*	*Zr-Nb*	*Ru*	*All Other*[a]
1st Cycle	1BP/1AF	9.998×10^{-6}	0.9985	9.000×10^{-4}	6.670×10^{-5}	9.000×10^{-5}
2nd Pu Cycle	2BP/1BP	0.9998	0.9998	1.503×10^{-3}	1.334×10^{-2}	8.919×10^{-3}

a. The 1AF stream is assumed to contain no tritium.

The spectra for neutrons from α,n and spontaneous fission reactions were combined with these calculations. The neutron and photon sources were multiplied by the dose conversion factors in SRL-ANISN and divided by 4π to obtain a calculated radiation dose (unshielded) at one centimeter from a point source.

1. M. J. Bell. *ORIGEN — The ORNL Isotope Generation and Depletion Code*. USAEC Report ORNL-4628 (1973).

Results are shown in Table 44 for the equilibrium uranium cycle case. Results for the plutonium recycle case are similar. Fission product photons contribute ∿100% of the dose rate in the 1AF stream, 92% in the 1BP stream, but only 5% in the 2BP stream. The photon source from actinides and daughter products in this 2BP stream contributes 95% of the dose rate, although this latter dose rate is only ∿10% of that produced by the fission product photons in the 1BP stream.

TABLE 44

Dose Rates at 1 cm from Point Source in Equilibrium Uranium Cycle

Solvent Extraction Stream[a]	*Total Dose Rate at 1 cm, rem/(hr) (g Pu)*	*Fraction of Total Dose from Actinides + Daughters*		*Fission Products*
		n	γ	γ
1AF	4.20×10^{5}	0.988×10^{-6}	0.652×10^{-4}	0.9999
1BP	8.44×10	0.132×10^{-3}	0.078	0.922
2BP	6.93	0.159×10^{-2}	0.946	0.053

a. 1AF = feed stream to first cycle solvent extraction.

1BP = plutonium product stream from first cycle solvent extraction and is feed stream to second plutonium cycle.

2BP = product stream from second plutonium cycle

The dose rate per gram of plutonium in the 2BP stream is about 3 mR/hr at 50 cm (with no shielding) and is almost entirely due to photons from the actinides and their daughters. Since the dose rate from fission products is only 5% of the total dose rate in the 2BP stream, a third cycle of solvent extraction would not significantly reduce radiation from the plutonium stream. However, if it were to be desired to increase the plutonium radiation levels for safeguards purposes, an increase of up to a factor of ten could be achieved by less complete removal of the fission products.

GENERAL SUPPORT

CORROSION AND MATERIALS DEVELOPMENT

Tests are continuing to evaluate Type 304L stainless steel for use in equipment to process LWR fuel. Type 304L specimens containing a weld joint made with Type 308 filler showed substantial pitting corrosion after 99 days exposure at 95°C in synthetic reprocessing solutions containing 0.05M HF, conditions much more severe than expected in service. Specimens exposed to pure HNO_3 solutions showed negligible corrosion of any type. These results were expected and are consistent with SRL-SRP experience with corrosion by HNO_3-HF dissolving solutions in 304L equipment. Type 304L steel would not be recommended for use in the presence of HF.

Corrosion test solutions were:

3M HNO_3

7M HNO_3

3M HNO_3 + 0.05M HF

7M HNO_3 + 0.05M HF

3M HNO_3 + 0.05M HF + 0.20M $Al(NO_3)_3$

Corrosion attack was most severe with the 7M HNO_3 + 0.05M HF solution (Figure 39) and moderately severe with 3M HNO_3 + 0.05M HF (Figure 40). The attack was most pronounced parallel to the rolling direction (end-grain attack) (Figure 39). In addition, the heat-affected zone of the 304L shows more extensive pitting than regions not affected by weld heating (Figure 40). The 308 filler shows negligible corrosion. The addition of 0.20M $Al(NO_3)_3$ to the HNO_3 + HF solution reduced, but did not eliminate, the pitting (Figure 41).

The results of weight loss measurements confirm our conclusion that 0.05M HF in the synthetic reprocessing solutions caused severe corrosive attack on 304L. Table 45 shows weight loss in test solution relative to weight loss in 3M HNO_3.

Evaluation of these and other test specimens is continuing, and tests of prospective materials for HNO_3 service are planned.

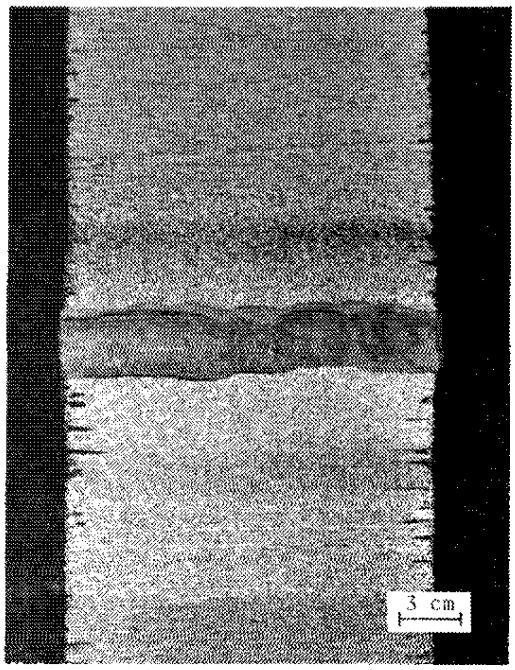

a. Attack in Heat-Affected Zone

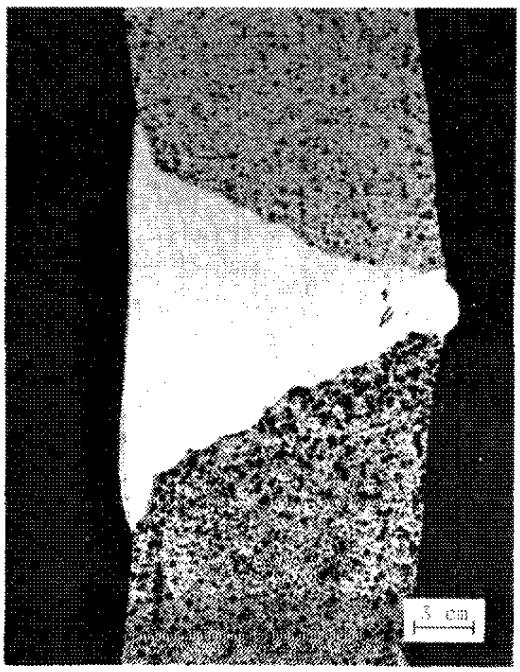

b. End-Grain Attack

c. Attack Parallel to Rolling Direction. Note deep pits.

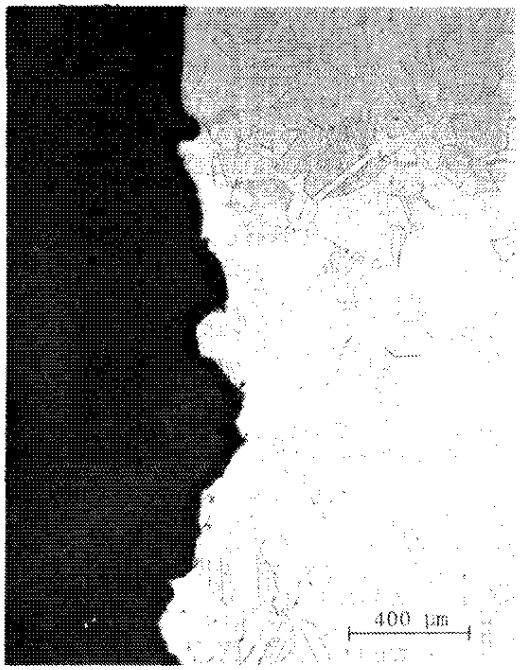

d. Perpendicular to Rolling Direction

FIGURE 39. Corrosion of Welded Type 304L Stainless Steel by 7M HNO_3 + 0.05M HF at 95°C

TABLE 45

Weight Losses

Test Solution	*Relative Weight Loss*
3M HNO_3	1.0
7M HNO_3	3.3
3M HNO_3 + 0.05M HF	248
7M HNO_3 + 0.05M HF	398
3M HNO_3 + 0.05M HF + 0.20M $Al(NO_3)_3$	52

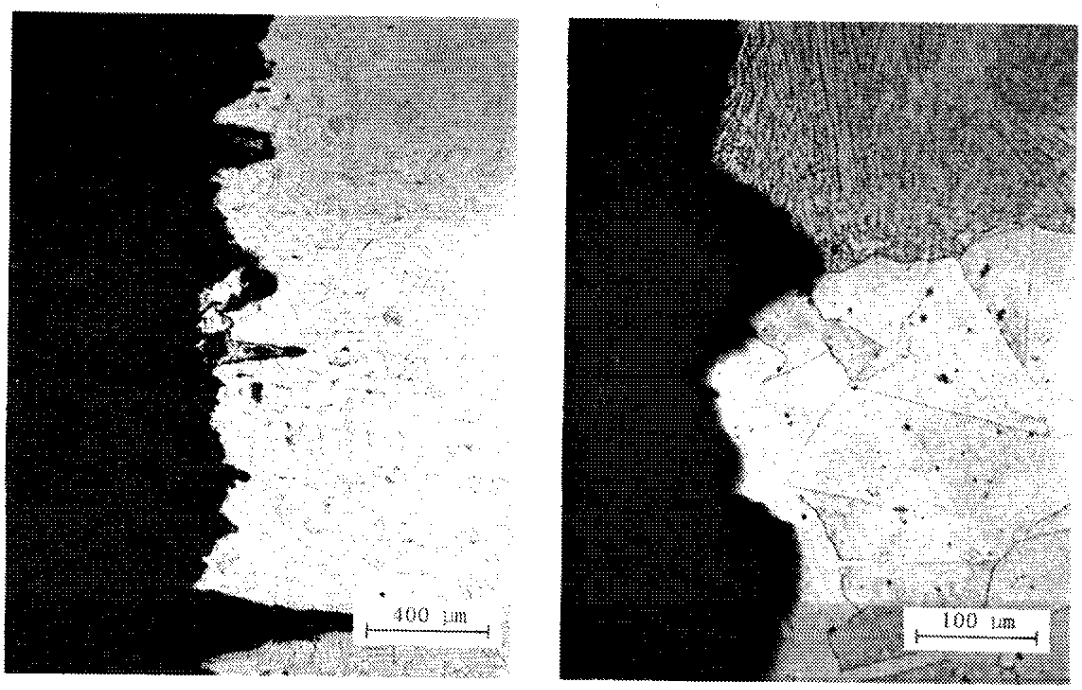

a. Pitting of End Grain

b. Attack Perpendicular to Rolling Direction

FIGURE 40. Corrosion of Welded Type 304L Stainless Steel in 3M HNO_3 + 0.05M HF at 95°C

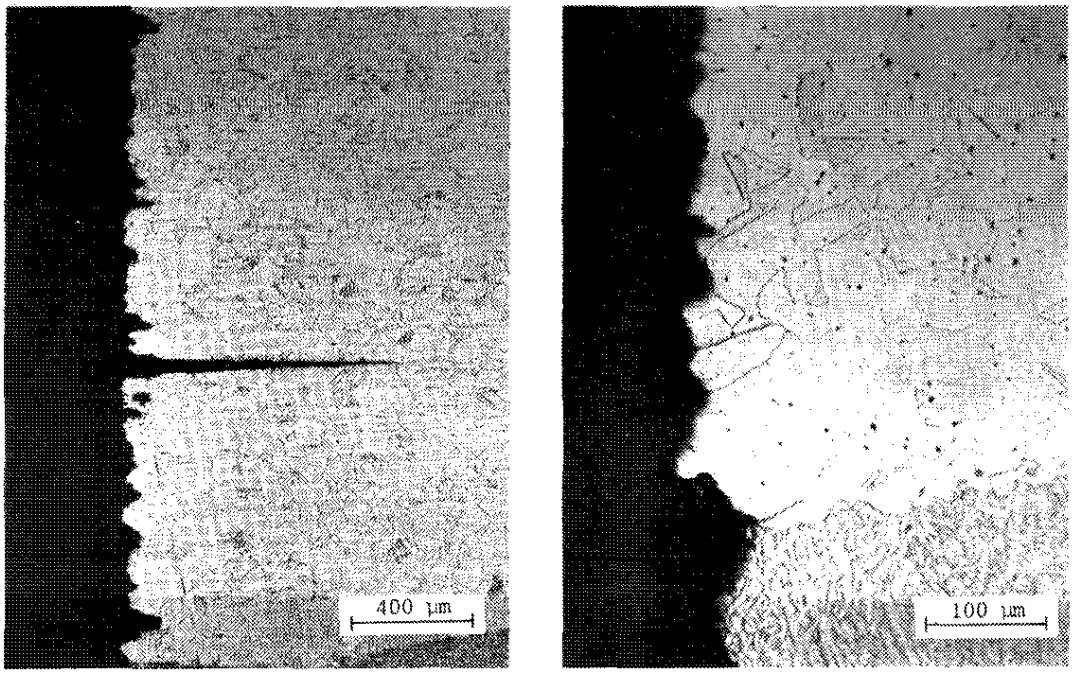

a. Pitting of End Grain

b. Attack Perpendicular to Rolling Direction

FIGURE 41. Corrosion of Welded Type 304L Stainless Steel in 3M HNO_3 + 0.05M HF + 0.20M $Al(NO_3)_3$ at 95°C

ANALYTICAL SUPPORT FOR THE AFCT PROGRAM

Determination of Lead in Zeolite

A method was developed for determining the lead content of zeolite by x-ray fluorescence spectrometry. The method is needed in studies of iodine retention in off-gas trapping systems for the head-end processes of a plant for processing light water reactor fuels (see page 47). The x-ray spectrometric method is faster and safer than the alternative method, atomic absorption spectrometry, because sample dissolution in potentially hazardous hydrofluoric acid is not required.

The x-ray spectrometric method is based on direct experimental determination of the intensity of the lead L_α x-ray. A 3% zeolite in $Na_2B_4O_7 \cdot 10H_2O$ pellet is used. The lead content of zeolite is calculated from the x-ray intensity of the sample, which is compared with the intensities of standards of known lead content. Precision is approximately 2% absolute between 20 and 50% lead in zeolite. The method could easily be adapted to determine silver in zeolite.

Calibration of Standards

Standards containing known concentrations of lead in zeolite were prepared by thoroughly mixing and pelletizing $Pb(C_2H_3O_2)_2 \cdot 3H_2O$, $Na_2B_4O_7 \cdot 10H_2O$, and zeolite containing no lead in the proportions indicated in Table 46. The lead content of the $Pb(C_2H_3O_2)_2 \cdot 3H_2O$ was determined by analysis to be 56.62 wt %. The lead-zeolite standards were analyzed by x-ray fluorescence spectrometry. The net intensities of the lead L_α x-rays are also reported in Table 46.

TABLE 46

Composition and Net X-ray Intensity of Lead-Zeolite Standards

Standard	*Component Weight, g*			*Lead in Zeolite, wt %*	*Net X-ray Intensity, counts*[a]
	$Pb(C_2H_3O_2)_2 \cdot 3H_2O$	*Zeolite*	*$Na_2B_4O_7 \cdot 10H_2O$*		
1	0.0	0.200	6.800	0.00	199
2	0.037	0.180	6.783	10.42	32,508
3	0.073	0.160	6.767	20.53	52,661
4	0.110	0.140	6.750	30.79	74,201
5	0.150	0.118	6.732	41.85	83,422
6	0.183	0.100	6.717	50.89	96,536

a. Average of two counts.

The calibration plot of lead x-ray intensity versus lead content of zeolite is shown in Figure 42. The weight percent lead in zeolite is related to the experimentally determined x-ray intensity I by Equation 1.

$$\% \text{ Pb} = 0.71 \times 10^{-2} + 0.2082 \times 10^{-3} I + 0.3265 \times 10^{-8} I^2 \qquad (1)$$

The precision of the x-ray spectrometric method was estimated by the standard error of the calibration points from their quadratic regression line (Equation 1) to be about 2% absolute.

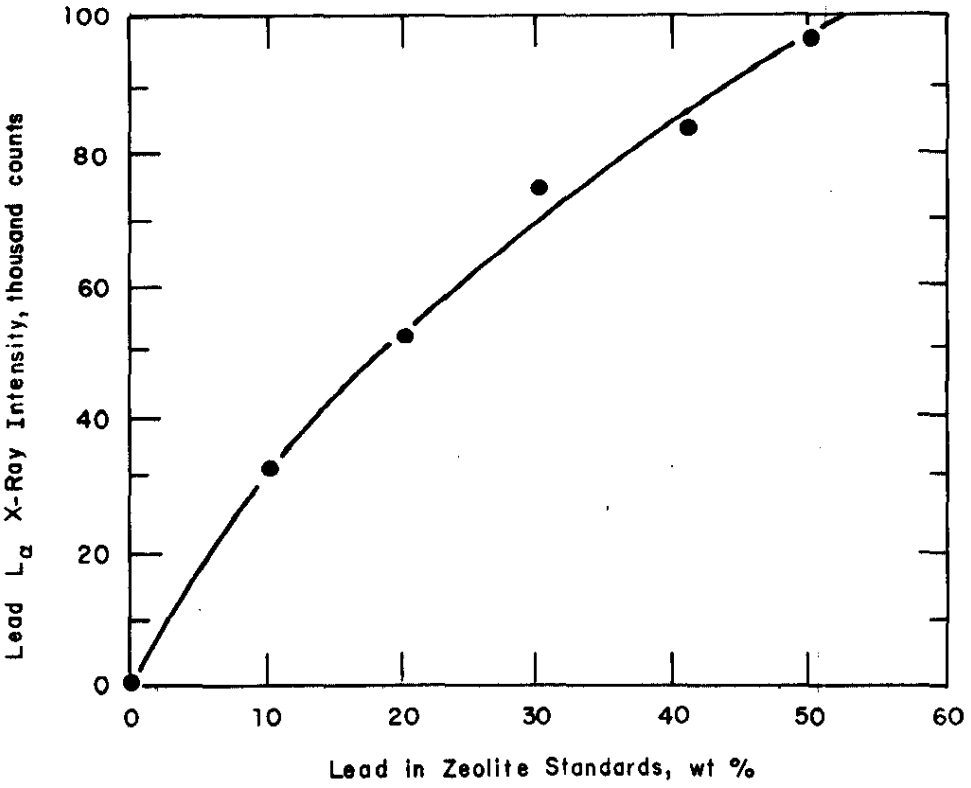

FIGURE 42. Calibration of Zeolite Standards

Comparison with Atomic Absorption Spectrometry

Analysis by x-ray spectrometry was compared with atomic absorption spectrometry by analyzing 12 samples of unknown lead content by both methods. The lead concentrations determined experimentally by x-ray spectrometry and by atomic absorption spectrometry are given in Table 47 and are compared graphically in Figure 43. These data show a good correlation between the two methods. The standard error of the points from their regression line through the origin (Figure 43) is only 1.3% absolute.

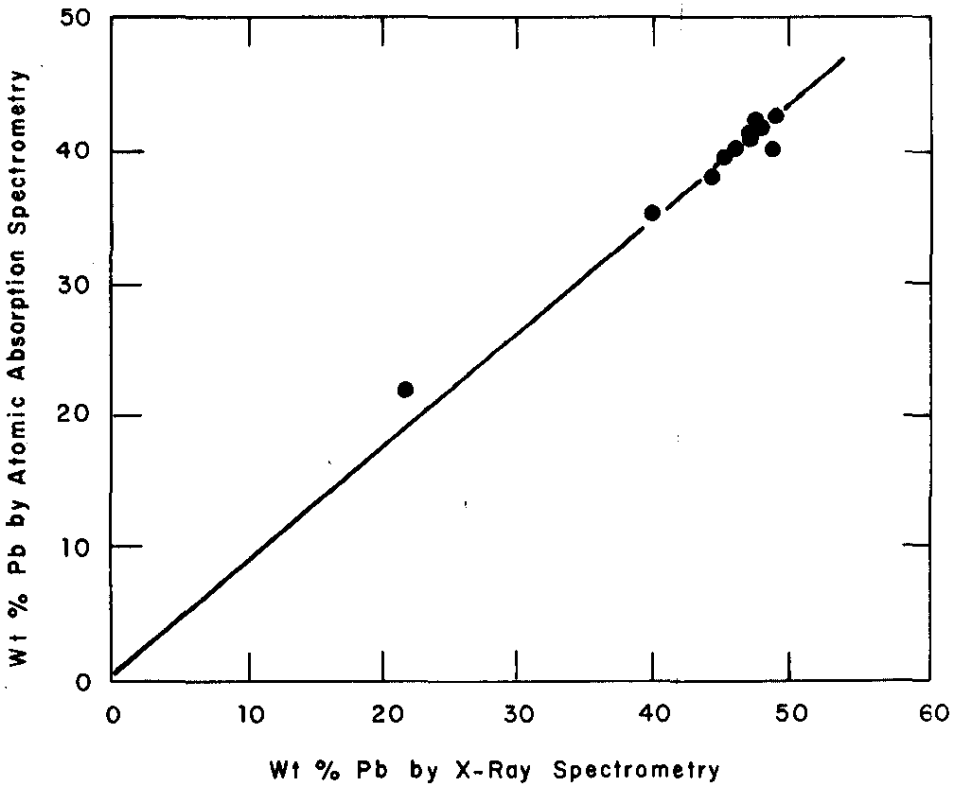

FIGURE 43. Comparison of X-ray and Atomic Absorption Spectrometry for Determination of Lead in Zeolite

Table 47 shows that the atomic absorption and x-ray fluorescence results, however, differ by approximately 14% relative. The reason for the analytical bias was not determined because the results of either method were adequate to establish relative absorption characteristics.

TABLE 47

Comparison of X-ray and Atomic Absorption Spectrometry for Determination of Lead in Zeolite

	Lead in Zeolite, wt %	
Sample	*X-ray Spectrometry*	*Atomic Absorption Spectrometry*
1	0.05	<9.7
2	22.0	21.7
3	40.3	35.2
4	44.9	37.8
5	45.7	39.4
6	46.5	39.8
7	47.4	41.2
8	47.6	42.1
9	49.2	39.9
10	49.4	42.2
11	48.1	41.7
12	47.5	41.0

Determination of HTO and $^{14}CO_2$ in Head-End Off-Gases

Procedures were developed to assay HTO and $^{14}CO_2$ adsorbed on molecular sieves during head-end operations (see page 47). In these procedures the molecular sieve is heated, the desorbed species are quantitatively trapped in a cold trap (HTO) or trapping solution ($^{14}CO_2$), and the activity of the species is determined by liquid scintillation counting. Tracer studies using these procedures demonstrate ∿90% recovery for $^{14}CO_2$ and ∿96% for HTO. Both methods are now used routinely.

Determination of HTO

The HTO procedure was adapted from one used for measuring tritium concentrated from SRP effluents. The apparatus used is shown in Figure 44. Up to six samples of molecular sieve are placed in glass traps. The traps are placed in an oven where each is connected to a corresponding cold trap in a refrigerated bath and to a small flask containing 3 ml of "push water." The cold traps are in turn connected to a vacuum manifold serviced by a mechanical pump. All the apparatus is contained in two adjoining stainless steel hoods specially constructed for this purpose and capable of handling large amounts (up to 5 curies) of activity.

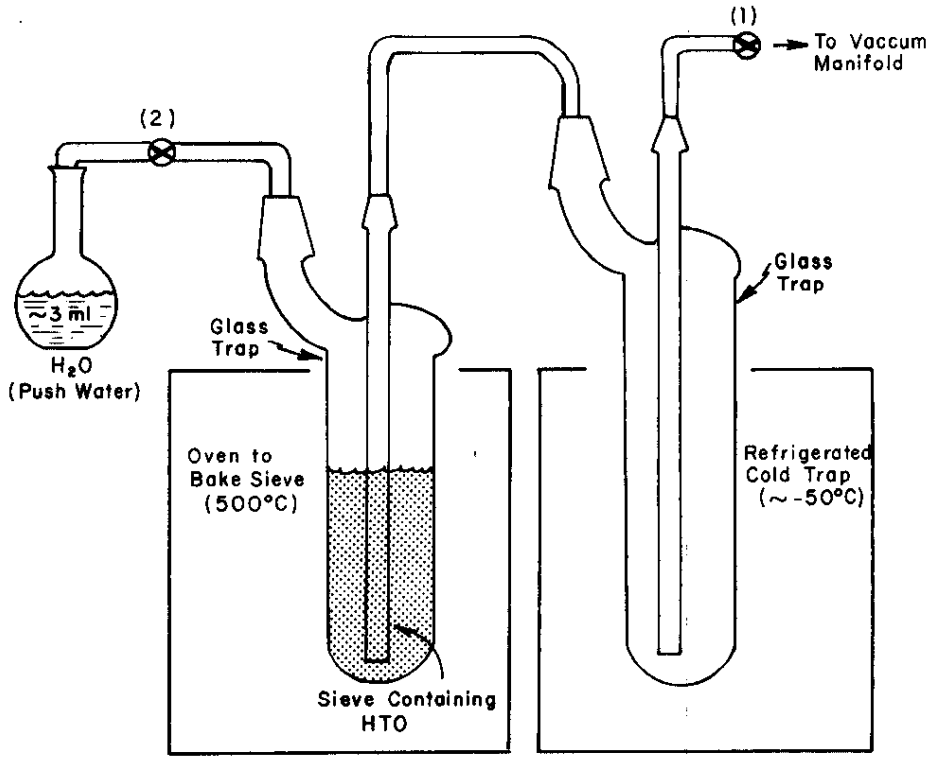

FIGURE 44. Apparatus for HTO Recovery from Molecular Sieve

Each sample consists of 275 grams of 1/16-inch pellets of 3A molecular sieve taken from one of the stainless steel traps in the off-gas system. After the samples have been loaded into the oven, Stopcock 2 is opened, and the system is evacuated. The samples are heated to 500°C overnight. After 4 or 5 hours at 500°C, Stopcock 1 is opened to permit the push water to sweep HTO from the sieve into the cold trap. After overnight operation, Stopcock 2 is closed, the sieves are cooled, the traps are vented, and the cold traps are warmed. A known aliquot of water from each cold trap is pipetted into a vial containing beta liquid scintillation medium, and the activity of the mixture is determined by liquid scintillation counting. The total HTO assay of each molecular sieve is then calculated by correcting the liquid scintillation counts for blank, counting time, counting efficiency, dilution, and volume of liquid in the cold trap.

Samples of molecular sieve containing known amounts of HTO were assayed to determine the per cent HTO recoverable from the sieve. These known samples were prepared from tritiated well water that had been assayed for tritium by comparison to standard HTO solutions. Measured amounts of this water were dripped slowly onto two 275-gram batches of 3A sieve, which were then assayed by the new method. For both samples, 96.4% of the tritium added to the sieves was recovered.

Determination $^{14}CO_2$

The apparatus and procedures for $^{14}CO_2$ assay trapped on molecular sieve are similar to those for HTO. The apparatus is shown in Figure 45. 250-gram batches of 13X molecular sieve from the stainless steel traps in the head-end off-gas system are placed in glass traps in an oven and heated to 500°C. In this case, dry air is used to sweep the desorbed $^{14}CO_2$ through a refrigerated cold trap and into a series of scrubbers, which remove the $^{14}CO_2$ from the flowing air. Each of the first two scrubbers (labeled 1 in Figure 45) contains a commercially available CO_2 trapping solution that is miscible with liquid scintillation mixtures. The buffer tube catches any splashover from the first two scrubbers. The last scrubber contains 1M NaOH and is placed in line in case the CO_2 capacity of the first two scrubbers is exceeded. Aliquots from these scrubbers are pipetted into liquid scintillation vials and counted. $^{14}CO_2$ is calculated as for HTO. The cold trap between the sieve and scrubbers from the flowing stream removes any HTO trapped by the 13X sieve in the off-gas system, which prevents HTO from interferring in the $^{14}CO_2$ liquid scintillation counting.

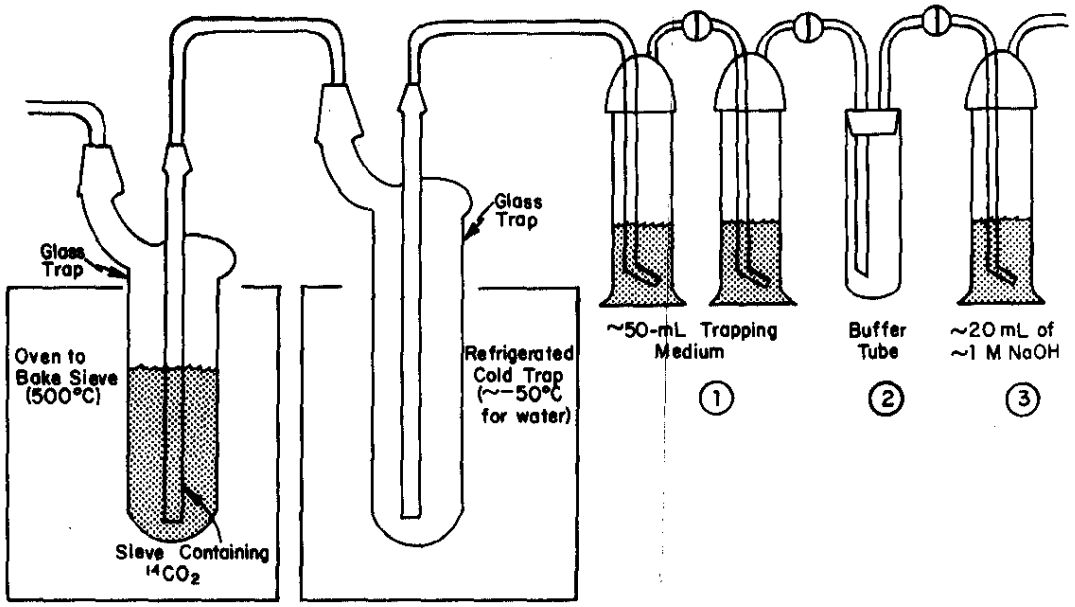

FIGURE 45. Apparatus for CO_2 Recovery from Molecular Sieve

Three sets of experiments demonstrated this procedure. The first set demonstrated quantitative $^{14}CO_2$ trapping by the commercial CO_2 trapping medium. Known amounts of $^{14}CO_2$ were produced by slowly dropping 2M HNO_3 into a solution of standardized $NaH^{14}CO_3$. An air purge swept the liberated $^{14}CO_2$ through two scrubbers connected in series and containing trapping agent. Counting of the standardized solutions and the scrubbers showed good material balance and demonstrated that ~99% of the liberated CO_2 was trapped in the first scrubber.

The second set of experiments demonstrated quantitative CO_2 trapping by the 13X sieve and produced two "standard" sieves containing known amounts of $^{14}CO_2$. For each sieve, a known amount of $^{14}CO_2$ was generated from standardized $NaH^{14}CO_3$ solution and was swept by dried air through a trap containing the sieve. The amount of $^{14}CO_2$ trapped on each sieve was calculated from the difference in activity of the standardized $NaH^{14}CO_3$ solution before and after acid addition. Scrubbers containing CO_2 trapping solutions were placed in series after the sieves and counting showed that essentially none of the liberated $^{14}CO_2$ passed through the sieves into these scrubbers.

In the third set of experiments, these "standard" sieves were assayed using the apparatus and procedures described above. Calculation showed that 90% of the $^{14}CO_2$ on the sieves was recovered.

Continuing Studies

Experiments are continuing, to demonstrate quantitative $^{14}CO_2$ assay in the presence of large excesses of HTO. Until these experiments are completed, a pulse height analysis is made of the liquid scintillation samples to ensure that HTO is not interfering with the $^{14}CO_2$ assay.

Fluorometric Method for Uranium

A new fluorometer with picoammeter readout was acquired, and a hexone extraction method coupled with a nonfusion, sintering technique for NaF pellets was adapted to measure trace concentrations of uranium. The linearity of the method has been demonstrated for uranium concentrations from 0.02 → 10 μg/ml. The precision of the method is ∿9% at 2 μg/ml. A second fluorometer head will be installed in a contained analytical facility and used for direct analysis of uranium in highly radioactive solvent extraction waste streams.

Densimetric Method for Uranium

An automatic, remote reading densimeter was acquired, and a remote densimeter cell was installed in an analytical shielded cell. The densimeter was calibrated for routine assay of high levels of uranium in fuel dissolver solutions. The rapid densimetric method agrees with the colorimetric method to within 5%.

ACCOUNTABILITY AND PROCESS MONITORING REQUIREMENTS FOR AN LWR FUEL REPROCESSING PLANT

Safeguards accountability and process monitoring requirements for a 10-MTU/day fuel reprocessing facility have been studied. Purposes and objectives and how to meet them have been defined for the facility in general. Instrumentation for accountability and process monitoring has been specified for the plutonium nitrate to oxide conversion process. A survey of current measurement technologies was completed, and a preliminary model of the conversion process was constructed and used to estimate the diversion detection sensitivity of the accountability system.

General Accountability Considerations

The purpose of accountability is to ensure that the removal of significant quantities of Special Nuclear Material (SNM) from a fuel reprocessing facility within a specified time interval will be detected. The accountability system should also be capable of providing a timely notification of diversion from any part of the process. Because of the statistical nature of SNM measurements, the accountability system cannot by itself guarantee that material cannot be diverted without detection. However, accountability combined with physical safeguards can both minimize the quantity of material that could be diverted and maximize the probability of rapid detection of diversion.[1]

For accountability purposes, any reprocessing facility will have designated "primary" and "secondary" accountability points. Primary accountability points are located in major material flows or where SNM can be measured in relatively pure chemical form. Examples of primary accountability points in the plutonium conversion process are input receipt tanks, product output stations, and recycle product blend tanks. Secondary accountability points are located in waste streams, minor side streams, and scrap, where SNM does not exist in pure form or where SNM concentrations are low. From these definitions, some general guidelines for an accountability system can be defined:

- Primary accountability measurements points are made offline with online backup.

1. International Atomic Energy Agency. *The Structure and Content of Agreement Between the Agency and States Required in Connection with the Treaty on the Non-Proliferation of Nuclear Weapons*. Rep. INFCTRC/153, IAEA, Vienna (1972).

- Secondary accountability measurements are made online.
- Variable material holdup is measured online.
- The process is divided into small accountability units.
- Accountability measurements are computerized for dynamic analysis.

Online nondestructive assay technology is not sufficiently developed at present to satisfy the requirements of high precision and accuracy for accountability measurements. Primary accountability analyses will have to be performed offline on samples taken from the process. To improve the timeliness of diversion detection, however, redundant online nondestructive assay instrumentation should supplement these offline measurements. At each primary accountability point requiring offline analysis, capabilities must be provided both for obtaining representative samples and for bulk (preferably weight) measurements. Measurements at secondary accountability points can be made by appropriate nondestructive assay instrumentation. The eventual goal is a completely online nondestructive assay accountability system as new measurement technologies are developed and field-tested.

The online nondestructive assay instrumentation specified for accountability measurements at secondary points and as backup for offline methods at primary points will provide timely information, which will also be useful for process control. In some locations, process monitoring and accountability measurements can be provided by a single instrument. However, in addition to measurement of SNM, process control variables include temperature, acidity, flow, and density.

In-process material (holdup) should be monitored at process locations where potential for variability of holdup exists. Holdup measurements at these locations are also necessary for process control and nuclear safety.

An effective means of improving the sensitivity, timeliness, and localization of diversion detection is to divide the process into discrete accounting units through which the flow of SNM is measured. Each discrete accounting unit (unit process) is composed of one storage area or one or more chemical or physical process. Unit processing allows control of quantities of material much smaller than the total process inventory. Duplicate accountability measurements are not always necessary before material leaves one unit process and after it enters the next. At the succeeding unit process, simple integrity/identity checks, such as volume and density measurements, are often adequate.

Automated process control and dynamic accountability systems require extremely reliable computers. Interconnected, doubly redundant processors with total data provided to each processor should provide sufficient reliability. Buffer storage capabilities should be provided to store accountability data during computer downtime. The design of the computer systems must ensure that accountability measurement data cannot be altered by the process control system.

The dynamic accountability concept complements but does not replace the need for physical inventories. The process should be designed to reduce the variability of the amount of SNM within each unit process. Often holdup measurements can be replaced with historical data derived from physical inventories. The expense of measurement systems to measure accurately and continuously the SNM content of minor sidestreams or waste streams may not be justified. Such streams can be accumulated and assayed on a less frequent, periodic basis. Estimating unmeasured SNM holdup or waste will reduce the sensitivity of diversion detection. The sidestreams and unmeasured holdup must be maintained unattractive or inaccessible for diversion. An ultimate update to the accountability system is made after shutdown for cleanout inventory.

General Process Control Considerations

The primary purposes of the process control systems are to provide operators with rapid access to key process variables, to provide "go, no-go" decisions based on predetermined ranges or specifications of process variables, and to provide rapid notification of process conditions requiring operator intervention. The process control system supports the accountability system by ensuring that variability of SNM content in all process locations is as low as possible.

Online techniques for nondestructive assay are sufficiently developed to provide adequate measurement of SNM concentrations for process control. Provisions for sampling should be made at all process control points for calibration and verification of the online measurement systems. Process monitoring instrumentation should be interfaced to the process control computer to permit rapid reduction of data from each measurement location. Interactive display terminals providing rapid readout of process variables should be provided at key locations on the process floor and in the control room. Whether the process control system is computer assisted or computer controlled, direct digital control should be provided for instances where safe plant operation (nuclear safety) requires immediate response.

Accountability and Process Monitoring Measurement Requirements for Plutonium Conversion

Plutonium Conversion Process

Purified plutonium nitrate streams from the solvent extraction facility (100 kg Pu/day), MOX recycle (11 kg Pu/day), and internal recovery (5.6 kg Pu/day) are converted to pure PuO_2 suitable for blending with UO_2 to form mixed oxide. The main steps of the process are valence adjustment, two-stage precipitation of Pu(III) oxalate, filtration, and calcination to PuO_2 (Figure 46). A recovery process operation (Figure 47) is designed to recover plutonium from filtrates, flush solutions, and reject solids.

The main process is a batch process (58.3 two-kg batches of plutonium per day); however, the two-stage precipitators operate continuously as do the filtrate evaporators in recovery. All other operations are batch operations.

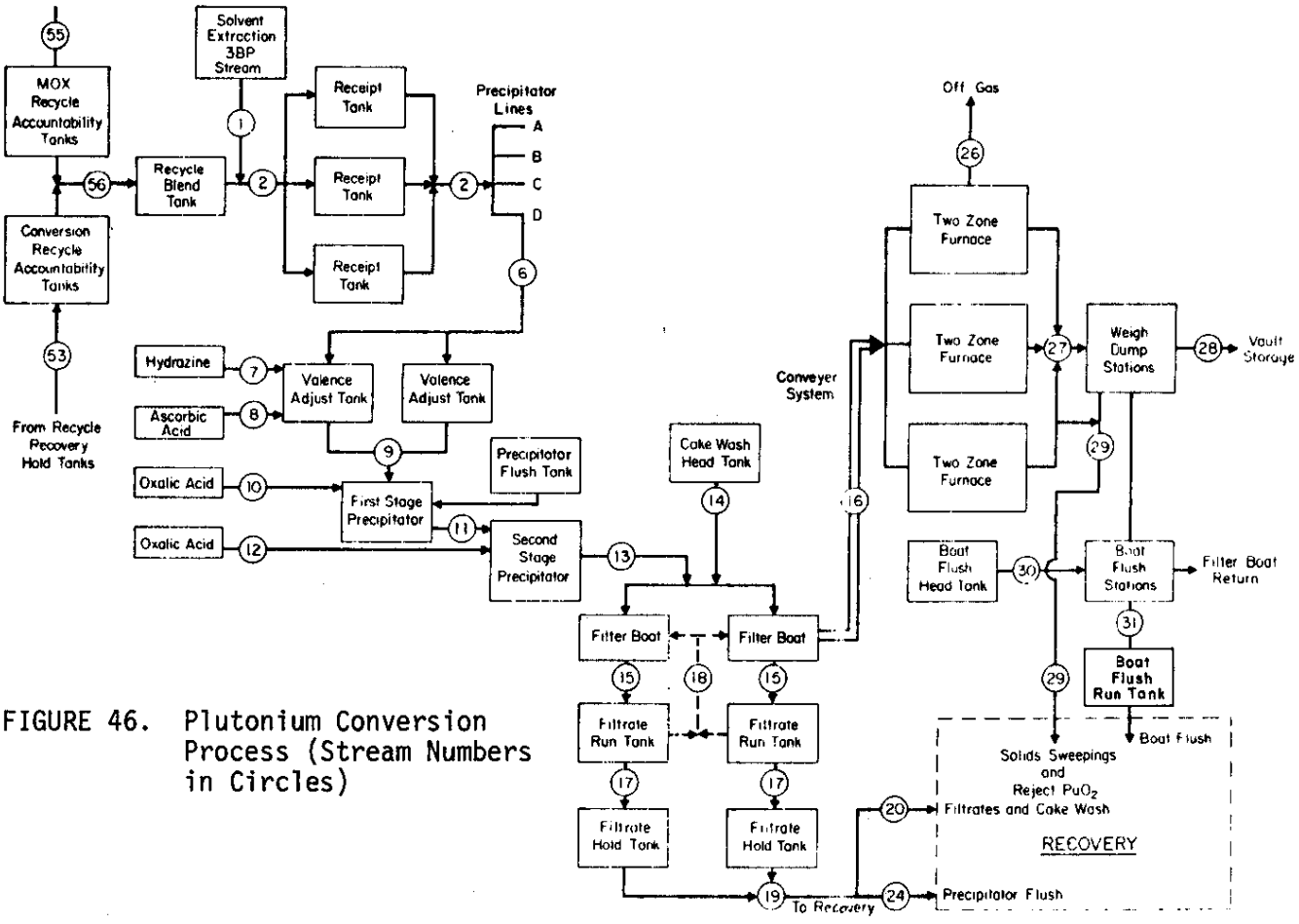

FIGURE 46. Plutonium Conversion Process (Stream Numbers in Circles)

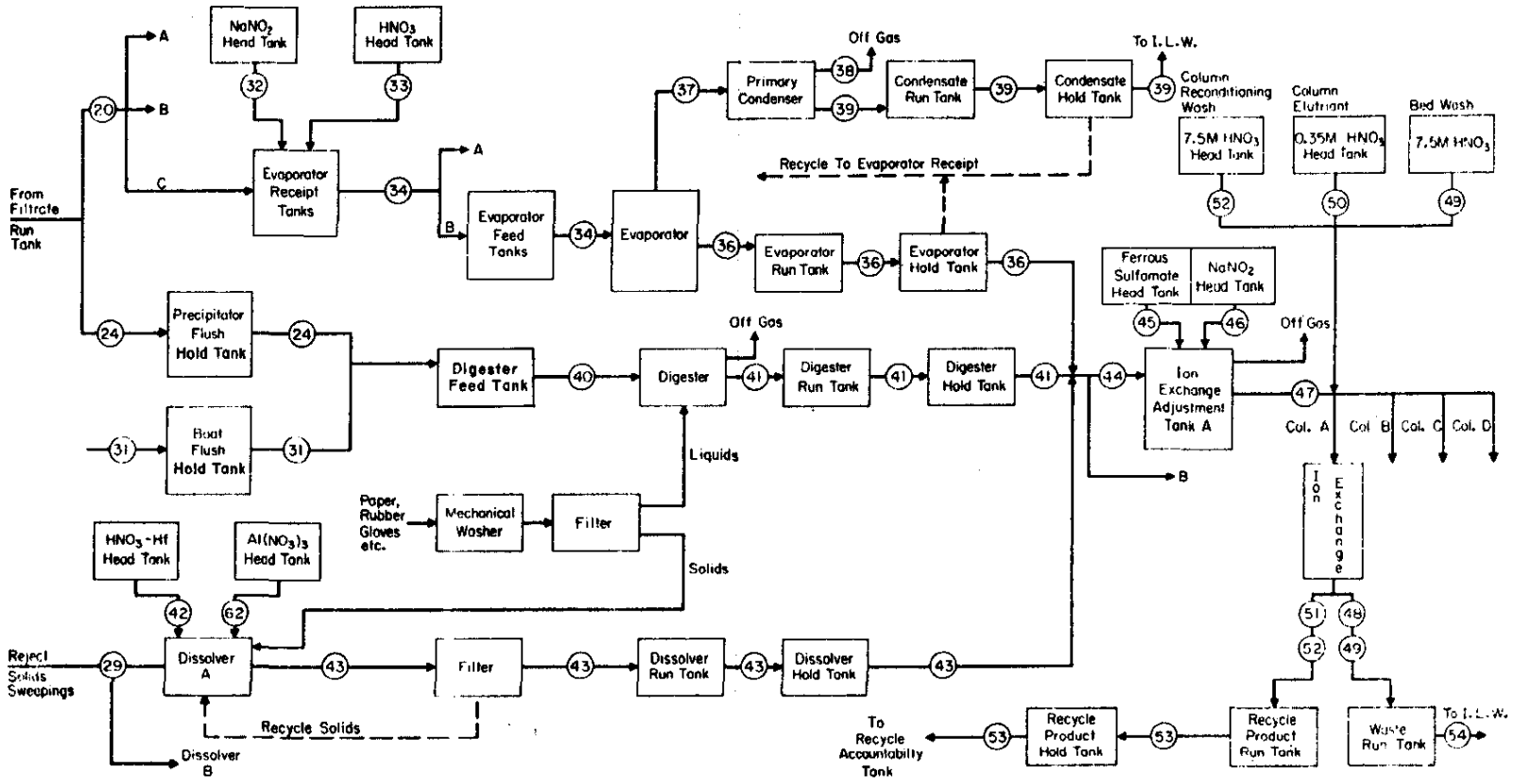

FIGURE 47. Plutonium Recovery Process
(Stream Numbers in Circles)

Accountability System Measurement Specifications

The design basis for the accountability measurement system is the rapid detection of unauthorized removal of significant quantities of plutonium from the conversion process. The computerized system operates on a near real-time basis and is designed to identify the process area from which any diversion occurs. The accountability measurement system utilizes both online nondestructive assay instrumentation and offline laboratory assay methods to measure material flows through three discrete accountability regions (unit processes) of the conversion process. Provision is made to convert to totally online measurements as nondestructive assay technology develops. The accountability system is integrated with physical safeguards to form the overall safeguards system.

The plutonium conversion facility is divided into three unit processes: Unit Process 1 is from receipt through filtration, including filtrate hold tanks. Unit Process 2 is from filtration through vault storage. Unit Process 3 is recovery.

Primary accountability points require the highest accuracy. Offline analyses are specified at these points. Backup online instruments for nondestructive assay measurements are listed in Table 48 and 49 under process control. At secondary accountability points, less accurate but more rapid online nondestructive assay methods are specified. Primary and secondary accountability points are listed in Table 50. Offline analyses require that provision be included for withdrawal of well-mixed, representative samples and for accurate bulk measurement of tank contents, preferably by weight.

Table 51 lists accountability measurement requirements for the plutonium conversion facility. For example, at the receipt tanks in Unit Process 1, plutonium concentration, plutonium isotopic analysis, and a tank solution weight are required each time a 6-kg plutonium batch is received into the process. The methods specified are x-ray absorption edge densitometry (XRAD) and gamma pulse height analysis (GPHA) for concentration and isotopic measurements accurate to 0.5%. The measurements would be performed offline at the analytical support facility. Bulk solution weight would be measured in process by load cells to an accuracy of 0.1% full scale. The methods specified represent reasonable extrapolations of current measurement technology. Table 52 summarizes the accountability measurement requirements according to analysis type for both online and offline analyses.

Performance of the Accountability System

Provisional safeguards criteria for material theft or sabotage have been issued for several design areas in the

10 MTU/day LWR fuel reprocessing plant.[2,3] Based on data from the plutonium conversion process and a survey of accountability measurement technology, a preliminary model was constructed to estimate diversion detection sensitivities for simple and multiple theft of SNM. The model has three accountability points: receipt, product, and recovery. The measurement uncertainty of each accountability point is determined by propagation of errors in bulk measurement, sampling, and laboratory analysis. The model indicates that if bulk solution measurement at the receipt tanks is performed by weight (0.1% accuracy full scale), a single theft from one 2-kg batch of plutonium of ≥105 grams plutonium could be detected. Also multiple, small thefts of ≥1.5 grams from each batch over a 90-day period (90-day sum of ≥7.6 kg Pu) would be detectable.

The results of the preliminary model must be considered as semiquantitative estimates. A more-detailed computer simulation of the conversion process was begun at Los Alamos Scientific Laboratory and will provide better estimates of detection limits. This advanced model will divide the conversion process into several unit processes through which flows of SNM will be monitored. Advanced statistical tests can be applied to signal diversion, and results of the model are expected to be available by October.

Process Monitoring Instrument Specifications for Plutonium Conversion

Instruments selected for process monitoring of the plutonium conversion facility provide rapid access of process data for plant operations and assist accountability functions. The online measurement sensors are part of a computer assisted process control system. Process control variables, measurement frequency, and analytical methods are listed in Table 48. Table 49 summarizes process monitoring requirements according to measurement type.

In general, plutonium concentration measurements are specified to provide rapid go, no-go information to process operators. Plutonium holdup measurements assist the accountability system but are included as process monitoring functions whenever potential process upset conditions could lead to criticality.

---

2. *Savannah River Laboratory Quarterly Report, Light Water Reactor Fuel Recycle, October-December 1976.* USERDA Report DPST-LWR-76-1-4, p. 64.

3. *Savannah River Laboratory Quarterly Report, Light Water Reactor Fuel Recycle, January-March 1977.* USERDA Report DPST-LWR-77-1-1, p. 64.

TABLE 48

Process Monitoring Requirements for Plutonium Conversion Facility

Measurement Location	*Measurement Required*	*No./day*	*Method*	*Accuracy, %*	*No. Online Instrument Inputs*
Stream 2	Flow	19.4	Meter	3	3
Receipt Tanks	Pu Concentration and Gamma Scan	19.4	XRAD[a] and GPHA[b]	5	3
Stream 6	Flow	58.3	Meter	3	8
Stream 9	Flow	58.3	Meter	3	8
Valence Adjust Tanks	Pu Holdup	Cont.	n-counter	10	8
Oxalic Head Tank (Stage 1)	Temperature	58.3		2[c]	8
Stream 10	Flow	58.3	Meter	3	8
Oxalic Head Tank (Stage 2)	Temperature	58.3		2[c]	8
Stream 12	Flow	58.3	Meter	3	8
Precipitator Stage 1	Temperature	Cont.		2[c]	4
	Pu Holdup	Cont.	n-counter	10	4
Precipitator Stage 2	Temperature	Cont.		2	4
	Pu Holdup	Cont.	n-counter	10	4
Stream 15	Pu Concentration	58.3	NaI[d]	10	8
2-Zone Furnaces	Temperature	Cont.	2	6	
	Pu Holdup	Cont.	n-counter	20	6
Filtrate Run Tank	Pu Holdup	Cont.	n-counter	20	8
Weigh-Dump Stations	Weight	58.3	Load Cell	1	2
	Pu Holdup	Cont.	n-counter	20	2
Off-gas Filter	Pu Holdup	Cont.	n-counter	20	3
Boat Flush Stations	Pu Holdup (boat)	58.3	n-counter	20	2
Evaporator Receipt Tanks	Pu Concentration	58.3	GPHA	10	3
Evaporator Feed Tanks	Pu Holdup	Cont.	n-counter	10	2

a. X-ray absorption edge densitometer.

b. Gamma Pulse Height Analyzer.

c. °C.

d. Sodium iodide detector.

e. Online alpha monitor.

(continued on next page)

TABLE 48, Continued

Measurement Location	*Measurement Required*	*No./day*	*Method*	*Accuracy, %*	*No. Online Instrument Inputs*
Stream 34 (to evaporator)	Flow	Cont.	Meter	3	2
Evaporator	Pu Holdup	Cont.	n-counter	10	1
Primary Condenser	Pu Holdup	Cont.	n-counter	25	1
Stream 37 (overheads)	Pu Concentration	Cont.	OLAM[e]	50	1
Off-gas Filter	Pu Holdup	Cont.	n-counter	50	1
Condensate Hold Tank	Pu Concentration	Cont.	OLAM	50	1
Evaporator Run Tank	Pu Holdup	Cont.	n-counter	10	1
Evaporator Hold Tank	Pu Concentration	8	GPHA	10	1
Stream 36	Flow	8	Meter	3	1
Precipitator Flush Hold Tank	Pu Holdup	Cont.	n-counter	10	1
Boat Flush Hold Tank	Pu Holdup	Cont.	n-counter	10	1
Digester Feed Tank	Pu Concentration	Cont.	GPHA	10	1
Digester	Pu Holdup	Cont.	n-counter	10	1
Digester Run Tank	Pu Holdup	5	n-counter	10	1
Digester Hold Tank	Pu Concentration	5	GPHA	10	1
Stream 41	Flow	5	Meter	1	
Digester Off-gas Filter	Pu Holdup	Cont.	n-counter	50	1
Dissolver	Pu Holdup	Cont.	n-counter	10	2
Dissolver Solids Filter	Pu Holdup	Cont.	n-counter	20	1
Mechanical Washer Liquids	Pu Conc.,	1	NaI	20	1
Dissolver Run Tank	Pu Holdup	5	n-counter	10	2
Dissolver Hold Tank	Pu Holdup	5	n-counter	10	2
Stream 43 (from dissolver hold)	Flow	5	Meter	3	1
Stream 44 (to ion exchange adjust)	Flow	11.2	Meter	3	2
Ion Exchange Adjust Tank	Pu Concentration	11.2	GPHA	10	2
Stream 47 (to ion exchange)	Flow	11.2	Meter	3	4
Stream 48 (Load Effluent)	Pu Concentration	11.2	NaI	10	1
Stream 49 (Column Wash)	Pu Concentration	11.2	NaI	10	1
Anion Waste Run Tank	Pu Holdup	Cont.	n-counter	50	2
Anion Product Run Tank	Pu Holdup	Cont.	n-counter	10	4
Anion Product Hold Tank	Pu Concentration	11.2	XRAD	5	2

TABLE 49

Summary of Process Monitoring Instrument Requirements

Measurement	*Method*	*No. of Instrument Inputs*
Flow	Meter	53
Pu Concentration	OLAM	2
Pu Concentration	NaI	11
Pu Concentration	GPHA	8
Pu Concentration	XRAD	5
Pu Holdup	n-counter	61
Temperature	Thermocouple	30
Weight	Load Cell	2

TABLE 50

Accountability Points

Primary Points	*Secondary Points*
Receipt Tanks (3)	Filter Stations (4)
Weigh-Dump Stations (2)	Filtrate Hold Tanks (8)
Anion Product Hold Tanks (2)	Weigh-Dump Stations (2)
	Boat Flush Run Tank (1)
	Evaporator Receipt Tanks (3)
	Evaporator Hold Tank (1)
	Precipitator Flush Hold Tank (1)
	Boat Flush Hold Tank (1)
	Digester Feed Tank (1)
	Dissolver Station (1)
	Dissolver Hold Tank (1)
	Anion Waste Run Tanks (2)

TABLE 51

Accountability Requirements for the Plutonium Conversion Facility

Measurement/Sampling Location	*Analysis/Measurement Required*	*No./Day*	*Analytical Method*[a]	*Analysis Location*[b]	*Accuracy, %*	*Online Instrument Inputs*
A. Unit Process 1						
1. Receipt Tank	Pu Conc. + Isotopic	19	XRAD, GPHA	ASF	0.5	-
	Weight	19	Load Cell	OL	0.1 FS	3
2. Filter Stations	Pu Factor[c]	58	n-count	OL	2	4
	Weight	58	Load Cell	OL	0.3 FS	4
3. Filtrate Hold Tank (Filtrates-washes)	Pu Concentration	58	GPHA	OL	5	8
	Volume	58	Liquid Level	OL	2	8
	Density	58	Densimeter	OL	0.1	8
4. Filtrate Hold Tank (Precipitator flush)	Pu Concentration	3	XRAD	OL	3	4
	Volume	3	Liquid Level	OL	2	8[d]
	Density	3	Densimeter	OL	0.1	8[d]
B. Unit Process 2						
1. Weigh-Dump Station	Pu Factor[c] + Isotopic	58	XRAD, GPHA	ASF	0.5	-
	Weight	58	Load Cell	ASF	0.1 FS	-
	Pu Residual	58	n-count	OL	10	2
	Product Purity	58	Emission Spectroscopy	ASF	2	-
2. Weigh-Dump Station (Solids and Sweepings)	Pu Factor[b]	1	n-count	OL	3	1
	Weight	1	Load Cell	OL	0.1 FS	1
3. Boat Flush Run Tank	Pu Concentration	2	XRAD	OL	3	1
	Volume	2	Liquid Level	OL	2	1
	Density	2	Densimeter	OL	0.1	1
C. Unit Process 3						
1. Evaporator Receipt Tank	Volume[e]	58	Liquid Level	OL	2	3
	Density[e]	58	Densimeter	OL	0.1	3
2. Evaporator Hold	Pu Concentration	~8	XRAD	OL	3	1
	Volume	~8	Liquid Level	OL	1	1
	Density	~8	Densimeter	OL	0.1	1
3. Precipitator Flush Hold Tank	Volume[e]	3	Liquid Level	OL	2	1
	Density[e]	3	Densimeter	OL	0.1	1
4. Boat Flush Hold Tank	Volume[e]	2	Liquid Level	OL	2	1
	Density[e]	2	Densimeter	OL	0.1	1
5. Digester Feed Tank	Pu Concentration	5	XRAD	OL	2	1
	Volume	5	Liquid Level	OL	1	1
	Density	5	Densimeter	OL	0.1	1
6. Dissolver Station	Weight[e]	1	Load Cell	OL	0.1	1
	Pu Factor[c]		n-count		3	1
7. Dissolver Hold Tank	Pu Concentration	5	XRAD	OL	2	1
	Volume	5	Liquid Level	OL	1	1
	Density	5	Densimeter	OL	0.1	1
8. Anion Waste Run Tank	Pu Concentration	11	NaI	OL	10	2
	Volume	11	Liquid Level	OL	5	2
	Density	11	Densimeter	OL	0.1	2
9. Anion Product	Pu Conc. + Isotopic	6	XRAD, GPHA	ASF	1	-
	Weight	6	Load Cell	OL	0.1 FS	2

a. XRAD x-ray edge absorption densitometry
GPHA gamma pulse height analysis

b. ASF analytical support facility
OL online nondestructive analysis

c. Grams of Pu/gram of oxide powder

d. Same input as in A,3 above

e. Integrity/identity check

TABLE 52

Summary of Accountability Requirements for Offline and Online Measurements

Offline Measurements in an Analytical Support Facility	*Number per Day*	*Method*	*Accuracy, %*
Pu Concentration	19, 6	XRAD	0.5, 1
Pu Factor[b]	58	XRAD	0.5
Pu Isotopic	82	GPHA[a]	0.1-0.5
Weight	58	Load Cell	0.1
Purity	58	Emission Spectroscopy	1 (relative)
Waste Assay	Est. 2	n-coincidence	10
Online Analysis Requirements			
Pu Concentration	10, 69	GPHA	
Pu Concentration	8, 23	XRAD	
Pu Factor[b]	8, 118	n-coincidence	
Weight	11, 75	Load Cell	
Volume	19, 155	Liquid Level	
Density	19, 155	Densimeter	

a. 200 Pu isotopic analyses per day can be performed with 3 PHA's (4K-24 bit) interfaced to a PDP-11 (64K).

b. Grams of Pu/gram of oxide powder.

DISTRIBUTION

Copy No.

1-2	N. Stetson, ERDA-SR
3-6	T. B. Hindman, ERDA-SR
7-73	TIS File, SRL
74	N. F. Sievering, Jr., Assistant Administrator for International Affairs, ERDA, Washington, DC 20545
75	G. W. Wensch
76	A. Giambusso
77	R. D. Thorne, Assistant Administrator for Nuclear Energy, ERDA, Washington, DC 20545
78	G. W. Cunningham, Director, Waste Management, Production, and Reprocessing, ERDA, Washington, DC 20545
79	D. R. Spurgeon
80	R. B. Chitwood
81	R. G. Bradley
82	G. B. Pleat
83	C. W. Kuhlman
84	J. L. Liverman, ERDA, Division of Biomedical and Environmental Research, Washington, DC 20545
85	ERDA Division of Reactor Development and Demonstration, Engineering and Technology, Washington, DC 20545
86	H. E. Lyon, ERDA, Division of Safeguards and Security, Washington, DC 20545
87	H. E. Roser, ERDA Albuquerque Operations Office
88	ERDA Oak Ridge Operations Office
89	ERDA Richland Operations Office
90	ERDA Idaho Operations Office
91	ERDA Nevada Operations Office
92	ERDA San Francisco Operations Office
93	ERDA Chicago Operations Office
94	ERDA Southern California Energy Office
95-122	ERDA-TIC, Oak Ridge
123	S. Levine, NRC Division of Reactor Safety Research
124	R. E. Cunningham, NRC Division of Fuel Cycle and Material Safety

125. Herman Postma, Director
Oak Ridge National Laboratory
P.O. Box X
Oak Ridge, TN 37830

126. H. M. Agnew, Director
Los Alamos Scientific Laboratory
P. O. Box 1663
Los Alamos, NM 87545

127. F. H. Anderson, Gen. Manager
Allied Chemical Corp.
550 Second Street
Idaho Falls, ID 83401

128. W. J. Wilcox, Technical Director
Oak Ridge Gaseous Diffusion Plant
Oak Ridge, TN 37830

129. Battelle-Columbus Laboratories
505 King Avenue
Columbus, OH 43201

130. Claude Stephens
Virginia Electric Power Co.
Nuclear Fuel Service Dept.
512 Franklin Building
P.O. Box 26666
Richmond, VA 32361

131. Wendell Johnson, Vice-President
Yankee Atomic Electric Co.
20 Turnpike Road
Westboro, MA 01581

132. R. D. Oldenkamp
Rockwell International
Atomics International Div.
8900 DeSoto Avenue
Canoga Park, CA 91304

133. S. Stoller
Western Reprocessors
The S. M. Stoller Corporation
1250 Broadway
New York, NY 10001

134. George Stukenbroeker
NL Industries
P.O. Box 928
Barnwell, SC 29812

135. Robert C. Adkins
Technical Representative
NUSAC
7926 Jones Branch Drive
McLean, VA 22101

136. K. Vickers
Phrasor Technology
110 S. Euclid Avenue
Pasadena, CA 91101

137. K. Bowlman
General Electric Co.
175 Curtner Avenue
San Jose, CA 95125

138. W. A. Kalk
Manager, Nuclear Power Systems
Holmes & Narver, Inc.
400 East Orangethorpe Ave.
Anaheim, CA 92801

139. Floyd W. Lewis, President
Middle South Utilities, Inc.
Box 61006
New Orleans, LA 70161

140. C. K. Anderson
Combustion Engineering
Nuclear Power Division
1000 Prospect Hill Road
Windsor, CN 06095

141. Justin Carp
Director for Energy Policy
Edison Electric
90 Park Avenue
New York, NY 10016

142. Dr. Uhrig
Florida Power & Light Co.
P.O. Box 013100
Miami, FL 33101

143. Richard G. Cross
DBM Corporation
1920 Alpine Avenue
Vienna, VA 22180

144. M. I. Naparstek
Manager of Proposals
Burns & Roe
Industrial Services Corp.
P.O. Box 663
Paramus, NJ 07652

145. Gordon R. Corey, Vice-Chairman
Commonwealth Edison Company
P.O. Box 767
Chicago, IL 60690

146. R. C. Baxter, President
Allied-General Nuclear Services
P.O. Box 847
Barnwell, SC 29812

147. R. H. Ihde
Manager Contracts & Marketing
Babcock & Wilcox
P.O. Box 1260
Lynchburg, VA 24505

148. C. A. Hirenda
Director of Marketing
Proposal Management, Inc.
121 N. Orionna Street
Philadelphia, PA 19106

149. B. H. Cherry
Manager of Fuel Resources
GPU Services Corporation
260 Cherry Hill Road
Parsippany, NY 07054

150. Martin Binstock
Kerr-McGee Nuclear Corp.
Kerr-McGee Building
Oklahoma City, OK 73102

151. Gerald K. Rhode
Vice-Pres. of Engineering
Niagara Mohawk Power Corp.
300 Erie Boulevard, West
Syracuse, NY 13202

152. Marvin G. Britton
Manager Technical Liaison
Corning Glass Works
Corning, NY 14830

153. R. L. Dickeman, President
Exxon Nuclear Company, Inc.
777 — 106th Avenue, NE
Bellevue, WA 98004

154. Andrew H. Hines, Jr., Pres.
Florida Power Corporation
P.O. Box 14042
St. Petersburg, FL 33733

155. Richard L. Grant
Director Nuclear Projects
Boeing Engineering and
Construction Division
P.O. Box 3707
Seattle, WA 98124

156. Larry E. Smith, Manager-Fuel
Carolina Power & Light Co.
P.O. Box 1551
Raleigh, NC 27602

157. F. J. Kiernan, Eastern Regional
Manager
Aerojet Energy Conversion Co.
1120 Connecticut Avenue, NW
Washington, DC 20036

158. L. M. Richards, Coordinator
Nuclear Commercial Development
Atlantic Richfield Co.
Box 2679 - TA
Los Angeles, CA 90071

159. Kay Killingstad
Contract Service
Battelle-Human Affairs Research
Centers
4000 NE 41st Street
Seattle, WA 98105

160. T. W. Ambrose, Director
Pacific Northwest Laboratory
P.O. Box 999
Richland, WA 99352

161. J. A. Kyger, Associate Director
Argonne National Laboratory
9700 S. Cass Avenue
Argonne, IL 60439

162-164. B. F. Judson, Manager
Advance Engineering -
Mail Code 858
Fuel Recovery Operation
General Electric Company
175 Curtner Avenue
San Jose, CA 95125

165. George Lehmkuhl
Rockwell International
Rocky Flats Plant
P.O. Box 464
Golden, CO 80401

166. G. H. Dyer
Bechtel Corp.
50 Beale Street
San Francisco, CA 94105

167. C. A. Preskitt
IRT Corporation
P.O. Box 80817
San Diego, CA 92138

168. E. Straker
Science Applications, Inc.
P.O. Box 2351
La Jolla, CA 92038

169. Robert L. Seale
University of Arizona
Dept. of Nuclear Engineering
Tucson, AZ 85721

170. Don Eldred
General Electric Company
Energy Systems & Technology Division
310 De Guigne Drive
Sunnyvale, CA 94086

171. B. L. Vondra
ORNL, Building 7601
Box X
Oak Ridge, TN 37830

172. R. O. Williams, Vice-President
Rockwell International
Rocky Flats Plant
P.O. Box 464
Golden, CO 80401

173. Kenneth Street, Associate Director
University of California
Lawrence Livermore Laboratory
P.O. Box 808
Livermore, CA 94550

174. W. T. Cave, Director
Monsanto Research Corporation
Mound Laboratory
P.O. Box 32
Miamisburg, OH 45342

175. Louis W. Nelms, Chief
Todd Company
Research Branch
Research and Technical Div.
P.O. Box 1600
Galveston, TX 77550

176. J. F. Bader, Manager
Plutonium Recycle Fuel Programs
Westinghouse Electric Corp.
Box 355
Pittsburgh, PA 15230

177. John Shefcik
General Atomic Company
P.O. Box 81608
San Diego, CA 92138

178. Dr. Ralph Fullwood
Science Applications, Inc.
2680 Hanover Street
Palo Alto, CA 94303

179. Ray Hoskins
Tennessee Valley Authority
217 Electric Power Board Bldg.
Chattanooga, TN 37401

180. W. H. Lewis, Vice-President
Nuclear Fuel Services
6000 Executive Blvd.
Rockville, MD 20952

181. A. Squire, Director
Hanford Engineering Development Laboratory
P.O. Box 1970
Richland, WA 99352

182. T. L. McDaniel
Babcock & Wilcox Co.
P.O. Box 1260
Lynchburg, VA 24505

183. E. Morgan
Babcock & Wilcox Co.
P.O. Box 1260
Lynchburg, VA 24505

184. D. M. Rohrer
Mail Stop 517
Los Alamos Scientific Laboratory
P.O. Box 1663
Los Alamos, NM 87545

185. D. D. Wodrich
Atlantic Richfield Hanford Co.
P.O. Box 250
Richland, WA 99353

186. R. W. Gilchrist
Electrical and Computer Engineering Dept.
Clemson University
Clemson, SC 29631

187. J. E. Bennett
Electrical and Computer Engineering Dept.
Clemson University
Clemson, SC 29631

188. J. K. Bryan
Electrical and Computer Engineering Dept.
Clemson University
Clemson, SC 29631

189. D. Orloff
College of Engineering
University of South Carolina
Columbia, SC 29208

190. V. Van Brunt
College of Engineering
U. of South Carolina
Columbia, SC 29208

191. T. Stanford
College of Engineering
U. of South Carolina
Columbia, SC 29208

192. C. Rhoades
College of Engineering
U. of South Carolina
Columbia, SC 29208

193. R. F. Duda
Westinghouse
P.O. Box 355
Pittsburgh, PA 15230

194. H. L. Browne
Bechtel Inc.
P.O. Box 3965
San Francisco, CA 94119

195. B. Smenoff
Hudson Institute
Quaker Ridge Road
Croton, NY 20520

196. H. A. Hurstadt
105 Randolph Hall
Virginia Polytechnic Institute
Blackburg, VA 34061

197. D. S. Webster
Argonne National Laboratory
9700 S. Cass Avenue
Argonne, IL 60439

198. M. J. Steindler
Argonne National Laboratory
9700 S. Cass Avenue
Argonne, IL 60439

199 G. Bernstein
Argonne National Laboratory
9700 S. Cass Avenue
Argonne, IL 60439

200. D. C. Nelson
Nuclear Commercial Development
Atlantic Richfield Co.
P.O. Box 2679-TA
Los Angeles, CA 90071

201. J. L. Fletcher
Hanford Engineering Development Laboratory
P.O. Box 1970
Richland, WA 99352

202. R. E. Dahl
Hanford Engineering Development Laboratory
P.O. Box 1970
Richland, WA 99352

203. B. R. Dickey
Allied Chemical Corp.
550 Second Street
Idaho Falls, ID 83401

204. B. Paige
Allied Chemical Corp.
550 Second Street
Idaho Falls, ID 83401

205. R. Brown
Allied Chemical Corp.
550 Second Street
Idaho Falls, ID 83401

206. D. Bowersox
Los Alamos Scientific Laboratory
P.O. Box 1663
Los Alamos, NM 87545

207. G. R. Keepin
Los Alamos Scientific Laboratory
P.O. Box 1663
Los Alamos, NM 87545

208. J. Dietz
Los Alamos Scientific Laboratory
P.O. Box 1663
Los Alamos, NM 87545

209. W. J. Maraman
Los Alamos Scientific Laboratory
P. O. Box 1663
Los Alamos, NM 87545

210. M. Dickerson
Lawrence Livermore Laboratory
University of California
P.O. Box 808
Livermore, CA 94550

211. R. C. Orphan
Lawrence Livermore Laboratory
University of California
P.O. Box 808
Livermore, CA 94550

212. Y. Ng
Lawrence Livermore Laboratory
University of California
P.O. Box 808
Livermore, CA 94550

213. D. Camp
Lawrence Livermore Laboratory
University of California
P.O. Box 808
Livermore, CA 94550

214 through 220 bear following ORNL address:

214. R. W. Stockdale
ORNL
P.O. Box X
Oak Ridge, TN 37830

215. M. J. Stephenson

216. S. V. Kaye

217. V. C. A. Vaughn

218. J. C. Mailen

219. D. O. Campbell

220. C. D. Watson

221 through 232 bear following PNL address:

221. W. Reardon
Pacific Northwest Laboratory
P.O. Box 999
Richland, WA 99352

222. C. L. Brown

223. E. D. Clayton

224. L. L. Wendell

225. R. C. Liikala

226. E. R. Irish

227. S. Goldsmith

228. W. J. Coleman

229. J. L. Swanson

230. L. Schwendiman

231. R. S. Kemper

232. H. H. Van Tuyl

233. E. D. Erickson
Rockwell International
Rocky Flats Plant
P.O. Box 464
Golden, CO 80401

234. D. Zeigler
Rockwell International
Rocky Flats Plant
P.O. Box 464
Golden, CO 80401

235. T. A. Sellers
Sandia Laboratories
P.O. Box 5800
Albuquerque, NM 87115

236. J. A. Stiegler
Sandia Laboratories
P.O. Box 5800
Albuquerque, NM 87115

237. J. L. Heffter
Air Resources Laboratories
National Oceanic and Atmospheric Administration
8060 13th Street
Silver Spring, MD 20910

238. Dr. Lester Machta
Air Resources Laboratories
National Oceanic and Atmospheric Administration
8060 13th Street
Silver Spring, MD 20910

239. Dr. W. G. N. Slinn
Atmospheric Sciences Dept.
Oregon State University
Corvallis, OR 97331

240. J. H. Pashley
Oak Ridge Gaseous Diffusion Plant
Oak Ridge, TN 37830

241. G. L. Ritter
Exxon Nuclear Corp.
2995 George Washington Way
Richland, WA 99352

242. R. B. Minogue
Office of Standards Development
Mail Stop NL5650
Nuclear Regulatory Commission
Washington, DC 20555

243. Dr. David Camp, L-233
Lawrence Livermore Laboratory
P. O. Box 808
Livermore, CA 94550

244. B. C. Blanke
USERDA-DA
P. O. Box 66
Miamisburg, OH 45342

245. P. Fairchild
Office Waste Isolation
Union Carbide Nuclear
P. O. Box Y
Oak Ridge, TN 37830

246. J. H. Jarrett
Pacific Northwest Laboratory
P. O. Box 999
Richland, WA 99352

247. D. Pence
Science Applications
P. O. Box 2351
La Jolla, CA 92038

248-330. TIS File